Rejuvenation of Aged Heart Explant-Derived Cells for Repair of Ischemic Cardiomyopathy

Ghazaleh Rafatian

This thesis is submitted to the Faculty of Graduate and Postdoctoral Studies as partial fulfillment of the Doctor of Philosophy program in Cellular Molecular Medicine.

Department of Cellular and Molecular Medicine

Faculty of Medicine

University of Ottawa, Ottawa, ON

Supervisors: Darryl R Davis, MD

Erik J Suuronen, PhD

Table of Contents

Sources of Funding

This study was funded by the Canadian Institutes of Health Research and the Heart and Stroke Foundation of Canada.

Abstract

In autologous stem cell therapy, cell characteristics determine the potency of stem cells for regeneration. Aging and ischemia are two factors that are often neglected in pre-clinical tests for stem cell therapy. Here, we characterized cardiac explant-derived cells (EDCs) with a focus on distinguishing the effect of age and ischemia and then we looked for the effects of the combination of the two factors. We observed that ischemia worsens the age effect on EDCs. EDCs that were derived from aged mice with a history of myocardial infarction showed the highest number of senescent cells with dysregulation of the DNA repair system resulting in activation of cell cycle checkpoints. We over-expressed the anti-senescence Mybl2 transcription factor in EDCs from ischemic aged mice. The senescent state, paracrine profile and superoxide dismutase antioxidant enzyme activity improved in these cells. *In vivo*, we observed a boost in the potency of the Mybl2-modified EDCs, with an increase in short-term engraftment leading to improved heart function in infarcted mice. In general, Mybl2 over-expression rejuvenates senescent EDCs.

List of Tables

List of Figures

List of abbreviations

7-AAD	7-Amino-Actinomycin D
BIO	6-bromoindirubin-3-oxime
BMDCs	bone marrow-derived cells
BRAF	B-Raf Proto-Oncogene
CDCs	cardiosphere derived stem cells
CDK2	Cyclin-dependent kinase 2
CEM	complete explant medium
CHIP	carboxy terminus of Hsp70-interacting protein
chk1	Checkpoint kinase 1
chk2	Checkpoint kinase 2
CM	Conditioned media
ct	cycle thresholds
cTNT	cardiac troponin T
DAPI	4',6-diamidino-2-phenylindole
DCF	2',7'–dichlorofluorescein
DCFDA	2',7'–dichlorofluorescin diacetate
DDR	DNA damage response
DF	dermal fibroblast
DMSO	Dimethylsulfoxide
DNA-SCARS	DNA segments with chromatin alterations reinforcing senescence
DP	Dimerization partners

EDCs	explant derived cells
ELISA	Commercial enzyme-linked immunosorbent assays
EMT	epithelial to mesenchymal transition
EPCs	endothelial progenitor cells
ESC	Embryonic stem cells
FBS	fetal bovine serum
FoxM1	Forkhead box protein M1
FoxO	Forkhead box O
GDF-11	Growth Differentiating Factor 11
GFP	Green fluorescent protein
GPx	Glutathione Peroxidase
GSK-3β	glycogen synthase kinase-3 beta
HBSS	Hank's Balanced Salt Solution
HIF1	hypoxia-inducible factor 1-alpha
HGF	hepatocyte growth factor
HUVECs	human umbilical vein endothelial cells
ICM	Ischemic
IGF-1	Insulin growth factor-1
IL	Interleukin
IMDM	Iscove’s Modified Dulbeccos Medium
iPS	induced pluripotent stem cells
LCA	Left Coronary Artery
LTS	long-term stratification score

LVEF	left ventricular ejection fraction
MI	Myocardial infarction
MMP	Matrix metalloproteinase
mTOR	mammalian target of rapamycin
mTORC1	mammalian target of rapamycin complex 1
mTORC2	mammalian target of rapamycin complex 2
MuvB	multi-vulval class B
Mybl2; B-MYB	Myb-Like Protein 2
NF-κB	Nuclear Factor Kappa light chain enhancer of activated B cells
NQO1	NAD(P)H dehydrogenase
NRM	normal
NYHA	New York Heart Association
PBS	phosphate buffered saline
PFA	Paraformaldehyde
PI3K	and phosphatidylinositide 3-kinase
pRB	phosphorylated retinoblastoma protein
Protein kinase B	AKT
RAGE	receptor for advanced glycation end-products
RB	Retinoblastoma
RMA	robust multi-array averaging
ROS	Reactive oxygen species
RRE	Rev Response Element
SAHF	senescence-associated heterochromatin foci

SASP	senescence associated secretory phenotype
SA-β-gal	Senescence associated β- galactosidase
sirt	sirtuin
SkM	skeletal myoblast
SDF-1α	stromal cell-derived factor 1 alpha
SOD	Super Oxide Dismutase
TERT	telomerase reverse transcriptase
TF	transcription factor
TIMP-1	tissue inhibitor of metalloproteinase-1
VEGF	vascular endothelial growth factor
vWF	von Willebrand factor
YF	Y RNA fragments
α-SMA	α-smooth muscle actin

Acknowledgments

I would like to acknowledge the following individuals for their contributions to this thesis:

Thesis Advisory Committee:

- Dr. Patrick Burgon, Dr. Marc Ruel and Dr. Katey Rayner

Laboratory Members:

- Dr. Maryam Kamkar: training, experimental design, tissue processing
- Richard Seymour: mouse surgeries
- Dr. Andre Molgat: project design, contribution in taking mice echo
- Bin Ye: training and project design
- Pushpinder Kanda: project design

University of Ottawa Heart Institute: Animal Care and Veterinary Service

University of Ottawa Department of Pathology: processing histological sections.

University of Ottawa OHRI StemCore microarray facility: processing microarray

I would also like to express my uttermost gratitude to Dr. Darryl R Davis and Dr. Erik J Suuronen for their continuous motivation, insight and continual guidance throughout my studies.

1. INTRODUCTION

1.1.1 Aging

Aging is the process of becoming older. The symptoms of aging are evident in the physiological function of organism, organs and their comprising elements, the cells and the cell molecules (Khan et al., 2017). Chronological age is a risk factor for many diseases including cardiovascular disease, hypertension, hearing loss, visual acuity and dementia (Dong et al., 2016). Although it inevitably occurs with time, biological aging is modulated by genetic factors (responsible for 20-30% of variability in life span (Kenyon et al., 2010)), epigenetic factors and environmental divergence. The process of aging in human involves deterioration in capacity for regeneration and repair causing a decline in the function of many organs including lung, kidney, immune and hematologic system, nervous system and musculoskeletal (Khan et al., 2017). The aged show an imbalance in hemostasis as newly formed cells cannot compensate for the number of cells with accumulated damage. These damaged cells undergo irreversible growth arrest termed senescence under normal physiological condition. Indeed, accumulation of senescent cells in an organ underlies age-related physiological deconditioning (Sousounis et al., 2014). The gradual accumulation of senescent cells is due to accelerated generation of these cells and/or impaired removal of the cells by immune system (Rodier F and Campisi J, 2011). López-Otín et al. proposed nine hallmarks of aging as follows. Cells in the aged have accumulated damage due to 1) genomic instability 2) telomere shortening 3) epigenetic alterations and 4) loss of proteostasis (protein homeostasis). In response to damage they show 5) deregulated nutrient sensing 6) cellular senescence and 7) mitochondrial

dysfunction, which cause 8) stem cell exhaustion and 9) altered intercellular communication (Figure 1.1; López-Otín et al., 2013).

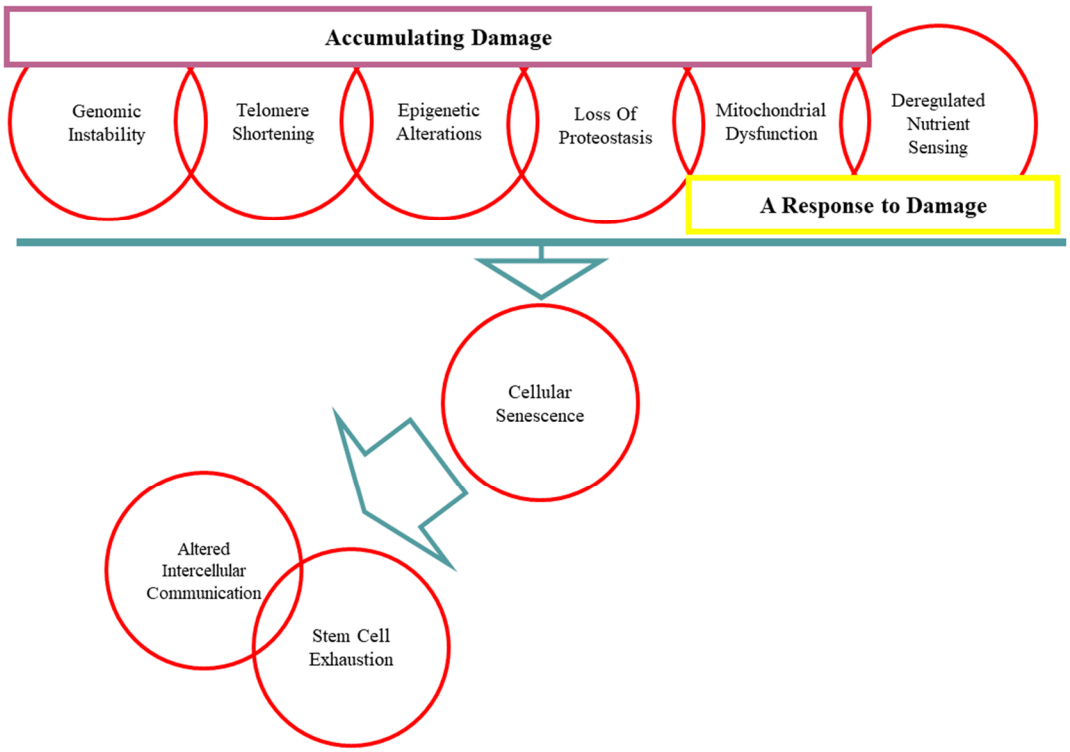

Figure 1.1. Hallmarks of cellular senescence. Senescence is a consequence of mechanisms that accumulate damage in cells and the response mechanism(s) to these damages. Senescence alters homeostasis by exhausting stem cells and changing cell-cell communication.

The hallmarks of aging with senescence triggering role are explained below in more details.

1.1.1.1 Genomic instability and telomere shortening

Telomeres are repetitive sequences at the ends of chromosomes, which are capped and protected by telomere binding proteins (de Lange, 2006). Telomere attrition occurs due to loss of part of telomere repeats after each chromosome replication as a consequence of incomplete lagging strand (5'-> 3' strand) synthesis. This leaves the new 5' end replicated from parental lagging strand

truncated (Shay and Wright, 2007). Telomere erosion or uncapping induce replicative senescence while genomic damage at non-telomeric sites results in single or double strand breakage and induces premature senescence (Figure 1.2). DNA damage turns on intrinsic DNA damage response (DDR) that induces senescence through activation of the p53 pathway (Hayflick and Moorhead, 1961; Shiloh, 2003; Herbig et al., 2004). p53 has multi-directional roles and its activation results in dose-dependent promotion of repair, cell-cycle arrest or if persisted senescence, or, eventual apoptosis (Vousden and Lane, 2007). When DNA damage occurs (as a result of oxidative stress, ionizing radiation or DNA replication errors (Dumont et al., 2000; Herskind and Rodemann, 2000)), repair proteins including ATR (Ataxia Telangiectasia and Rad3-Related Protein) and ATM (Ataxia Telangiectasia Mutated) come to the site of damage and phosphorylate H2A histone which facilitates recruitment and assembly of other DNA repair factors and checkpoint proteins to correct DNA damage whilst the cell cycle is halted. Recruited Checkpoint kinases become phosphorylated by ATR and ATM, and sequentially activate cell cycle arrest proteins p53, p21 and Retinoblastoma (RB) while inhibiting cell cycle promoting protein Cyclin-dependent kinase 2 (CDK2) (Passos et al., 2007).

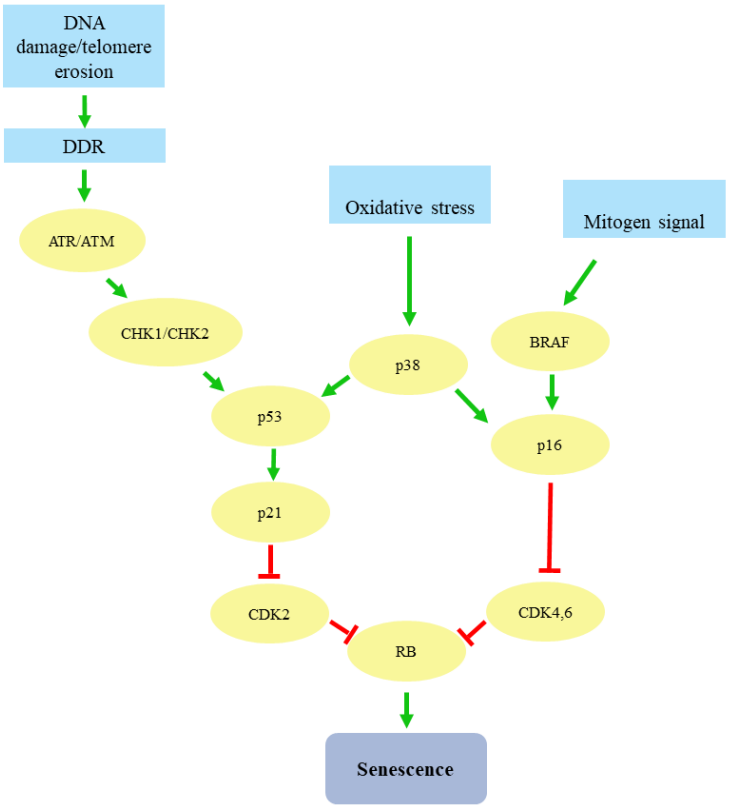

Figure 1.2. Senescence effector pathways. Senescence triggers induce permanent growth arrest through different pathways. CHK: checkpoint kinase; CDK: cyclin-dependent kinase; BRAF: B-Raf Proto-Oncogene

In some cell types, oxidative stress also reduces telomerase activity speeding up replicative senescence, thus, telomere shortening is stress dependant (Haendeler et al., 2004; Matthews et al., 2006). In support of this notion, Bernandes et al. showed that Telomerase Reverse Transcriptase (TERT) gene transfer to (1 and 2 years old) mice delayed aging and increased longevity. These mice showed improvement in symptoms of aging such as insulin resistance, osteoporosis and age biomarkers (Bernardes et al., 2012). Also, humans with exceptional longevity were carrying longer telomeres and hTERT gene mutations that improved maintenance of telomere. These individuals with longer telomeres experienced healthier aging with normal lipid profiles, less diabetes, less hypertension and less cognitive dysfunction (Atzmon et al., 2010). Smoking, obesity and life

stressors also influence telomere length by manipulating the generation of oxidative stress with obesity reducing telomeres by 240 bp, on average, over time, and smoking reducing telomeres by 5 bp per pack year (Valdes et al., 2005; Epel et al., 2004).

1.1.1.2 Oncogenic stress and oxidative stress

While replicative senescence may be the case in proliferative cells, post-mitotic cells have different triggers responsible for senescence. Strong mitogen signals (such as oncogenic compounds or oxidative stress) trigger senescence by activating p16/p19 or p53/p21 pathways that promote growth arrest (Lujambio, 2016; Zhu, J et al., 1998). As shown in Figure 1.2, the mediators of this effect are instigator dependent with oncogenic stress inducing BRAF which activates p16 and suppresses CDK4,6 while oxidative stress leads to activation of p38 (MAPK) which activates both the p16 and p53 pathways (Lujambio, 2016). Mitochondrial dysfunction is the main culprit for production of excess reactive oxygen species (ROS) in cells. ROS as an active compound reacts with lipids and proteins to generate dysfunctional/toxic oxidized products within cells. ROS also reacts with both mitochondrial and genomic DNA, thus increasing genetic mutations resulting in further functional abnormalities (Passos et al., 2007). Chronic oxidative stress increases rates of single strand breakage, hence, controlling ROS level by increasing nicotinamides which are reducing agents within cells improves mitochondrial function and results in longevity (Kang et al., 2006; Gomes et al., 2013). ROS also activates p53. In response to moderate ROS elevation, p53 induces expression of antioxidants genes and protection (Sablina et al., 2005). However, excessive ROS result in mitochondrial dysfunction and profound DNA damage that leads to p53 mediated induction of apoptosis or senescence (Vousden and Lane, 2007). Thus, while low levels of p53 and ROS promote repair and are beneficial for cells, high levels are malignant and trigger senescence.

1.1.1.3 Nutrient sensing

Cell metabolism is another important determinant of aging. It has been shown that caloric restriction increases longevity while activation of anabolic pathways is associated with aging (Colman et al., 2014; López-Otín et al 2013). For instance, 20 years of caloric restriction in monkeys reduces mortality by 30% with less cancer incidence, cardiovascular disease and brain atrophy as compared to those on a regular diet (Colman et al., 2009). Among the metabolic pathways involved in aging, insulin and phosphatidylinositide 3-kinase (PI3K) signaling pathways are well-known for their pro-aging effects through downregulation of Forkhead box O (FoxO) and activation of mamnalian Target of Rapamycin (mTOR) (Kenyon 2010; Barzilai et al., 2012). The much publicised sirtuins (sirts) are also mediators of the beneficial effects of caloric restriction. These established longevity factors are often altered with age, but their activity is necessary to combat the effects of aging by stabilizing the genome. Sirtuins convey their effect through modulation of p53, Protein kinase B (Akt), hypoxia-inducible factor 1-alpha (HIF1-α) and Nuclear Factor Kappa light chain enhancer of activated B cells (NF-κB) (Cencioni et al., 2015).

1.1.1.4 Loss of protein homeostasis (proteostasis)

Cells have two distinct mechanisms for elimination of damaged organelles and materials, the autophagy and ubiquitin systems (collectively termed the proteolytic system). While enhanced proteostasis is important for maintaining youthful phenotype of cells, this process is slowed down in senescent cells (Tomaru et al., 2012). Aged cells exhibit a greater amount of oxidized or misfolded proteins due to protein oxidation and impaired proteolytic system clearance. In support of this principle, Min et al. showed that mice with carboxy terminus of Hsp70-interacting protein

(CHIP; a chaperone/ubiquitin ligase that involves in damaged protein elimination process) deficiency accelerated aging and accumulation of senescent cells (Min et al., 2008).

1.1.1.5 Epigenetic alterations

Within the epigenome, senescence is controlled by histone deacetylases (Histone deacetylase 1 and Sirt1) or by their inhibitors. Histone deacetylase inhibitors relax chromatin which alters DNA structure resulting in signals similar to DDR to induce senescence (Ogryzko et al.,1996). Pluripotency factors like SOX2 and Nanog also decrease with age which lessens their influence on the epigenetic state towards a youthful phenotype (Sousounis et al., 2014).

1.1.1.6 Cellular senescence

Regardless of senescence initiators, growth arrest associated with biological aging involves persistent phosphorylated retinoblastoma protein (pRB), p16 or p53 activation. Both p16 and p53 induce cell cycle arrest via activation of RB protein. Senescent cells display a distinct phenotype (Figure 1.3) including prominent cell cycle arrest, larger size (sometimes more than twice the original size), flat morphology, higher autofluorescence, expression of Senescence associated β-galactosidase (SA-β-gal; reflecting increased lysosomal content and mass (Kurz et al., 2000), up-regulation of tumor suppressor genes (p16 and p19), displaying senescence-associated heterochromatin foci (due to silencing of pro-proliferative genes by p16/pRB), displaying DNA segments with chromatin alterations reinforcing senescence (in cells with persistent DDR signal) and displaying the senescence associated secretory phenotype (SASP; excessive secretion of inflammatory cytokines, immune modulators, chemokines, growth factors and matrix metalloproteinases) with autocrine and paracrine activity to communicate with other cells (Dimri et al., 1995; Lee et al., 2006; Narita et al., 2003; Rodier et al., 2011).

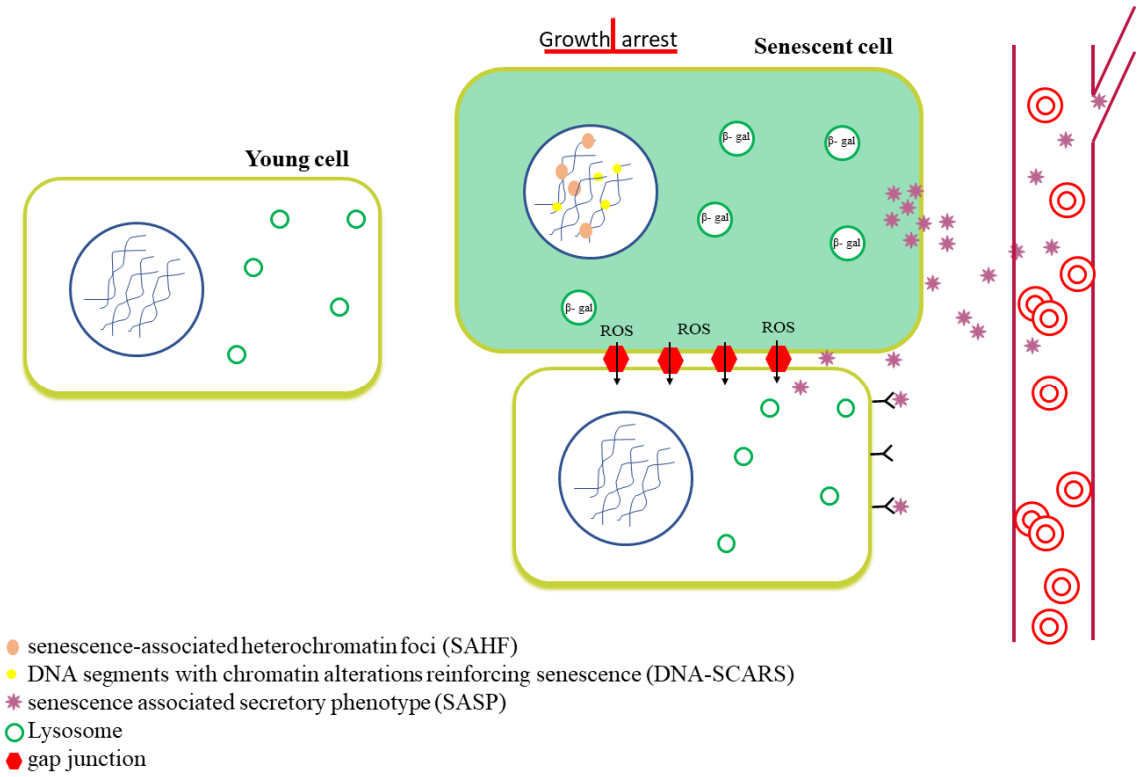

Figure 1.3. Senescent cell phenotype relative to young cell phenotype. Senescent cells secrete SASP to their microenvironment or the circulation which influences neighboring and distant cells. Excess ROS from senescent cells also enter neighboring cells through gap junctions.

This secretory phenotype occurs due to activation of NF-κB mainly by interleukin 1 alpha (IL-1α) pathway stimulation soon after cell-cycle arrest (Orjalo et al., 2009). DDR and mTOR activate NF-κB by translation of IL-1α and MAPK-Activated Protein Kinase 2 (Laberge et al., 2015). Coinciding with this, p38 in the senescence signaling pathway orchestrates SASP by directly activating NF-κB (Lujambio, 2016). NF-κB downstream molecules (IL-1α in particular) generate a low-level chronic inflammation which has systemic effects (Kuilman et al., 2010). While NF-κB and IL-1α have a positive feedback loop, NF-κB increases expression of miR-146 a/b which transcriptionally downregulates NF-κB expression (negative feedback mechanism) (Bhaumik et

al., 2009). Senescent cells are thought to use these miRNAs as a control mechanism to prevent extremely high expression of SASP factors.

Aside from stimulating the expression of surface bound molecules that flag senescent cells, SASP factors send signals to stimulate immune cell recruitment (macrophages, neutrophils and natural killer cells) that clear senescent cells (Sagiv and Krizhanovsky, 2013). Senescent cell clearance is important for the beneficial outcomes of this pathway and prevention of disease. For example, functional macrophages and natural killer cells suppress liver tumor formation and fibrosis via senescent cell resolution (Sagiv et al., 2013). However, SASP is a double-edged sword that helps tissue repair and removes senescent cells but also induces chronic inflammation which damages surrounding cells via oxidants produced by inflammatory cells and disturbs tissue function to eventually promote most of age associated diseases (Chung et al., 2009). In addition, SASP factors alter the tissue microenvironment by loosening epithelial cell adhesion to basement membrane (Matrix metalloproteinase (MMP)-2 and -3, IL-8) and promoting endothelial cell migration (vascular endothelial growth factor (VEGF) secretion and chemokine gradients); hence changing cells toward a malignant metastatic phenotype (Krtolica, et al., 2001; Coppé et al., 2010). SASP factors such as IL-6 or tissue inhibitor of metalloproteinase-1 (TIMP-1) counteract senescent cell removal by shielding tumor cells from being targeted for removal (Gilbert and Hemann, 2010). Therefore, senescence has polytrophic effects as in young individuals it plays a tumor suppressor role to improve tissue regeneration and repair, but in older individuals cellular senescence contributes to aging and tumor progression (Campisi, 2005; Campisi, 2013).

By affecting on neighboring cells or even distant cells, SASP propagate senescence phenotype in those cells. Nelson and colleagues showed that ROS enter to neighboring cells via gap junctions, which induce senescence in bystander cells (Figure 1.3; Nelson, 2012). Senescent cells can affect

physiology of other cells or organs distant from senescent tissue by producing and secreting different cytokines or miRNA into blood that can travel far from the tissue (Grillari and Grillari-Voglauer, 2010). Heterochronic parabiosis studies in which the circulation system of animals with different age are surgically connected confirmed this distant effect of senescent cells as aged mice in these studies showed phenotype of mice with younger chronological age due to the change in levels of factors in circulation system like Growth Differentiating Factor 11 (GDF-11) and C-C motif chemokine 11. In this model, the aged mice were showing enhanced regenerative potency for satellite cells and hepatocytes (Conboy et al., 2005; Laviano, 2014).

1.1.2 Cardiac aging

Most morphometric and functional changes in aged hearts result from changes in aorta and large vessels compliance, as progressive calcium/collagen deposition and loss of elastic fibers, increase the systolic blood pressure and decrease diastolic blood pressure (Vaitkevicius et al., 1993). Subsequently, left ventricular afterload and wall thickness (due to cardiomyocyte hypertrophy) increase influencing the shape of left ventricle making it more spherical shape, while cavity size remains unchanged (Hees et al., 2002). While 25% of a young adult heart is composed of cardiomyocytes, some of these cells are lost with age and given that cardiomyocyte renewal is very low instead of replacement with new cardiomyocytes older cells hypertrophy in compensation. Apoptosis increases with age and, curiously, is greater in males; suggesting a responsiveness to hormones and environmental changes (Olivetti et al., 1995). Mechanistically, murine heterochronic parabiosis studies have shown that these effects may be partially explained by loss of circulating GDF-11 as GDF-11 within young mice circulation leads to regression of age-related cardiomyocyte hypertrophy (Loffredo et al., 2013). Increased age is also associated with

remodeling of the extra-cellular matrix as deposition of collagen, fibronectin and amyloid increases. As such, aged hearts become more fibrotic and less compliant (Burgess et al., 2001).

In addition to cardiomyocytes, macrophages represent another significant population within heart as these cells are resident and maintained in the heart tissue since the embryonic state. Macrophages are spindle shaped cells and are found in close proximity to cardiomyocytes, endothelial cells and fibroblasts. Resident macrophages play important roles in clearing senescent cells, defending against infection, accelerating myocyte repolarization and facilitating electrical conduction from atrioventricular node via gap junction to cardiomyocytes (Ma et al., 2018; Hulsmans et al., 2017). The phenotype and markers of these cells resemble classic anti-inflammatory "M2 macrophages" (Pinto et al., 2012). With age, the number of cardiac resident macrophages decreases and instead more monocytes from the circulation infiltrate into cardiac tissue (Molawi et al., 2014). Influenced by the increased production of SASP factors during cardiac aging, these monocytes differentiate into macrophages that are polarized toward an inflammatory "M1 phenotype"; thus, shifting the phenotypic make-up within the heart (Chiao, 2011; Ma et al., 2015). As aging progresses, macrophages show diminished response to activating signals and impaired ability in phagocytosis of senescent cells (Ding et al., 1994).

Finally, fibroblasts compose almost 70% of the cells within the heart and actively participate in adaptations to advancing age. Given that fibroblasts participate in the ongoing turn over of the cardiac extracellular matrix (deposition of collagen and secretion of MMPs which degrade extracellular matrix), this response increases with age in steady state heart (Meschiari et al., 2017). After cardiac injury (such as a myocardial infarction), aged senescent fibroblasts with increased p53 expression accumulate in the heart. These cells are unable to produce critical collagen which is urgently needed to maintain cardiac function after injury and, in part, accounts for the increase

in early myocardial rupture seen in elderly patients after large myocardial infarctions (Horn et al., 2012; Zhu et al., 2013).

1.1.3 Cardiomyocyte aging

The cardiac aging phenotype in the heart arise from cells losing functionality due to senescence. Senescent cells show disturbed expression of cell molecules that has role in cardiomyocyte contractile dysfunction and myocyte death (Boon et al., 2013). Cardiomyocytes lose contractile function through altered expression of contractile proteins, disorganized sarcomere arrays and malignant calcium handling (Lakatta, 1990). Cardiac cells are highly metabolic; therefore, susceptibility to senesce is linked with mitochondrial function. During oxidative phosphorylation, ROS forms as a by-product of the mitochondrial electron transport chain. Increased exposure to relatively high ROS levels in cardiac cells harm mitochondrial and genomic DNA initiating senescence (Dai and Rabinovitch, 2009; Balaban et al., 2005). For example, the number of cardiomyocytes with defective mitochondrial cytochrome C subunits accelerate with age resulting in defective electron transport chain reaction that brings about formation of further abnormal proteins (Muller-Hocker, 1989). Reducing ROS stress through catalase over-expression or modulation of p66shc which are critical for ROS handling, decrease age-related effects on heart function and improve longevity (Zhang et al., 2003; Gertz and Steegborn, 2010). Nutrition sensing pathways are also critical in cardiac aging. Mammalian target of rapamycin complex 1 (mTORC1), which acts as a sensor for nutrients, stress and cellular growth, responds to several growth hormones such as angiotensin II, insulin growth factor-1 (IGF-1) or catecholamines. Over-stimulation of this molecule results in cardiac senescence. mTORC pathologies usually coincide with increased stress-induced protein synthesis and reduced protein degradation by autophagy (Domenighetti et al., 2005). mTOR suppression using inhibitors (rapamycin in appropriate doses)

or caloric restriction (through upregulation of autophagy and downregulation of ROS by sirtuins) improve cardiac inflammation, fibrosis and hypertrophy and prevent myocyte senescence or death (Siddiqi and Sussman, 2013; Alcendor et al., 2007; Sundaresan et al., 2009; Vakhrusheva et al., 2008).

1.2.1 Myocardial infarction

Myocardial ischemia occurs when the metabolic and oxygen demand of the heart is greater than the supply. When this condition is prolonged beyond a few minutes, it causes myocardial infarction whereby cells undergo necrosis and apoptosis. In most cases, ischemia is the consequence of a blockage in the coronary blood vessels that nourish the myocardium. Usually the rupture of atherosclerotic plaques and release of thrombogenic lipids activate platelets causing thrombosis and obstruction of blood flow that leads to ischemia. Atherosclerotic plaques narrow blood vessels and only very rarely result in downstream supply-demand imbalances causing ischemia at rest (Falk, 1982). However, when a fixed supply is not equal to demand, flow limiting lesions (i.e., greater or equal to 70% stenosis) may result in ischemia proportional to demand (ischemia with effort). Other conditions like embolism, coronary artery dissection, anemia and hypotension by decreasing the oxygen supply or exercise, cocaine use and thyrotoxicosis by increasing oxygen demand can also cause ischemia or even infarction. Myocardial infarction damages the heart muscles and decreases cardiac function (Frangogiannis, 2015).

1.2.2 Myocardial infarction risk factors

With medical advances, more people are living to an older age. Thus, more people also suffer from age-associated disease such as myocardial infarction. Myocardial infarction risk factors can be categorized as non-modifiable and modifiable risk factors. The recognized non-modifiable risk

factors are age, gender and genetic disorders. Within the modifiable risk factors, some of which are also controlled by genetic factors too, such as: dyslipidemia, hypertension, diabetes and obesity (Ounpuu et al., 2001). The comprehensive study of INTER-HEART identified 9 potentially modifiable risk factors among people of different ethnicity in 52 countries worldwide that significantly increase the incidence of myocardial infarction. These risk factors are cigarette smoking, raised ApoB/ApoA1 ratio, hypertension, abdominal obesity, diabetes, diet (vegetable and fruit consumption), physical activity, alcohol use, and psychological factors. Together these factors are responsible for a 94% of the population attributable risk in women and 90% in men which can be avoided to prevent myocardial infarction (Yusuf et al., 2004). In other studies, a relationship between the incidence of myocardial infarction (MI) and air pollution was identified (Colombo et al., 2014).

1.2.3 Myocardial infarction consequences

Thanks to the advancement of pharmaceutical therapies and development of cardiovascular intensive care units and reperfusion strategies, mortality after MI has dropped considerably during the last few decades (Levy et al., 2002). For example, anticoagulation and antiplatelet drugs decrease the prevalence of another thrombosis. However, these advances cannot repair damaged or lost myocardium. Depending on the severity of damage, survivors may develop heart failure as the infarcted area heals and heart remodel to compensate for lost myocardium. In cardiac remodelling, myocardium within the infarcted area is replaced by fibrotic tissue as a means of reducing wall tension and the prospect for cardiac rupture, fibroblast cells stretch, the ventricle dilates, and the heart gets a spherical shape at the apex (Pfeffer and Braunwald, 1990). During systole, this non-contractile area bulges and eventually assumes an aneurysmal shape. To compensate for the lost tissue, the healthy non-infarcted myocardium becomes thicker as

individual cardiomyocytes hypertrophy. This remote myocardium area also shows inflammation and fibrosis (Lee et al., 2012). The cardiomyocytes rearrangement in the border zone combines with extracellular matrix turn over to dilate the ventricular chamber and expand the infarct region (i.e., the scar) (Mukherjee et al., 2003). Because of these changes, systolic dysfunction develops, and the altered electrical coupling increases the chance for malignant cardiac arrhythmias (St John Sutton et al., 2003). In heart failure, the heart cannot pump blood efficiently to itself worsening the infarct (further necrosis and infarct extension) and to other vital organs such as kidneys causing their ischemic dysfunction (Cleland et al., 2005; Hutchins et al., 1978).

1.2.4 Cellular changes during ischemia

Lack of cardiac perfusion for short time period is tolerable for cardiomyocytes. If anoxia persists, the contractile function and energy expenditure of cardiomyocytes is reduced to prolong cell survival by reducing dependence upon high energy phosphate storage. Mitochondrial oxidative phosphorylation stops and instead the glycosylation pathway becomes the dominant source of energy. As glycosylation is relatively inefficient, energy production reduces and lactate content (by-product of glycosylation pathway) increases which results in acidosis (Elliott et al., 1992; Kubler et al.,1970). Accumulation of lactate through chemical equilibrium prevents further glycosylation, but increased acidosis leads to ion channel inhibition which electrophysiologically manifests in prolongation of the cardiac action potential duration (Coraboeuf et al., 1980). Maintaining the ion gradient is an energy-dependant process, so ischemia disturbs the electrophysiologic balance resulting in cardiomyocyte inexcitability and blockage of electrical conduction (Carmeliet, 1999). As an adoptive response, activation of autophagy pathways during ischemia provides cells with energy and may save cardiomyocytes from death (Matsui et al., 2007; Kanamori et al., 2011). Intriguingly, the key autophagy regulator, Sirt1, decreases with age and

may increase the risk of heart failure development (Sciarretta et al. 2011; Lee et al.,2008). Cessation of blood flow longer than 5-10 minutes can cause irreversible loss of cardiomyocytes with the extent of damage proportional to the area exposed to anoxia. Disturbed mitochondria and sarcolemma ultrastructures are early signs of this damage. Cardiomyocyte necrosis is evident few hours after ischemia (Jennings and Reimer, 1981). In ischemia, the main pathways leading to cardiomyocyte death are necrosis and, to a lesser extent, apoptosis (Gottlieb, 2011). In both pathways, mitochondrial dysfunction plays a major role (Ong et al., 2012). Ischemia activates apoptosis through increased permeability of the outer mitochondrial membrane by altering Bcl-2 family interactions. This leads to release of cytochrome C from the mitochondria into cytoplasm which activates the effectors of cell death, caspases. Necrosis is triggered when permeability transition pores in the inner mitochondrial membrane open and water influx into the mitochondrial matrix results in swelling and loss of electron transport chain integrity. While necrosis is the main death mechanism in cardiomyocytes after infarction, apoptotic cell death occurs more frequently after re-perfusion (Gottlieb et al., 1994; Gottlieb, 2011) through the generation of oxygen free radicals, microvasculature injury and alteration in calcium handling (Verma et al., 2002).

1.2.5 Myocardial healing after infarction

Myocardial infarction starts a cascade of events leading to replacement of millions of cardiomyocytes with a collagen-based scar that maintains structural integrity of the heart but fails to contract and maintain cardiac output. These events are categorized in three phases (Figure 1.4). The very first phase is inflammatory phase associated with infiltration of immune cells and clearance of dead cardiomyocytes. Simultaneously, MMPs degrade matrix within the damaged area. The proliferative phase soon follows in which anti-inflammatory mechanisms are activated, fibroblast cells proliferate in the damaged area and differentiate into myofibroblast that secrete

matrix proteins to remodel the lost extracellular matrix. The maturation phase then ensues whereby myofibroblasts undergo apoptosis or become quiescence and matrix cross-links to increase mechanical stability. Also, new blood vessels form (neo-angiogenesis) which feed fibroblasts and pro-healing macrophages within the infarct region (Frangogiannis, 2006; Frangogiannis, 2014).

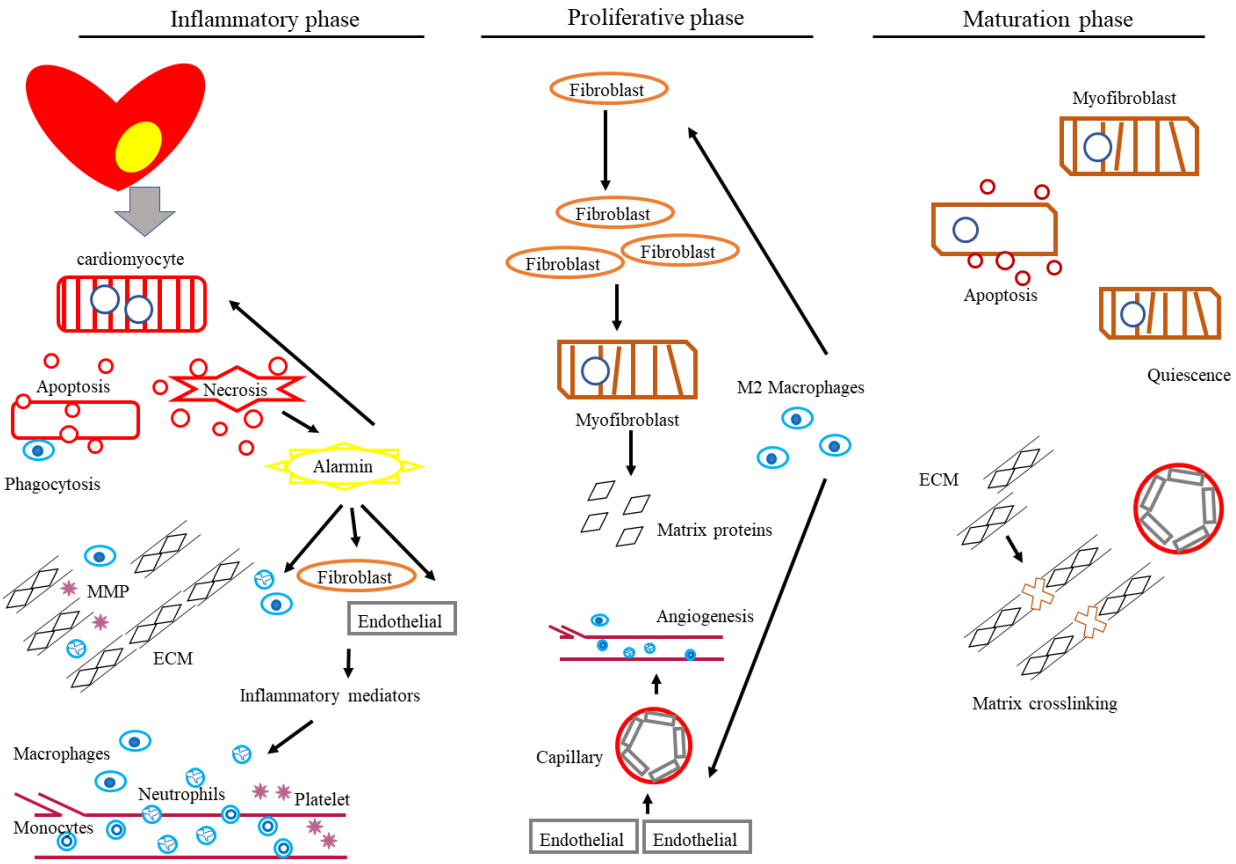

Figure 1.4. Phases of myocardial healing after infarction. The events are categorized in three phases: 1) Inflammatory phase in which cardiomyocytes die while immune cells infiltrate to clear dead cardiomyocytes and secrete MMPs which degrade matrix in the damaged area. 2) Proliferative phase in which anti-inflammatory mechanisms are activated and fibroblast cells proliferate within the damaged area to differentiate into myofibroblast that secrete new matrix proteins. Cytokines secreted from different cells promote endothelial cell differentiation and capillary formation. 3) Maturation phase characterized by apoptosis or quiescence of myofibroblasts and matrix cross-linkage.

The inflammatory phase starts with the death of cardiomyocytes. Necrotic cells in the damaged area of the heart release some factors called alarmins to signal fibroblast cells, endothelial cells, leukocytes and even surviving cardiomyocytes in infarct and border zone. High mobility group box 1 is the best known alarmin in myocardial infarction but other alarmins also participate in signaling (such as DNA fragments, heat shock proteins, IL-1α and matrix protein fragments). After receiving the signal of necrotic cells through appropriate receptors, in most cases Toll-Like Receptors or Receptors for Advanced Glycation End-products, activation of the NF-κB pathway in target cells results in secretion of inflammatory mediators. These chemoattractants recruit leukocytes to the site of injury to digest and eliminate dead cells and damaged molecules (Ghigo et al., 2014. Arslan et al., 2011). ROS stress and activation of complement system after MI also generate a chemoattracting signal for leucocytes (Hensley et al., 2000; Hill et al., 1971). Matrix degradation is another consequence of MI, happening early in the inflammatory phase. Soon after MI, both collagenase and MMPs activate to degrade matrix into fragments (Cannon ROIII., 1983; Etoh et al., 2001). This matrix replaces with a provisional matrix of fibrin base. Platelet aggregates contribute to formation of this provisional matrix that accommodates leukocytes and later fibroblasts and vascular cells (Dobaczewski, 2006). Platelet aggregation at the site of injury also promotes migration of reparative mesenchymal cells and infiltration of mononuclear cells (Frangogiannis, 2015).

During prolonged ischemic insults, resident macrophages also die. Circulating monocytes infiltrate into infarct very early after MI and differentiate into macrophages replacing lost resident cardiac macrophages (Heidt, 2014). These macrophages phagocytose both dead cardiomyocytes and apoptotic neutrophils. They also secrete a diverse array of cytokines, chemokines and MMPs associated with matrix degradation. As immune-modulators, they change the infarct environment

toward an anti-inflammatory or pro-healing setting by promoting fibroblast activation and growth, matrix remodeling and new vessel formation (Ben-Mordechai, 2015).

Clearance of the wound from dead cells is essential for activation of anti-inflammatory pathways. IL-1α has an inhibitory effect on the transition from inflammatory to the proliferative phase and continued expression of IL-1α ensues until all cell and matrix debris are removed (Shinde and Frangogiannis, 2014). At this point, most macrophages adopt an M2 anti-inflammatory phenotype secreting pro-angiogenic and pro-reparative factors (ter Horst et al., 2015). Resident fibroblast cells become proliferative and transdifferentiate into myofibroblasts which express smooth muscle actin. Non-resident fibroblast cells also migrate into the infarct area. These cells may be blood-derived fibroblasts or may have endothelial origin undergoing mesenchymal transition (Zeisberg et al., 2007). These cells produce matricellular proteins which incorporate into matrix and regulate signaling in fibroblasts, macrophages, and vascular cells (Frangogiannis, 2012; Shinde and Frangogiannis, 2014). One such matricellular protein with regulatory role is Thrombospondin-1 that conducts its reparative effect through activation of TGF-β and inhibition of MMPs (Frangogiannis et al., 2005). Pre-mature new vessels form to feed the myofibroblasts and macrophages. In the last phase of healing after MI, these vessels develop a pericyte coating (Ren et al., 2002). In the maturation phase, collagen matrix proteins cross-link to maintain cardiac structure and reinforce the infarct region. Matricellular protein production decreases and myofibroblasts undergo apoptosis or become dormant (Matsui et al., 2010; Frangogiannis, 2015).

1.2.6 Effects of age on endogenous responses to myocardial infarction

Age not only increases the risk of myocardial infarction, but it also fundamentally influences the outcome of myocardial infarction. Mice with advanced age develop greater infarct sizes and

ventricular chamber dimensions with reduced systolic function as compared to young individuals after MI (Bujak et al., 2008). Infiltration of leukocytes is greater in young rats rather than old rats after ischemia reperfusion injury. Aging also increases the number of cardiomyocytes with apoptotic factors (Liu et al., 2002). These findings are generalizable between different species and models as left coronary artery (LCA) ligation in aged mice results in greater activation of the caspase pathway and cardiomyocyte apoptosis as compared to younger mice (Boyle et al., 2013). Aging also alters the fibrotic response after myocardial infarction. Although aged hearts show excess deposition of extracellular matrix after MI, aged fibroblasts fail to form a mature scar increasing the risk of heart failure due to infarct expansion and maladaptive cardiac remodeling (Shih et al., 2010). The quantity and timing of cytokine release is also reduced and delayed, respectively, which alter the kinetics of scar formation in aged individuals. The delay in leukocytes infiltration to remove dead cells increases inflammation and damages surviving bystander myocytes in the area at risk (Bujak et al., 2008).

1.3.1 Cardiac regeneration

Studies on primitive species such as zebra fish have shown that adult fish can fully regenerate their hearts after major cardiac damage through direct proliferation of cardiomyocytes (Poss et al., 2002; Jopling et al., 2010). Mammals also possess this capacity as neonatal mice can fully regenerate their injured hearts through cardiomyocyte division and (possible) direct differentiation of resident stem cells (Jesty et al., 2012; Porrello et al., 2011; Porrello et al., 2013). However, this regenerative potential is lost soon after birth, which shows that the repair process is an age specific process rather than species-specific. For humans, it was at the turn of the century that some outstanding studies changed the dogma that human heart is a post-mitotic organ. Instead, the heart undergoes life-long repair through *de novo* differentiation of stem cells and by proliferation of existing

cardiomyocytes (Uygur and Lee, 2016; Kajstura et al., 1998; Beltrami et al., 2001; Bergmann et al., 2009). In normal myocardial homeostasis, new cardiomyocytes mainly form through division of pre-existing cardiomyocytes (Hsieh et al. 2007; Senyo et al. 2013). Whereas following cardiac injury, cardiomyocytes division increases and the generation of cardiomyocytes from other cells (possible pre-existing stem cells) becomes a contributor. However, this renewal rate is obviously insufficient for complete cardiac repair (Hsieh et al. 2007). Although the innate regeneration potential of the heart is inadequate to fully restore the lost tissue after injury and the identity of resident cardiac stem cells is controversial, the recognition that cardiac stem cells exist, opened the possibility of delivering exogenous cells and raised speculation that if cells are used with intrinsic capacity to differentiate into cardiac lineages these cells may be more effective than stem cells of non-cardiac origin.

1.3.2 Stem cells for cardiac dysfunction

The first type of stem cell proposed to replace the myocardium of the damaged heart was skeletal myoblast (SkM). These cells are abundant within skeletal muscle tissue and respond to injury by migrating to the site of injury and forming new working skeletal tissue. Early studies on skeletal myoblast transplant confirmed enhanced cardiac function by differentiation of myoblasts into working skeletal myocytes (Marelli et al., 1992, Murry et al., 1996). The promising results encouraged a rapid translation into clinical studies (Menasche et al., 2001) where they showed long-term engraftment of SkMs with persistent functional benefits (Hagege et al., 2003; Siminiak et al., 2004). However, the absence of gap junction in SkMs resulted in improper coupling with adjacent cardiomyocytes thus electronically isolating these cells and increasing chance of life-threatening arrhythmia (Fernandes et al. 2006). These findings raised caution toward clinical use of SkM cells. Ultimately, a pivotal doubled-blind randomized trial data put a halt to further

investigations due to prevalence of ventricular tachycardia and strong signal indicating failure to improve cardiac function (Menasche et al., 2008; Povsic et al., 2011)

The widespread use of bone marrow cells for hematological bone marrow replacement therapy propelled studies investigating the capacity of bone marrow cells to differentiate into cardiomyocyte and promote cardiac repair (Eisenberg et al., 2003). Early studies revealed that bone marrow mononuclear cells were incapable of trans-differentiation into cardiomyocytes, although they improved myocardial function after transplantation (Murry et al., 2004; Balsam et al., 2004). This realization led to the understanding that improvements in heart function occurred largely via indirect paracrine mechanisms that resulted in recruitment of endogenous cardiac stem cells, stimulation of angiogenesis and the prevention of cardiomyocyte apoptosis and fibrosis (Kocher et al., 2001; Fazel et al., 2006). Promising preclinical reports are driven by more than 50 clinical trials on bone marrow mononuclear cells treatment. While the outcome from these clinical trials are contradictory, a recent comprehensive systemic review showed no beneficial effect for bone marrow mononuclear cells treated patients immediate after acute ST elevation myocardial infarctions (Jeyaraman et al., 2017). Growing insight into the fundamental biology underlying hematological cells led to culture guided techniques or antigenic selection markers to derive several different types of cell products from haematological source (Davis and Stewart, 2014). These refined stem cell products were generated to improve paracrine signatures but were still incapable of true cardiomyocyte differentiation. Preclinical studies reported that intramyocardially injected mesenchymal stem cells differentiated into encapsulated structures with calcifications and ossifications (Yoon et al., 2004) and even formed tumors in some cases (Wolf et al., 2009; Jeong et al., 2011), raising caution upon using these cells due to ectopic differentiation into cell line of non-cardiac tissue or forming malignancy.

Embryonic and engineered induced pluripotent stem cells (iPS) are able to transdifferentiate to all different cell types in the body including cardiac lineages (He et al., 2003; Zhang et al., 2009). Autologous iPS are more advantageous compared to embryonic stem cells as they do not activate immune system with raising minimum ethical concerns. iPS cells have shown to have similar transdifferentiation capacity and regenerative potency as embryonic stem cells (Singla, 2011). However, both cell types are showing electrophysiological heterogeneity and premature ventricular depolarizations after injection into infarct heart particularly become noticeable after injection of cells into large animal models (Chong, 2014).

Overall, arrhythmogenicity or lack of ability to fully differentiate into cardiomyocyte may suggest that non-cardiac stem cells would not be the first choice to repair damaged heart tissue, and motivate the search for better alternatives.

1.3.3 Cardiac stem cells

Current research suggests a non-cardiomyocyte source within the heart tissue that plays a role in post infarct repair. Akin to myoblast properties of skeletal muscle tissue, a side population of cells was identified in digested heart tissue that could efflux Hoechst dye via Multi-Drug Resistant-1 pumps that were also negative for markers of cardiac identity and were able to adopt cardic lineages *in vitro* (Hierlihy et al., 2002). These cells were also found to express abcg-2 marker on their surface and were partly positive for other stem cell markers including c-Kit and Sca-1 (Martin et al., 2004). However, the physiological role of these cells has not been determined in any clinical trials (Hao et al., 2017).

Akin to hematopoietic stem phenotype, the c-Kit marker was actively investigated as a clue to stem cell identity within the heart. Concurrent with the identification of side population cells,

another research group detected c-Kit+/Lin− cells as a cluster of cells residing within myocardium. These cells were shown to be self-renewing, clonogenic and cardiomyogenic (Quaini et al., 2002; Beltrami et al., 2003). c-Kit cells were found to be comprised of two subpopulations that were proposed to be largely vasculogenic (KDR+) or cardiomyogenic (KDR-). However, lineage tracing methods suggested that adult c-Kit+ cells within the heart were only capable of differentiating into endothelial cells and their contribution towards the formation of new cardiomyocytes was negligible (Jesty et al., 2012; van Berlo et al., 2014; Sultana et al., 2015). Although formation of mature cardiomyocytes capable of electrical coupling has never been examined, antigenically selected and *ex vivo* expanded c-Kit+ cells entered phase I clinical trial (Bolli et al., 2011). The SCIPIO open-labelled trial confirmed the safety and efficacy of c-Kit+ cells and noted a 13.7% improvement in ejection fraction 1-year after intra-coronary injection (Chugh et al., 2012). However, the result from SCIPIO trial was viewed with skepticism after journal editors raised significant concern regarding integrity of the data (The Lancet Editors, 2014), and by early 2019 more than 10 papers from the discoverer of c-Kit cells were retracted from various journals.

There are further suggested cardiac stem cell markers including SSEA-1 and Isl-1 that are co-expressed with other proposed stem cells markers (Davis & Stewart, 2011) but to date, there is no consensus on any marker to detect authentic cardiac precursor cells. It is important to note that antigenic selection and further expansion of cells to achieve therapeutically relevant doses requires prolonged culture time (D'Amario et al., 2011), along with increasing cost and risk of phenotypic drift. Therefore, instead of using a single marker for which there is no consensus, other groups focused on obtaining heterogeneous population of cells from cardiac tissue. In this method, cardiac outgrowth or explant derived cells (EDCs) spontaneously emigrate from plated heart tissue to form

a monolayer of cells on the cultureware surrounding the plated tissue. Interestingly, the origin of these cells is not cardiomyocytes (Davis et al., 2010a) but has yet to be fully defined. EDCs are competent to fully differentiate into functional electrically coupled cardiomyocytes (Messina et al., 2004; Smith et al., 2007). Akin to the neurosphere technology, plating EDCs on poly-D-lysine coated plates was developed as a means of enriching the expression of stem cell markers. While loosely adherent cells aggregate together and form spheres, fibroblast-like cells adhere to plate surface. Within cardiospheres, cells expressing progenitor cell markers proliferate to form the body of the sphere (Messina et al., 2004). These cells express stem, endothelial, mesenchymal and cardiomyocyte differentiation markers (Davis et al., 2009) that may enhance the cardioprotective effect of monolayer EDCs (Li et al., 2010a). As intracoronary administration of these cell balls theoretically confers a high probability of micro-infarction due to their size (70–100μm), administration is limited to intramyocardial injection (Latham and Davis, 2014). To accommodate intracoronary injection of cells, cell monolayers (termed cardiosphere derived stem cells; CDCs) were generated by transferring cardiospheres to a fibronectin coated plate for *in vitro* disaggregation and expansion. The phenotype analysis of CDCs demonstrated a combination of cells with endothelial and mesenchymal origin similar to cardiospheres. Both porcine and human CDCs form mature cardiomyocytes expressing connexin proteins that are able to couple electrically with surrounding cells to conduct spontaneous calcium transients and generate spontaneous action potential (Smith et al., 2007). Pre-clinical studies in large animal models assured the non-arrhythmogenesis property of CDCs (Johnston et al., 2009; Lee et al., 2011). A head to head comparison of CDCs to non-cardiac originated cells or antigenically selected c-Kit+ cells of cardiac origin, revealed greater paracrine secretory properties for CDCs and superior functional benefit after injection into infarcted heart (Li et al., 2012). This promising pre-clinical

data prompted the phase I CADUCEUS trial that reported improvement in viable tissue and decrease in scar size of ischemic heart with no increased incident of arrhythmia (Makkar et al., 2012; Malliaras et al., 2014b). Davis and colleagues refined the CDC culture protocol by shortening the culture time. They showed that the cardiosphere step in CDC generation is unnecessary as the EDCs have equal capacity to improve myocardial function as CDCs, with greater potential for cardiomyogenic differentiation. This technique improved the cell yield collected in shorter period of time that is important for clinical application (Davis et al., 2010a).

Cardiac explant derived cells are primary products in CDC generation process. Like CDCs, these cells are CD105+/CD45- cells of intrinsic cardiac origin that expand through entry into an endothelial to mesenchymal transition (Zakharova et al., 2012). EDCs express markers of mesenchymal (CD90), endothelial (CD31 and CD34) and cardiac (abcg2, SSEA-1) progenitors while they are negative for hematopoietic lineages (CD45) (Davis et al., 2009). EDCs can also be cultured from cryopreserved tissue with no change in their characteristic which facilitates the transportation and processing of tissue biopsies (Jackson et al., 2017). Unpublished data from our lab confirmed GMP compatibility of this method while showed no evidence for teratogenicity. EDCs are capable of genuinely differentiating into cardiac lineages (Davis et al., 2010a) and improving post ischemic heart function (Latham et al., 2013; Molgat et al., 2014). Akin to their progeny CDCs, EDCs are capable of electrically coupling with surrounding cardiomyocytes as they are expressing connexin 43 (Davis et al., 2010a).

Although promising, not all patients are capable of achieving maximal benefit from stem cell therapy. Several factors are involved in defining the ability of EDCs to impart therapeutic benefits; factors including age, gender, diabetes and congenital heart failure are elements that influence the regenerative capacity of EDCs (Mayfield et al., 2016). All these factors combined, were reported

as long-term stratification score (LTS). The higher this score is, the more susceptible patients are for repeat myocardial events. When the regenerative potency of EDCs derived from human patients were correlated with their LTS score, Mayfield et al showed that the EDCs sourced from patients with higher LTS score had a reduced ability to induce angiogenesis and cell migration. The secretion profile of these patient also changed showing fewer exosomes, reduced stromal cell-derived factor 1 alpha (SDF-1α) production and greater IL-6 production (Mayfield et al., 2016).

1.3.4 Stem cell aging

As outlined above, the manifestations of aging has been partially attributed to stem cell aging. Healthy stem cells renew themselves through symmetric division that gives rise to identical daughter cells or asymmetric division which gives rise to an identical daughter cell and a differentiated cell (Sharpless and DePinho, 2007). Aged stem cells lose their capacity for self-renewal or differentiation; thus, fail to replace senescent cells within organs. Reduced proliferation capacity of stem cells has been related to a decline in the number of newly generated neurons (Kuhn et al.,1996), or endothelial progenitor cells (EPCs) (Jie, 2009). Even if aged stem cells do not decrease in number, they may display compromised function, reduced ability to differentiate into descendant cell or impaired responsiveness to stimuli. For example, the EPCs response to migratory stimuli reduces with age (Heiss et al., 2005), as does the c-Kit cells' ability to translocate within the heart. Also, increased age corresponds to increased mortality in bone marrow cells transplanted from aged donors (Kollman et al. 2001).

Aging of stem cells shares similar initiators as differentiated cells which involves tumour suppressor pathways. In stem cells, high duplication number shortens telomeres and induces senescence (Sharpless and DePinho, 2007). The impact of tumour suppressor pathways is marked

as p21 knockout prevents senescence in transgenic telomere dysfunctional mice which improves stem cell function in various organs and increases longevity (Choudhury et al., 2007). Within the heart, increased age leads to shorter telomere length, increased senescent marker expression and reduced differentiation capacity within c-Kit+ cells (Anversa et al., 2006). Moreover, with age unrepaired DNA damage accumulates and induces replicative senescence. Oxidative and oncogenic stress are involved in stem cell senescence, as well. Under physiologic conditions, resident stem cells are kept in dormant state and resided within hypoxic stem cell niches (Cheung and Rando, 2013; Sanada et al., 2014). This dormant state is accompanied by slower metabolism rate and low ROS production but exposure to DNA damaging factors may increase ROS stress leading to irreversible growth arrest (Rossi et al., 2005). As a proof of concept, activation of PI3K, the negative regulator of FoxO induces ROS formation so depletes stem cells (Paik et al., 2009; Tothova and Gilliland, 2007). Likewise, mTOR pathway activation in hematopoietic stem cells leads to increased ROS to impair stem cell mobilization and function (Gan et al., 2008). Mitochondrial function also plays an important role in stem cell senescence as mice with dysfunctional mitochondrial DNA polymerase have an increased burden of mitochondrial DNA mutations leading to compromised hematopoietic stem cell (Chen et al., 2009). Stem cells communicate with their surroundings, thus, environmental stress factors and negative signaling from niche deteriorate stem cell function. For instance, any change that results in increased oxygen level within stem cell hypoxic niches leads to stem cell activation and possible exhaustion. Similarly, SASP factors secreted by senescent neighboring cells into microenvironment may promote stem cell apoptosis or senescence (Siddiqi and Sussman, 2013).

The effects of aging have been evaluated in cardiac stem cells. As there is no consensus on characteristics of authentic cardiac stem cells, studies have been conducted on various cells with

different markers. Advanced donor age increased expression of p53 and p21 in CDCs while no significant effect was detected on expression of cytokines, senescence markers, proliferation rate and DNA damage markers (Nakamura et al., 2016). However, CDCs derived from congenital heart failure patients in adulthood or at neonatal stage showed a reduced capacity to adopt marker indicative of a cardiac lineage with advanced age (Mishra et al., 2011). These neonatal cells also had higher expression of FLK-1 and a broader cytokine profile. After injection into a rat infarct model, neonatal derived CDCs provided superior benefit in terms of heart function, scar size and new vessel formation (Simpson et al., 2012). Antigenically selected c-Kit+ cells from healthy donor hearts for transplantation and unhealthy explant hearts demonstrated a change in all age-related factors including p53, p21 and p16 levels, telomere length, telomerase activity and telomere induced foci. Relating chronological age with each age-related factor showed that p16 level and telomere induced foci change by age but chronological age does not significantly change the telomere length, telomerase activity and p21 levels (Cesselli et al., 2011). In a mouse model, aging reduced CDC yield (Hsiao, 2014) and lessened the ability of antigenically selected Sca-1+ CD31− cells for proliferation and differentiation (Wu, 2017).

1.3.5 Stem cell and myocardial infarction

As outlined, cardiac stem cells are not sufficient to fully restore myocardial function after a damage like ischemia, which causes the loss of a tremendous number of myocytes. Angiogenesis decreases after MI because aged hearts possess less pro-angiogenic cytokines, such as Platelet Derived Growth Factor impairing stem cell response (Edelberg et al., 2002). The data from c-Kit+ cells (which contribute largely to formation of endothelial cells) has shown that myocardial infarction promotes recruitment and proliferation of these stem cells within both injured and viable myocardium. While cardiac lineage commitment and mitosis increase, many c-Kit+ cells also

express greater amounts of p16 or p53 markers as compared to cells isolated from the non-infarcted heart (Urbanek et al., 2005). *In vitro*, healthy donor heart c-Kit+ cells were noted to be more clonogenic, more proliferative and less prone to senesce. Unsurprisingly, senescence related factors (such as p21, p16, telomere length attrition, reduced telomerase activity and p53) were lower in healthy c-Kit+ cells as compared to c-Kit+ cells cultured from explant hearts at end stage heart failure (Cesselli et al., 2011). In contrast, a study using CDCs derived from end stage heart failure patients showed that a history of chronic heart failure increased the regeneration potential of these cells- presumably related to increased production of SDF-1α. In their study, they also showed that CDCs from patients with acute MI had similar regenerative potency relative to CDCs from healthy donor hearts and they were secreting equal amount of SDF-1α (Cheng et al., 2014).

1.4 Refining cardiac stem cells

There are two principle mechanisms proposed to account for the benefit conferred by stem cell therapy. Specific to CDCs, direct differentiation was considered as an important mechanism of action. Transplanted human CDCs engraft and differentiate into cardiac lineages (Smith et al., 2007) to contribute into working myocardium (Davis et al., 2010b). Quantification of newly formed cardiomyocytes and endothelial cells combined with human specific antigen staining, however, revealed that a large number of newly formed cells originate from the host rather than cell donor thus indicating that the mechanism of benefit is not limited to direct differentiation alone. Paracrine mechanism was proposed as an indirect mechanism for formation or preservation of host originated cells (Chimenti et al., 2010). Paracrine stimulation conveys its effect through many different pathways including: activation of native cardiac stem cells to migrate and differentiate at the site of injury (Segers et al., 2007) into working myocytes (Malliaras et al., 2014a) or to promote endogenous vasculogenesis and angiogenesis to improve blood flow at the

ischemic site (Chimenti et al., 2010; Latham et al., 2013), promoting cardiomyocyte cell cycle re-entry to increase viable tissue (Malliaras et al., 2013), reducing inflammation and death signaling resultant of ischemia, reducing fibrosis and improving remodeling via TGF-β inhibition (Tseliou et al., 2014), and modulating the immune response by controlling macrophage polarization to a distinct cardioprotective subtype (not the classical M1/M2) (de Couto et al., 2015). CDCs also secrete extracellular vesicles that are carrying pro-survival molecules (such as miRNA-146-a) to reduce ROS and preserve cardiomyocytes by attenuating cardiomyocyte apoptosis (Barile et al., 2014; Ibrahim et al., 2014). In addition to protective miRNAs, CDCs secrete extracellular vesicles containing distinct non-coding Y RNA fragments such as YF-1 which induces IL-10 secretion to protect cardiomyocytes toward oxidative stress (Cambier et al., 2017). Recognizing these mechanisms highlights opportunities to boost the salutary effects of cell transplantation.

It goes without saying that following ischemia, continued anoxia and nutrition deficiency, and lack of an efficient repair system make a desert-like environment in the site of injury (Matsui et al., 2010). Thus, any mechanism that helps with the survival of transplanted stem cells in ischemic heart microenvironment, would augment the therapeutic effect of stem cells. Moreover, the properties of cardiac stem cells for autologous therapy influence by patients' characteristics such as age, diabetes, obesity, ischemia and other medical co-morbidities (Mayfield et al., 2016). Strategies that would assist the stem cells to reach a higher potency for therapy should be applied to meet stem cell need based on their characteristics. Hence, next generation stem cells require specific modulation designed for each patient condition.

1.4.1 Genetic modification

One strategy to boost the stem cell effects is through modulation of signaling pathways by over-expressing (a) key salutary gene(s) to the cells. Although the cytokine profile of EDCs is important for their reparative effects, not all beneficial cytokines are robustly secreted by primary cultured cells. Given the importance of SDF-1α in the heart healing after infarction, this represents a logical candidate to focus attention. SDF-1α conveys its effects by chemoattracting bone marrow cells and circulating angiogenic cells. Targeted over-expression of SDF-1α within EDCs increased the ability of cells to adopt a cardiac phenotype and to withstand apoptosis which conferred greater functional improvement after myocardial infarction while reducing fibrosis (Tilokee et al., 2016). In another strategy, EDCs armed with the pro-survival molecule, IGF-1, enhanced survival and consequently engraftment of transplanted cells to protect cardiac tissue from further damage by reducing apoptosis (Jackson et al., 2015). Not all effects are conditional upon modifying solely the paracrine profile of transplanted cells as shown by targeted overexpression of the pro-survival transcript Pim-1 in slow growth senescent cardiac c-Kit+ cells to improve telomere length, mitochondrial function and proliferation. When injected into mice after myocardial infarction, these enhanced cells show better cell retention and myocardial function (Mohsin et al., 2012; Mohsin et al., 2013). Nucleostemin over-expression confers similar anti-aging effect on c-Kit+ cells (Hariharan et al. 2015).

Genetic modification has been used to combat the effect of disease modifiers on function as well. Of the different conditions that influence regenerative potency is diabetes which reduces the ability of EDCs to enhance heart function after myocardial infarction. This functional deterioration is associated with the accumulation of methylglyoxal from high glycolytic reaction rate and results in excessive oxidative stress (Rabbani et al., 2008). Elimination of methylglyoxal by over-

expressing the key de-toxification enzyme glyoxalase 1 in the diabetic EDCs successfully restores the salutary effects of EDC transplant after myocardial infarction and represents the prototypical example of designed therapy based on patient condition (Molgat et al. 2014).

1.4.2 Biomaterials

Akin to all cell types (Müller-Ehmsen et al., 2006), less than 5% of cardiac-derived cells engraft in the heart 3 weeks after injection (Terrovitis et al., 2009). Successful long-term engraftment is influenced by route of administration with highest retention seen after direct intramyocardial injection and lowest retention seen after intravenous injection. Clinically, the intracoronary route is the most practical means of delivery with reasonable retention after delivery by a procedure similar to balloon angioplasty (Bonios et al., 2011a). Cell retention is strongly influenced by cell death or complete wash out after injection. Minimizing cell death can be limited by addressing several steps used during stem cell mobilization for transplant including reducing detachment-induced cell death (anoikis) (Karoubi et al., 2009). Also, immediately after injection, cells confront hypoxia, nutrition deprivation and inflammatory clearance (Kanda and Davis, 2017). Besides genetic enhancements that improve survival, biomaterials can improve engraftment. Cocooning cells within protective capsules enriched with attachment proteins prevents anoikis and reduces wash out of these cells. Therefore, these cells exhibit improved secretion phenotype and persistence in the heart compared to non-encapsulated cells (Mayfield et al., 2014).

1.4.3 Other enhancement strategies

Simple changes in culture conditions have a marked impact on stem cells. Changing the oxygen level within cell culture incubators from 20% to a more physiologic 5% increases EDC yield and their ability to migrate while reduces cellular senescence (Li et al., 2011). Glucose free media

stimulate survival pathways in bone marrow mesenchymal stem cells by activating Sirt1 expression (Choudhery et al., 2012), and even a slight decrease in the pH of media can stimulate bone marrow c-Kit+ cells to increase expression of SDF-1α and its receptor CXCR4 (possibly enhancing the ability of cells to function within ischemic environments) (Cencioni et al., 2013). Targeted small molecules pre-conditioning is another option; however, pre-conditioning effects are usually transient. Statin, through modulation of pro-survival genes, has anti-senescent effects and improves vasculogenesis after transplantation (Zhu et al., 2004a; Assmus et al., 2003; Walter et al., 2002). Finally, providing complimentary paracrine stimulation by combining different supporting cells or stem cell sources represents another means of enhancing the functional properties of cell administration. Many studies have shown that combination of heart derived cells with other cell sources synergistically boosts cardiac function greater than monotherapy alone (Latham et al., 2013; Williams et al., 2013; Nguyen and Sussman, 2015).

1.5 Mybl2 (Myb-Like Protein 2)

As will be shown, molecular phenotyping of EDCs from ischemic old and young mice revealed differential expression of Mybl2 (Myb-Like Protein 2; B-MYB). Mybl2 is a potent transcription factor (TF) which regulates cell cycle, differentiation and epigenetic changes (Zhan et al., 2012). In human, MYBL2 gene is located on chromosome 20q13.1 and encodes a 700 amino acid protein (http://www.genecards.org/cgi-bin/carddisp.pl?gene=MYBL2) which shares homology with retroviral v-Myb oncogene (Musa et al., 2017). The Myb family of TFs are present in all vertebrates (Oh and Reddy,1999) and consists of 3 members (Mybl1, Mybl2 and Mybl3). Unlike the other members of Myb family that are expressed in specific tissues or developmental stages, Mybl2 is expressed in all proliferating cells and plays a vital role in cell cycle progression (Martinez and DiMaio, 2011), which explains the embryonic lethality of Mybl2 double knockout

mice due to abortive formation of the blastocyst inner cell mass (Tanaka et al., 1999). Mybl2 is highly expressed in embryonic and pluripotent stem cells sharing similar target genes with the key somatic reprogramming transcripts SOX, NANOG and OCT4. These target genes consequently regulate several of the epigenetic modifications needed for differentiation of stem cells and embryonic development (Zhan et al., 2012). In conjunction with MuvB (multi-vulval class B) and FoxM1 (Forkhead box protein M1) and E2F transcription factors, Mybl2 regulates the cell cycle transition through the G1/S and G2/M phases (Sadasivam and DeCaprio, 2013; Musa et al., 2017; Mowla et al., 2014). In this regard, a strong relationship has been detected between Mybl2 and the expression of 23 other genes implicated in DNA replication and cell cycle checkpoint control (Clarke et al., 2013). Although upregulation of Mybl2 has been observed in several cancers (Musa et al., 2017), Mybl2 has tumor suppressor properties through regulation of DNA replication and checkpoint control pathways genes, regulation of mitotic spindle function and maintenance of genome stability (Garcia and Frampton, 2006; Lorvellec, 2010; Yamauchi, 2008; Fung et al., 2002). Interestingly, Mybl2 expression below 20% of normal results in growth arrest but sub-haploinsufficiency dose-dependently induces myeloid malignancy. Greater than 60% of patients with myelodysplastic syndromes show Mybl2 levels less than half of normal cell expression (Heinrichs et al., 2013). One possible mechanism for low expression of Mybl2 is increased mir-29a expression that reduces Mybl2 level by degrading mRNA leading to acute myeloid leukemia in mice (Han et al., 2010). Mybl2 haploinsufficiency (gene knock out) in mice leads to a variety of myeloid disorders upon aging. Tellingly, transplant of Mybl2+/- bone marrow cells increases the generation of haematopoietic neoplasia when the cells go through the proliferative stress of transplantation, confirming the key role for Mybl2 in maintenance of genomic stability (Clarke et al., 2013). Mybl2's role in maintaining genome stability originates from its function in progression

of S and G2/M phases of cell cycle. Loss of Mybl2 increases double-strand breakage, replication fork defects, centrosome defects, unequal chromosome segregation and aneu/polyploidy (Tarasov et al., 2008; Lorvellec et al., 2010). Loss of Mybl2 also makes DNA more vulnerable to UV radiation effects on chromosomal fragmentation, end-to-end fusion and chromatid loss (Ahlbory et al., 2005; García and Frampton, 2006). In addition, Mybl2 forms a complex with clathrin and filamin and carries them to mitotic spindles. By helping to properly localize these filaments, Mybl2 stabilizes kinetochore fibres during mitosis and maintains genome integrity (Yamauchi et al., 2008).

1.5.1 The role of Mybl2 in regulation of the cell cycle

Mybl2 is known to have a major role regulating cell cycle progression while simultaneously being regulated by the cell cycle. Mybl2 is expressed at late G1/S phases and subsequently transcribes many of the genes that are required for G2/M phases (Joaquin and Watson, 2003). Hence, low levels of Mybl2 correspond with reduced expression of cell cycle and mitotic genes (Sadasivam et al., 2012; Zhan et al., 2012) and conditional Mybl2 inactivation leads to accumulation of stem cells at the S and G2/M phases of cell cycle (Baker et al., 2014).

When cells are at G_0 stage in the cell cycle, a group of proteins come together to form the DREAM complex (Figure 1.5 A). Immunoprecipitation revealed that this complex is composed of MuvB core, retinoblastoma-like proteins (p130 and p107), repressor E2Fs (E2F4 and E2F5) transcription factors and Dimerization partners (DP1, -2, -3) (Litovchick et al., 2007). This complex binds to its binding site in the promoter of several cell cycle re-entry genes and inhibits their expression to maintain cells in a quiescent state. One of these genes is Mybl2 whose transcription is repressed in G_0 (Sadasivam and DeCaprio, 2013). Mybl2 promoter has a binding site for MuvB named

Downstream Repression Site which is similar to the well-conserved cell Cycle genes Homology Region element on promoter of DREAM targets whose expression maximize at early (G1/S) or late (G2/M) phases (Figure 1.5 B; Catchpole et al., 2002; Muller and Engeland, 2010).

A

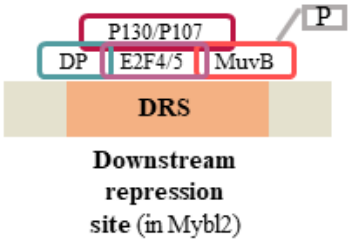

B

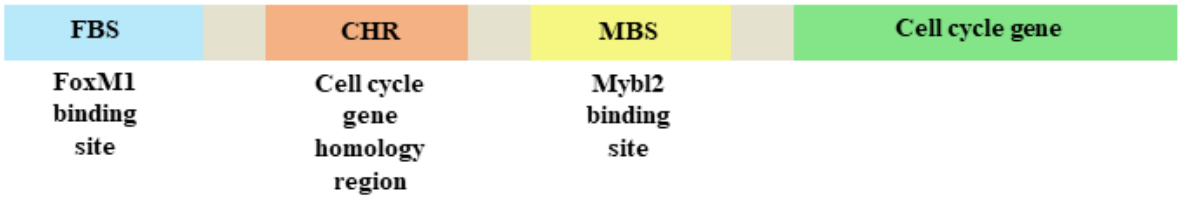

Figure 1.5. (A) Mybl2 promoter in G_0. The DREAM complex attaches to the Mybl2 promoter and inhibits its transcription. (B) Cell cycle gene's promoter. The promoter of cell cycle genes has binding site for DREAM complex, FoxM1 and Mybl2.

To exit quiescence or senescence states, MuvB is dephosphorylated at Serine 28 of the LIN52 subunit and its binding affinity to RB-like proteins weakens (Table 1; Litovchick et al., 2011). p130 or p107 dissociate from MuvB and repressor E2Fs, so the DREAM complex disengages from cell cycle re-entry promoters. Meanwhile, activator E2F1, E2F2 or E2F3 are recruited to trans-activate expression of genes important in DNA synthesis and the G1/S transition (Sadasivam and DeCaprio, 2013). Mybl2 transcription increases with peak expression at the S phase (Litovchick et al., 2007). Consequently, Mybl2 and MuvB increase binding to their binding sites on the promoter of G2/M effector genes such as *Cyclin B* and *Cdc2* (Zhu et al., 2004b). Table 1.1 shows

the chorological order of Mybl2 and related transcription factor activation in the cell cycle. During the S phase of cell cycle, Mybl2 expression increases and Mybl2 becomes activated through phosphorylation by Cyclin A-Cdk2, often in combination with acetylation by p300 co-activator (Lane et al., 1997; Sala et al., 1997; Schubert et al., 2004). This sequential activation results in a burst in expression of FoxM1 and other G2/M- specific gene transcripts. Despite being required for activation, phosphorylation of Mybl2 eventually promotes its ubiquitination and proteasome-mediated degradation (Charrasse et al., 2000) but prior to degradation, Mybl2 recruits FoxM1 (Down et al., 2012). FoxM1 become phosphorylated and activated by Plk1 at G2 phase (Fu et al., 2008) which together with MuvB express the late cell cycle genes (such as Cyclin B, surviving and Aurora B). Akin to the effects of phosphorylation on Mybl2, FoxM1 phosphorylation makes it more susceptible for ubiquitination and degradation which occur at the end of mitosis (Sadasivam and DeCaprio, 2013; Musa et al., 2017). Cyclin D-Cdk4/6 also phosphorylates FoxM1 which activates and stabilizes this TF to promote the expression of genes important in detoxification of ROS and DNA repair thereby reducing senescence (Anders et al., 2011; Khongkow et al., 2013). Finally, when cells enter G_0 or G1, nuclear receptor co-repressors interact with non-phosphorylated Mybl2 keeping Mybl2 inactive (Li and McDonnell, 2002).

Late G1 phase	- Loss of MuvB phosphorylation due to reduced DYRK1A-dependent phosphorylation - Dissociation of Retinoblastoma like proteins from MuvB and E2Fs - Replacement of repressor E2Fs with activator E2Fs -Transcription of Mybl2 - MuvB binding to Mybl2
S phase	- Phosphorylation of Mybl2 by Cyclin A/E-CDK2; Acetylation by p300 - Activation of ubiquitin mediated proteolysis - Expression of genes having role in G2/M phase of cell cycle (Cyclin B1, CDK1, Cyclin A2)
Late S/G2 Phase	- Recruitment of FoxM1 - Degradation of Mybl2 - Phosphorylation and activation of FoxM1
M phase	FoxM1 degradation

Table 1.1. Mybl2 and cell cycle: What happens upon entry into cell cycle?

1.5.2 Mybl2 role in senescence

Stressors induce senescence by consistent activation of tumor suppressor genes (p53 and pRB) to inhibit cyclin dependant kinases and repress the G1/S transition (Lowe and Sherr, 2003). Interestingly, all these molecules are linked to Mybl2 and the concentration of Mybl2 determines if a cell should stay in quiescent state, enter the cell cycle or become senescent. The role of Mybl2 in controlling senescence first became clear when it was observed that Mybl2 was reduced in p53 conditional expression cell lines. But, constitutive Mybl2 expression in these cells overrode senescence and bypassed G0/G1 cell cycle arrest (Lin et al., 1994). Mybl2 overexpression in

primary fibroblasts stimulates proliferation in low growth factor media (Sala and Calabretta, 1992) to forestall senescence (Huang et al., 2011) while conferring resistance to RAS induced premature senescence (Masselink et al., 2001). Conversely, MYBL2 downregulation induces senescence in both primary fibroblast cells and Hela cells (Johung et al.,2007).

Mybl2 is regulated at the transcriptional, post-transcriptional and post-translational levels (Martinez and DiMaio, 2011). Among tumor suppressors, RB is one of the most important regulators of Mybl2 at pre-transcriptional and post-translational levels. RB is active during both replicative and induced senescence. Within DREAM complex, RB like proteins (p130 and p107) either directly inhibit Mybl2 mRNA transcription by binding to the Mybl2 promoter or by competing with Mybl2 protein to bind to MuvB thus resulting in the detachment of Mybl2 from MuvB and a shift from the Mybl2-MuvB complex toward formation of DREAM complex which induces quiescence or senescence (Wells et al., 2000; Quaas et al., 2012). RB also indirectly regulates Mybl2 post-transcriptionally by controlling miRNA-29 and miRNA-30 levels that are known to bind to 3' untranslated region (UTR) of Mybl2 RNA to promote degradation (Martinez et al., 2011). Interestingly, the transition factor c-Myc is responsible for binding to miR-29 and miR-30 promoters to repress them. However, as an E2F target gene, c-Myc itself is repressed by RB during senescence (Chang et al., 2008; DeFilippis et al., 2003). In a positive feedback loop, miR-29 represses Cdc42 and stabilizes p53 which combine to promote apoptosis (Park et al., 2009). Other Mybl2 regulators (direct or indirect) include Cyclin D-Cdk 4/6, p16Ink4a, p53/p21, Cyclin A,-E Cdk2 (Rufini et al., 2013; Quaas et al., 2012; Mannefeld et al., 2009). As mentioned before, besides regulation at transcriptional levels, Mybl2 is regulated at post-translational levels by Cyclin A/Cdk2 phosphorylation, p300 acetylation and phosphorylation induced ubiquitination.

2. STUDY RATIONALE, AIMS & HYPOTHESES

2.1 Rationale

The prevalence of MI is greatest in elderly people and the literature shows that age is a predictor of stem cell weakened potency (Mayfield et al., 2016). Following the discovery of resident cardiac stem cells, a great number of studies have been conducted to characterize the behavior and function of these cells, however, most studies have largely focused on stem cells cultured from young animal models (Fransioli et al., 2008; Van der Bogt et al., 2008; Oh et al., 2003). To date there have been no studies characterizing the effect of age and/or ischemia on the regenerative performance of heart-derived cells. There are studies that have characterized the effect of age on patients suffering from congenital heart failure with possible other co-morbidities (Mishra et al., 2011; Simpson et al., 2012). Work by Cesselli et al. Cheng et al. had similar issues as they studied the effect of ischemia in end stage heart failure patients with variable risk factors including age or disease etiology (Cesselli et al., 2011; Cheng et al., 2014). Therefore, a need for differentiating the effect of aging and ischemia alone without the complexity of other co-morbidities is obvious. Knowing the underling mechanism behind the changes in aged cardiac stem cells and their response toward ischemia helps us with designing stem cells with restored function. Hence, we characterized stem cells from healthy aged hearts and aged hearts after ischemic injury (Figure 2.1). Although primarily focusing on the impact of aging, this is the first study to separate the effect of aging and ischemia on heart-derived stem cells. To this end, we selected a mouse model aged to an extent reminiscent to patients that may require cell therapy in the future (Figure 2.1). EDCs from old mice (12±1 months old) were *ex vivo* proliferated and compared with EDCs from traditional young mice (2 months old). The interaction between age and ischemia was probed by comparing cells from old mice 4 weeks after LCA ligation with cells cultured from aged matched

non-infarcted mice. The 4-week timeframe allows the heart to develop a mature scar to reflect clinical realities and enhance direct translation to the patient setting.

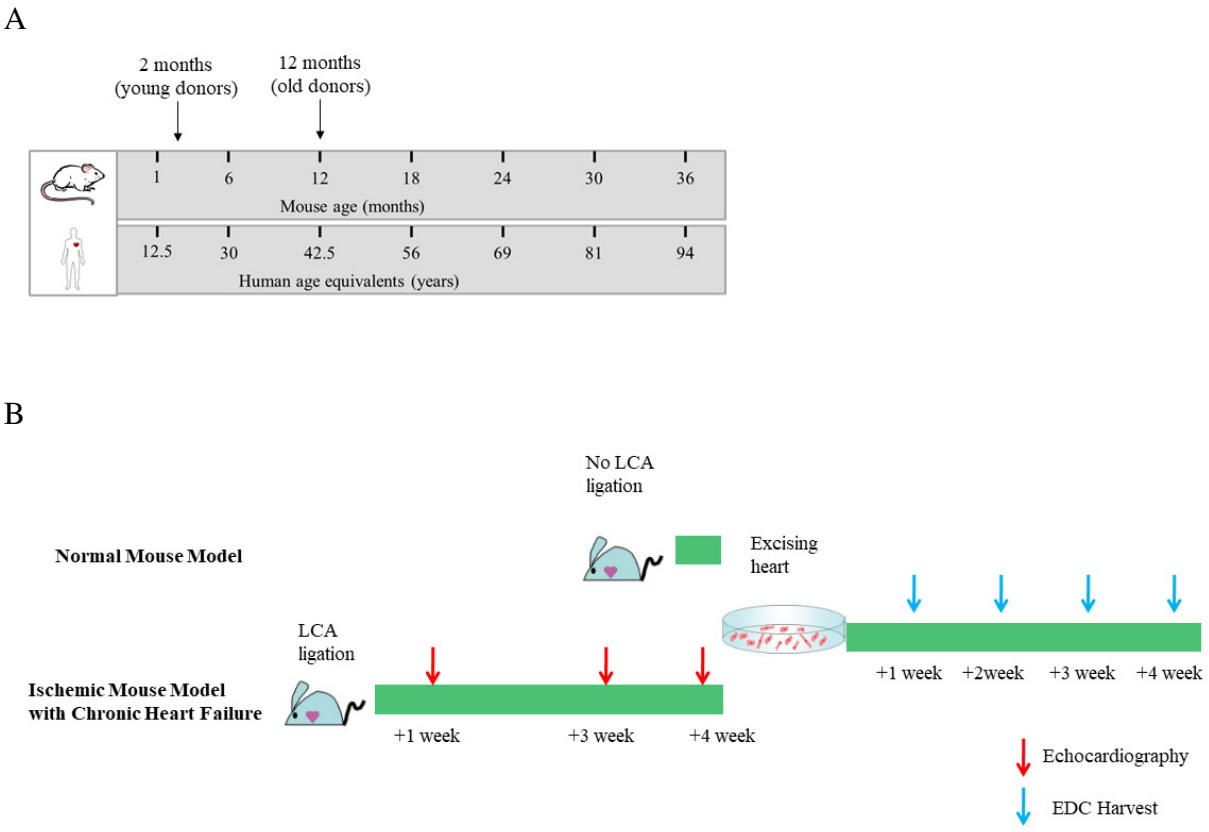

Figure 2.1. Mouse model. In this project (A) EDCs were derived from hearts of young and old mice. (B) Some of these mice were randomized to receive LCA ligation 4 weeks prior to tissue collection. The excised hearts were processed, and the EDCs were harvested serially.

After profiling the effects of age and ischemia on EDC function, this project then focused on measures to rejuvenate aged EDCs by targeting the specific molecular pathways that underlie age-related senescence. As outlined below, we performed unbiased microarray analysis on our experimental cohorts which revealed age and ischemia effects on pathways related to cell cycle control, checkpoints and DNA repair system. Among the genes that were expressed significantly less was Mybl2 which we chose to target based on its role in maintaining genome integrity and

resisting senescence (Mowla et al., 2014; Heinrichs et al., 2013). EDCs derived from old ischemic mice were genetically modified to over-express key transcription factor, Mybl2, to demonstrate if modulation of this TF will provide downstream benefits in cardiac repair. The results were compared to both backbone-transduced and non-transduced controls.

2.2 Research Aims

Aim 1: To determine the effect of age on EDC phenotype and cell-mediated repair after ischemic injury.

Aim 2: To determine the effect of remote ischemic injury on EDC phenotype and cell-mediated repair after ischemic injury.

Aim 3: To determine the effect of recipient age on the ability of EDCs to improve myocardial function after ischemic injury.

Aim 4: To evaluate the effect of Mybl2 overexpression on the ability of EDCs to improve myocardial function after ischemic injury.

2.3 Hypotheses

Hypothesis 1: Post-infarct functional improvements will be greater in mice treated with young EDCs as transplanted cell will be more resistant to apoptosis and less senescent.

Hypothesis 2: Post-infarct functional improvements will be greater after intra-myocardial injection of EDCs cultured from mice without a history of myocardial infarction as transplanted cells will be less senescent.

Hypothesis 3: Increased recipient age will decrease the salutary effects of cell transplantation on myocardial function after ischemic myocardial injury.

Hypothesis 4: Mybl2 overexpression will reduce cell senescence and will provide better cardiac function after transplant into a model of ischemic cardiac injury.

3. METHODS

3.1 Experimental animals.

Menopausal old (54 weeks) and young (8 weeks) female C57BL/6mice (Charles River) were handled in accordance with the Canadian Council on Animal Care Guide to the Care and Use of Experimental Animals under a protocol approved by the University of Ottawa Animal Care and Use Committee. Mice used to culture EDCs for experimentation were randomized to receive no intervention (n=94) or surgical ligation of the LCA (n=86) prior to eventual sacrifice and EDC cell culture.

3.1.1 Generation of chronic ischemic model.

Animals were injected with sustained-release buprenorphine (0.05 mg/kg; subcutaneous) and meloxicam (0.2 mg/kg) 1 hour prior to surgery. Meloxicam was then administered twice daily thereafter for 3 days. During surgery, mice were anesthetized with isoflurane (maintained at 2-3%), intubated and maintained under physiologic temperature control (37˚C). After opening the chest, the left coronary artery was visualized and ligated ~2 mm below the tip of the left atrial appendage (inducing ~40–50% ischemia of the left ventricle) with a 7–0 silk suture. Occlusion was confirmed by the anterior wall of the LV becoming pale and then the chest cavity was closed. Immediately after surgery, animals were placed in a 30˚C incubator with supplemental oxygen and moistened food to recover. Once animals recovered to a normal state, they were returned to their holding room. All animals were housed in Techniplast ventilated cages with at least bi-weekly cage changes and were given food and water ad libitum. The food was supplied by Envigo (irradiated #2019 extruded chow) and the water was autoclaved and prepared on site. The overhead lighting in the holding room was alternated every 12 hours between light and dark cycles. A

University of Ottawa Animal Care Technician monitored animals at least twice daily for 3 days post surgery and then at least once per day until the end of the study.

3.1.2 Evaluation of cardiac function using echocardiography

Mice underwent echocardiographic imaging 7, 21 and 28 days after LCA ligation. Transthoracic echocardiography was performed using a Vevo 770 system (VisualSonics Inc.). During the procedure, mice were anesthetized with 1-2 % isoflurane. The chest was prepped using a calcium and Sodium hydroxide solution to minimize ultrasound attenuation. After applying warmed Aquasonic 100 gel (Parker Laboratories), parasternal long-axis images were acquired. Chamber dimensions were quantified from the images at end systole and end diastole while left ventricular ejection fraction (LVEF) was calculated using following formula by Vevo software (EF (%)=100 × (end-diastolic volume- end-systolic volume)/end-diastolic volume; v3.0.0, VisualSonics Inc.).

3.2 Explant-derived cardiac stem cell culture

Four weeks after randomization, animals were sacrificed, and hearts were collected for EDC culture. Myocardial biopsies were minced to 1 mm^3 pieces, washed three times with cold Hank's Balanced Salt Solution (HBSS) containing 2% fetal bovine serum (FBS), 100 U/ml penicillin G, 100 µg/ml streptomycin and 2 mmol/l L-glutamine prior to enzymatic digestion (Collagenase IV; 1mg/mL) for 30 min at 37°C (all from Life Technologies). After digestion, the tissue fragments were washed three times with complete explant medium (CEM; Iscove's Modified Dulbeccos Medium (IMDM), 20% FBS, 100 U/ml penicillin G, 100 µg/ml streptomycin, 2 mmol/l L-glutamine and 0.1 mmol/L 2-Mercaptoethanol (all from Invitrogen) prior to plating on fibronectin (BD Biosciences) coated dishes at 37°C in 5% CO_2 (Davis et al. 2009; Davis et al. 2010a). EDCs that spontaneously emigrated from plated tissue were collected at 7-day intervals using mild

enzymatic digestion for direct experimentation. Five harvests from plated tissue were collected prior to discarding the used plates. To harvest cells, they were first washed with HBSS followed by incubation with TrypLE Select (Life Technologies) for 3 min at 37°C. Suspended/detached tissue was removed using a 100µm cell strainer (Fisher Scientific). For cryopreservation, EDCs were stored at -140ºC in freezing-medium (70% IMDM, 20%FBS, 10% dimethylsulfoxide (DMSO, Sigma)).

3.3 EDC cell count

The total number of harvested cells was counted with a Neubauer hemocytometer by averaging 4 squares. The collective number of cells from all harvests was totalled and normalized to heart weight measured right after excision.

3.4 Quantification of EDC proliferation

Cellular proliferation was examined by counting the number of cells at baseline (100,000 cells) and after 48h of culture in ambient (20% O_2) or hypoxic (1% O_2) conditions. Population doubling time was calculated as the difference between the time(t) and cell counts(N) of the starting population(1) and the final population (2) [Doubling time = (t2-t1)log2/(logN2-logN1)] (Sun et al., 2004).

3.5 Flow cytometry

EDC surface markers were profiled using flow cytometer (Guava easyCyte, Millipore) for c-Kit (Primary antibody: sc-168, Santa Cruz; Secondary antibody: A-11034, Invitrogen), CD34 (119309, Biolegend) and CD90 (A14726, Invitrogen) cell content. Briefly, 100,000 cells were fixed with 4% paraformaldehyde (Electron Microscopy Sciences). After washing with phosphate

buffered saline (PBS), the cells were labeled with fluorophore conjugated primary antibody or unconjugated primary antibody and secondary antibody for 30min at 4ºC. Non-stained EDCs and single stained EDCs were used as controls for gating. A minimum of 10,000 single cells events were collected. The percentage of positive cells was calculated by proprietary software (GuavaSoft Software, Millipore).

The capacity of EDCs to withstand programmed cell death was assessed after 48 hours exposure to hypoxic (1% oxygen) and low serum (1% serum) condition. Apoptosis was assessed by staining the cells with 7-Amino-Actinomycin D (7-AAD) and Annexin V-PE (559763, BD Biosciences) for 15 minutes at room temperature. Flow cytometry was used to quantify the percentage of early and late apoptotic EDCs.

3.6 Cardiogenic culture conditions

Two hundred thousand EDCs were seeded in 6-well plates and cultured for 24 hours in CEM media. The media was then replaced with cardiogenic media (60% DMEM (Dulbecco's Modified Eagle's Medium; Invitrogen), 40% MCDB-201 (Cellular, and Developmental Biology media; Sigma), 0.75% DMSO, 0.1% 10 mmol/l L-ascorbic acid (Sigma), 0.01% ITS liquid media supplement (Insulin-Transferrin-Selenium; Sigma), 0.01% linoleic acid-albumin (Sigma), 1% anti-anti (Gibco), 0.0002% 0.25 mmol/l dexamethasone (Sigma), 0.001% 2-mercaptoethanol (Gibco), 10 ng/ml recombinant mouse fibroblast growth factor 8b, 100 ng/ml fibroblast growth factor 4, 10 ng/ml recombinant human Dickkopf-related protein 1 and 10 ng/ml recombinant human bone morphogenetic protein 2 (all from PeproTech)). Media was changed every other day for 1 week.

3.6.1 Quantitative polymerase chain reaction (qPCR) evaluation of cardiac transcripts

After 7 days of culture in cardiogenic media, mRNA was extracted (RNeasy Micro Kit, Qiagen). Predesigned qPCR primers with FAM-labelled probes were used to quantify expression of α-SMA, cTnT and vWF with loading evaluated using GAPDH (Integrated DNA Technologies). Quantitative PCR was performed using LightCycler® 480 RNA Master Hydrolysis Probes (Roche). Samples were amplified for 35 cycles by LightCycler 480II (Roche). Cp values were used to determine the mRNA levels in relation to GAPDH.

3.6.2 Flow cytometry evaluation of cardiac markers

After 7 days of culture in cardiogenic media, cells were permeabilized with 0.2% Triton X-100 (Bio-Rad) and then blocked for 15min in 3% albumin (Sigma) and 3M Glycine (Bio-Rad). Once permeabilized, cells were stained for cardiomyocyte (Anti-Cardiac Troponin T-FITC, 130-106-687, Miltenyi Biotech), endothelial cell (anti von Willebrand Factor, ab9378, Abcam) or smooth muscle cell (anti alpha-smooth muscle actin, ab66133, Abcam) markers. The number of differentiated cells were quantified by flow cytometry.

3.7 Generation of conditioned media for angiogenesis, migration and paracrine profiling

Conditioned media was generated by culturing EDCs in hypoxia (1% O2) and low serum (1% serum) media (IMDM, 100 U/ml penicillin G, 100 ug/ml streptomycin, 2 mmol/l L-glutamine and 0.1 mmol/l 2-mercaptoethanol) for 48 hours to simulate the ischemic transplant environment.

3.7.1 Paracrine profiling of EDC conditioned media

Commercial enzyme-linked immunosorbent assays (ELISAs) were used to measure the abundance of cytokines known to be produced by EDCs: angiogenin (MBS160147, MyBiosource), angiopoietin-1 (MBS163055, MyBiosource), hepatocyte growth factor (HGF, MHG00,RD systems), interleukin-6 (IL-6, M6000B, RD systems) and VEGF (MMV00, RD systems) (Latham et al., 2013). Unbiased proteomic screening was used to evaluate the pro-angiogenic cytokines within EDC conditioned media using the Proteome Profiler Mouse Angiogenesis Array according to the manufacturer's instructions (ARY015, R&D Systems). We profiled the secretion of 53 angiogenic related cytokines. Conditioned media from mouse C57BL/6 primary dermal fibroblast (DF; cell biologics c57-6067) cells was used as negative control. Densitometry of dots was determined by ImageJ software (Protein Array Analyzer plugin, NIH) corrected to number of seeded cells. A second proteomic array of 111 mouse cytokines (Proteome Profiler Mouse XL Cytokine Array (ARY028, R&D Systems)) was used to evaluate the effect of Mybl2 lentiviral overexpression or transduction (backbone) on cytokine secretion within conditioned media. The signal intensity of dots was quantified using ImageJ (Protein Array Analyzer plugin, NIH) after normalization to the internal controls and the number of plated cells.

3.7.2 Angiogenesis assay

The *in vitro* potential of EDC conditioned media to induce angiogenesis was evaluated through tubule formation assay by exposing Human Umbilical Vein Endothelial Cells (HUVECs) plated within a cytokine-depleted matrigel (ECM625, Millipore) to conditioned media. HUVECs were purchased from Lonza and cultured on fibronectin coated dish in Endothelial Cell Growth Medium-2 with growth supplements (Catalog #: CC-3162; Lonza). Angiogenesis was performed

by seeding 10,000 HUVECs per well in triplicate on µ-Slide Angiogenesis (ibidi) filled with ECMatrix. Sixteen hours after incubating HUVECs within EDC conditioned media, the picture of whole well was taken using AxioVision microscope (Carl Zeiss Microscopy). Tubule length was measured in each well using ImageJ (NeuronJ plugin, NIH). To evaluate the influence of proliferin on angiogenesis, tubule formation assay was conducted after depleting proliferin by incubating conditioned media with goat anti-mouse proliferin antibody (sc-47347; Santa Cruz Biotechnology) or goat IgG isotype control (ab-37373, Abcam) at 4 °C for 2 h prior to magnetic separation using protein A/G magnetic beads (88802, Life Technologies) for 3 h at 4 °C (Yang X et al. 2012). Tubule length was calculated in each well using ImageJ (NeuronJ plugin, NIH).

3.7.3 Migration assay

The ability of EDCs to recruit circulating stem cells was evaluated by exposing bone marrow-derived cells (BMDCs) to a gradient of EDC conditioned media using a transwell plate (24 wells, 3.0 µm pores; Corning). BMDCs were isolated from C57BL/6 femurs and tibias prior to 7 days of culture (EGM-2 media, CC-2935; Lonza). Specifically, 1 x 10^5 BMDCs in 100 µl of serum-free IMDM were seeded in the upper well of the transwell while 600 µl of EDC-conditioned media was placed in the bottom well. Cells that successfully migrated through the polycarbonate membrane over 18 h of incubation were then fixed in 4% paraformaldehyde and stained with 4',6-diamidino-2-phenylindole (DAPI; Sigma-Aldrich). To evaluate the effect of IL-6 on migration, conditioned media was incubated with rat anti-mouse IL-6 antibody (16-70611-85; eBioscience) or rat IgG1 isotype control (400402, Biolegend) at 4 °C for 2 h and then incubated with 300 µl of anti-rat Dynabeads (11035, Life Technologies) for 3 h at 4 °C. Migration assay was performed using IL-6 depleted conditioned media followed by quantification of the total number of cells in six random fields of view.

3.8 Characterization of extra-cellular vesicles secreted by EDCs

Extra-cellular vesicles were collected from EDCs cultured in hypoxic (1% oxygen) and low serum (1% exosome depleted serum; System Bioscience) for 2 days. Conditioned media was centrifuged at 2000 x g for 10 minutes to remove cellular debris prior to centrifugation at 8000 rpm for 30 minutes to remove the large particles/vesicles (L8-70M, Beckman). The supernatant was then centrifuged at 28000 rpm for 3 hours to pellet extra-cellular vesicles (L8-70M, Beckman). The total vesicles pelleted from 6 ml of EDC conditioned media were resuspended in PBS for quantification and evaluation of the particles size distribution by NanoSight (LM10; Malvern Instruments).

3.9 Cellular senescence

β–galactosidase staining was used to evaluate senescence. Briefly, EDCs at 80–90% confluence were fixed and incubated overnight at 37ºC with SA-β-gal Detection Solution (KAA002, Millipore). After washing, blue stained cells were counted in 6 random fields of view under phase contrast microscope (Moticam Camera). The percentage of senescent cells was calculated by dividing the number of β –gal+ cells to the total number of cells.

3.10 Evaluation of telomere length and telomerase system

Telomere length and telomerase activity was evaluated in the c-Kit+ and c-Kit- sub-populations within EDCs after antigenic sorting (c-Kit, Sc-168, Santa Cruz; anti-rabbit IgG Dynabeads, 11203D, Life Technologies). Following magnetic separation, the c-Kit+ cells were retained on the tube wall by magnetic attraction (DynaMag-2, Invitrogen), while the c-kit- cells remained in the supernatant.

Genomic DNA was extracted (DNeasy kit, Qiagen) for qPCR. To perform quantitative PCR, 16ng of total DNA was added to each reaction well with 12µl of master mix (LightCycle 480 SYBR Green I Master, Roche) and the primers of interest. Two sets of forward and reverse primers were used, one to detect telomere repeats (telg, ACACTAAGGTTTGGGTTTGGGTTTGGGTTTGGGTTAGTGT and telc, TGTTAGGTATCC CTATCCCTATCCCTATCCCTATCCCTAACA) and another set to detect a single copy gene (albumin) (albu: CGGCGGCGGGCGGCGCGGGCTGGGCGGAAATGCTGCACAGAATCCTTG and albd: GCCCGGCCCGCCGCGCCCGTCCCGCCGGAAAAGCATGGTCGCCTGTT. Signal acquisition was read at 74ºC to provide the C_T values for the amplification of the telomere template and at 88ºC to provide the C_T values for the amplification of the single copy gene template (LightCycler 480II; Roche) using 40 cycles. A reference DNA extracted from cardiac tissue with different concentrations was used to generate standard curves for telomere repeats and Albumin. The level of telomere length and single copy gene (albumin) was calculated in each sample using the standard curves. The telomere and single copy gene (albumin) (T/S) ratio was calculated to estimate relative telomere length such that greater T/S ratio indicates longer telomeres while lower T/S ratio infers shorter telomeres (Cawthon, 2009).

Telomerase activity was quantified using qPCR detection of TTAGGG telomeric repeats according to the manufacturer's directions (MT3011, Allied Biotech Inc).

In brief, cells were lysed and, centrifuged at 12,000g for 30 minutes prior to incubation with proprietary solutions that permit telomerase addition of telomeric repeats (TTAGGG) onto the 3' end of the substrate oligonucleotide for qPCR quantification (45 cycles, LightCycler 480II; Roche).

3.11 Reactive Oxygen species content

Cell ROS content was quantified using fluorometric detection according to the manufacturer's directions (ab113851, Abcam). The ROS level was detected by formation of oxidized form of 2',7'–dichlorofluorescein (DCF) from 2',7'–dichlorofluorescin diacetate (DCFDA). The final product is highly fluorescent and is detectable under green fluorescent channel settings. In brief, 2',7-dichlorofluorescein diacetate (25mM) was added to EDC cell cultures and incubated for 45 minutes followed by direct quantification of fluorescent emission (529nm) in response to excitation at 495nm using plate reader (PowerWave HT Microplate Spectrophotometer, BioTek Instruments). The assay was performed with 2 technical repeats. EDC treatment with Tert-Butyl Hydrogen Peroxide (50μM) for 1 hour was used as positive control.

3.12 Antioxidant reserves evaluation

The activity of Super Oxide Dismutase (SOD) and Glutathione Peroxidase (GPx) that catalyze dismutation of superoxide free radicals to molecular oxygen and reduction of hydroperoxides, respectively, was evaluated. GPx activity within EDCs was measured using a colorimetric assay according to the manufacturer's directions (703102, Cayman Chemical). Briefly, 200,000 EDCs were collected and sonicated. The supernatant was collected and centrifuged (10,000g for 15 minutes) before addition of the co-substrate mixture. The assay was performed with 2 technical repeats and the reaction was initiates by addition of Cumene hydroperoxide. Change in light absorption at 340nm per minute corresponds to oxidation of $NADH+H^+$ was used to quantify GPx activity (PowerWave HT Microplate Spectrophotometer, BioTek Instruments).

SOD activity was measured using a colorimetric assay according to the manufacturer's directions (706002, Cayman Chemical). Briefly, the supernatant from sonicated EDCs was centrifuged

(1,500g for 5 minutes) prior to addition of radical detector. The assay was performed with 2 technical repeats and the reaction was started by adding Xanthine oxidase. Colorimetric absorption of formazan dye at 440 nm was used to quantify the total amount of superoxide produced by Xanthine oxidase. SOD dismutates the superoxide, and reduces the generation of superoxide and consequently the sample absorption at 440nm.

3.13 Microarray

Total RNA was extracted from EDCs according to the manufacturer's directions (RNeasy Mini Kit, Qiagen) prior to quantity/quality evaluation (NanoDrop 2000, Thermo Fisher Scientific; 2100-Bioanalyzer system, Agilent Technologies). The same RNA samples were used for subsequent qPCR validation. RNA was submitted to the StemCore microarray facility (OHRI) for hybridization to Affymetrix based GeneChip Mouse Gene 2.0 ST arrays (902119, Thermo Fisher Scientific). Signal intensities were normalized by applying robust multi-array averaging (RMA; Expression console software by Affymerix, Thermo Fisher Scientific) to use as an input for different analyzing software programs. Of the 45,101 probe sets screened, 26,788 probe sets were determined to be present. Expression data was analyzed using statistical analysis of microarray software (Array Star v12, DNASTAR), with a calculated median false discovery rate of =5%. Genes with 1.5-fold different expression rate were used for hierarchical clustering (Array Star v12, DNASTAR). Among these genes, those that were related to the senescence pathway or mitochondrial function were distinguished. Ingenuity Pathway Analysis, was used for pathway analysis (QIAGEN Bioinformatics). Some differentially expressed genes according to microarray data with 0 to 8-fold expression change between groups (ppp1r16b, Tnf, Cxcr4 and Rgs1) were arbitrarily chosen for subsequent microarray validation using qPCR (PrimeTime Predesigned qPCR probes, Integrated DNA Technologies).

3.14 Lentiviral vector production and transduction

3.14.1 Plasmid constructs

Commercial 3rd generation packaging plasmids i.e. RSV-REV, Rev Response Element (RRE) and VSV-G plasmid (addgene), 2nd generation packaging plasmids (LV003, abmgood), green fluorescent protein (GFP) expression vector (12154, addgene) and Mybl2 lentiviral vector (pLenti-GIII-CMV-GFP-2A-Puro; LV437429, ABM Inc.) were purchased. Also, custom made firefly luciferase reporter plasmid (pCDH-EF1-FLuc-IRES-Puro, Dr. Duncan Stewart lab gift) and custom-made Backbone control vector were used in this study.

3.14.2 Transformation

Mybl2 plasmid was received in the form of DNA. The plasmid was transformed into E-coli bacteria DH5-α strain (Life technologies) by heat shock method. Briefly, 1µl of plasmid was added to 50 µl of bacteria and the mixture was kept for 30 minutes on ice, 20 seconds at 42ºC and 2 minutes on ice. The transformed bacteria were grown in LB media for one hour at 37ºC followed by culture on LB agar gel containing Kanamycin (0.5mg/ml) to select for transformed bacterial colonies. Few colonies were picked, and their plasmid DNA was extracted by miniprep (QIAprep Spin Miniprep Kit). The DNA was digested by EcoRV restriction enzyme (NEB) for 1h at 37 ºC before loading on 1% agarose gel, to assure the presence of Mybl2 plasmid in bacterial colonies. The Mybl2 insert was detected at around 2k band of the ladder.

3.14.3 Viral packaging

To amplify plasmids, the transformed bacteria were grown in LB media overnight. The DNA was extracted from bacteria using maxiprep (PM025, Geneaid). Lentivirus was produced using HEK

293T cells in about 70% confluence after transfection with transfection reagent (Lipofectamine 2000, Thermo Fisher Scientific) packaging plasmids and plasmid containing gene of interest, with harvest 48 and 72 hours later followed by concentration (Lenti-X concentrator; Clontech) according to the manufacturer's instruction.

3.14.4 Virus titration and transduction

The virus titration was measured by qPCR of LV vector gene (IDT primer). Briefly, the HEK 293 cells (Clontech) were treated with 0.8 µg/ml polybrene (Sigma) for 10min prior to transduction by desired Lentivirus. Seventy-two hours after transduction, the HEK DNA was extracted (DNeasy kit, Qiagen) and the stably integrated lenti gene was quantified using a standard curve for plasmids containing the LV gene (Sastry et al., 2002). To transduce EDCs, cells were treated with 0.8 µg/ml polybrene for 10min before transduction with desired lentivirus. EDCs were then allowed to recover for at least 48 hours before further experimentation on them.

3.15.1 Mybl2 plasmid validation and Backbone plasmid generation

pLenti-GIII-CMV-GFP-2A-Puro (Figure 3.1A) was transformed into E-coli DH5 strain and cultured on LB agar. Successful transformation was confirmed by the presence of ≈2200 Mybl2 DNA fragment after plasmid DNA digestion by EcoR V and running it on agarose gel (Figure 3.1B). The HEK cells were then transfected by Mybl2 plasmid. The expression of GFP in HEK cells showed that the plasmid is functional (Figure 3.1C). Also, the qPCR for Mybl2 RNA in HEK cells showed increased Mybl2 transcript expression in transfected cells relative to non-transduced HEK cells (Data not shown). Mybl2 virus was produced using 2nd generation packaging plasmids. We used non-transduced EDCs sourced from old donors with a history of ischemia and EDCs transduced with Backbone lentivirus as controls. To generate a viral control for our experiment,

Mybl2 plasmid construct was digested by EcoRV restriction enzyme overnight. The product was loaded on agarose electrophoresis gel and the desired section (around 6Kbp, Figure 3.1B) containing the plasmid backbone without Mybl2 gene was cut using UV light and a scalpel. The agarose was melted, and the plasmid DNA was extracted according to manufacturer's protocol (DF100, Geneaid). Backbone plasmid was reconstructed by ligation of the two ends of plasmid DNA using T4 DNA ligase (NEB; 16 ℃ overnight) after excision of Mybl2 gene. The backbone plasmid was then transformed into DH5-α E-coli strain for further amplification and virus generation.

A

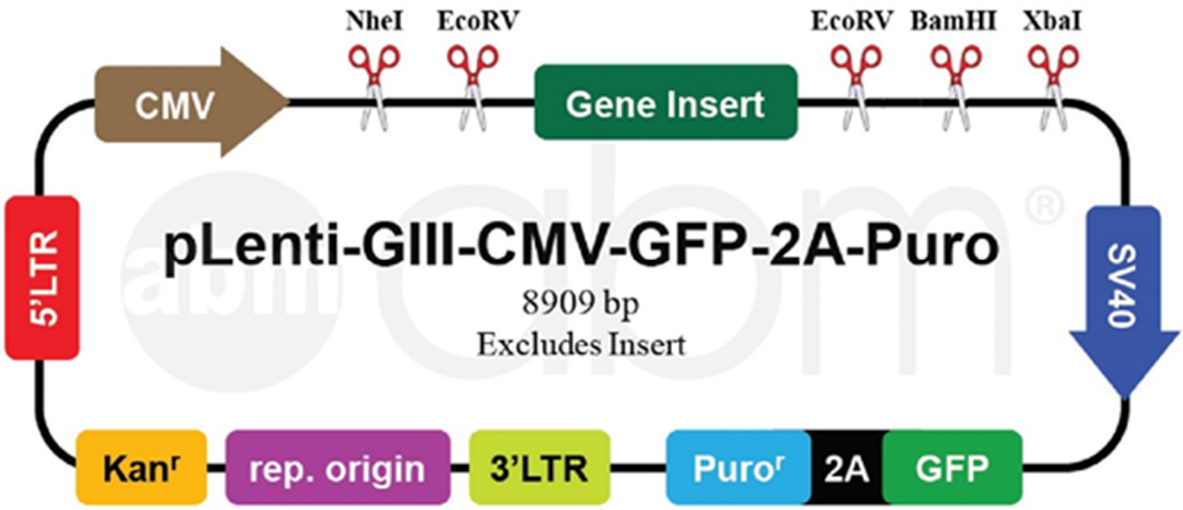

B

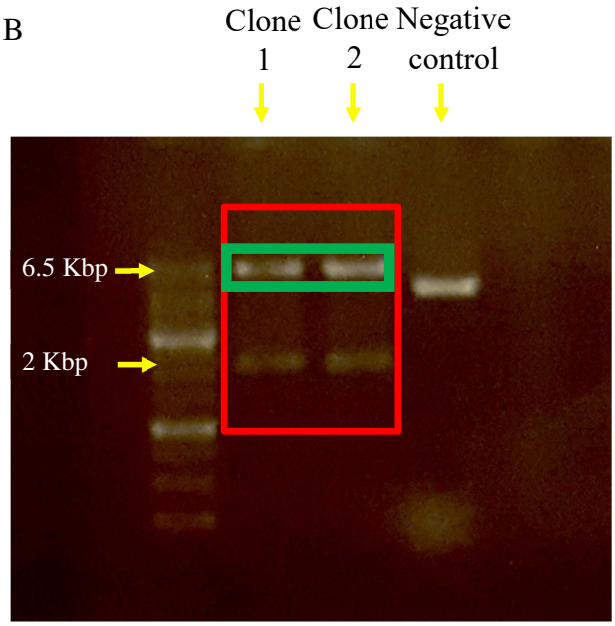

C

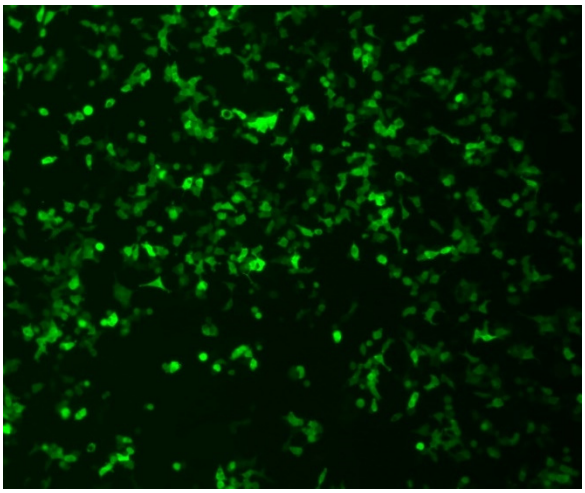

Figure 3.1. Mybl2 plasmid**.** (A) Plasmid map reproduced with permission from abm Inc. (B) Agarose gel showing successful transformation. The E-coli cells were transformed with Mybl2 plasmid. The DNA from different colonies were extracted and digested with EcoRV. The green box shows the backbone DNA which was later extracted from the gel and ligated to form backbone plasmid. Negative control is undigested plasmid (C) Transfection of HEK cells by Mybl2 plasmid.

3.15.2 Mybl2 over-expression

Mybl2 and its target genes expression was confirmed at RNA level. Mybl2, Cyclin B, FoxM1 and CDK1 mRNA was quantified 48 hours after lentiviral transduction using qPCR detection of mRNA (PrimeTime Predesigned qPCR probes, Integrated DNA Technologies). At protein level Mybl2 was evaluated 48 hours after transduction using CytoGlow B-Myb Cell-Based ELISA detection Kit (CB5077, Assay Biotech). Moreover, the effect of Mybl2 over-expression on EDC function was evaluated 72 hours after EDC transduction using appropriate techniques.

3.16 Rapamycin and bromoindirubin-3-oxime (BIO) cell treatment

EDCs were treated with 2μM of glycogen synthase kinase-3 beta (GSK-3β) inhibitor, 6-bromoindirubin-3-oxime (BIO, 361556, CALBIOCHEM), 2μM of the inactivated methylated control (meBIO, 361550, CALBIOCHEM) and high (10 μM) and low (50 nM) doses of mTOR inhibitor, Rapamycin (R0395, Sigma).

3.17 *In vivo* testing

For this cohort study, groups of 8-week old and 54-week old C57BL/6 recipient mice underwent LCA ligation under a protocol approved by the University of Ottawa Animal Care Committee. Seven days after LCA ligation, mice were randomized to receive 100,000 EDCs derived from young normal donors, young ischemic donors, old normal donors or old ischemic donors. Also, a separate subset of 8-week old mice, were randomized to receive 100,000 EDCs from old ischemic donors which were non-transduced or were transduced with Mybl2 or Backbone virus. EDCs were split into 2 doses delivered at the cardiac apex and lateral border zone using echocardiographic guidance (VisualSonics V1.3.8, VisualSonics). Allowing for an alpha error of 5%, the sample size

for each experimental group was calculated with 80% confidence based on the mean of compared groups and their standard deviation.

3.17.1 Functional evaluation

Fourteen and 21 days after EDC injection, the effect of cell therapy was evaluated by echocardiogram tracing of endocardium at end systole and end diastole in a blinded fashion as described in section 3.1.2. After the final echocardiogram, the mice were sacrificed, and their hearts were collected once the animals were anesthetized (2% isoflurane anesthesia).

3.17.2 Histology

A subset of hearts was excised and perfused with saline prior to fixation for 72 hours in 4% Paraformaldehyde (PFA; Alfa Aesar) and stored in 70% Ethanol until paraffin embedding and sectioning. The hearts were sectioned into 5μm slices from the base of the heart starting from suture to the apex (Histology lab, RGN). Four sections per heart from four different levels of infarct area with 20 slice intervals (sections 1, 20, 40 and 60) were stained for Masson's trichrome. The scar size was evaluated (ImageJ, NIH) by calculating the percentage of fibrotic tissue within the left ventricle. A second four sections per heart was deparaffinized in gradients of Xylene (Fisher Scientific) and ethanol prior to antigen retrieval performed by boiling slides in Tris-EDTA-Tween buffer for 1 hour. The sections were blocked in serum-PBST (37.5 ml PBS, 12.5ml FBS and 125ul triton -X) for 1 hour and stained for Isolectin B4 expression (B-1205, Vector Laboratories) for 30 minutes at room temperature. After DAPI (Sigma) counter-staining, the number of vessels per field of view within the infarct and border zone was assessed by fluorescent microscope (Carl Zeiss). For CD68 staining, following deparaffinization and antigen retrieval, tissue sections were blocked in serum-PBS and stained for CD68 (ab125212) overnight at 4ºC. The tissue was then

incubated with DyLight 594 goat anti-rabbit IgG (ab96897, Abcam), and DAPI was used to identify cell nuclei. The number of CD68 cells per field of view was quantified within the infarct and border zones of each section assessed by florescent microscope (Carl Zeiss).

3.17.3 Retention

3.17.3.1 Measurement of long-term EDC retention by GFP-labeling

To measure retention of transplanted EDCs within host myocardial tissue, EDCs were transduced with GFP lentivirus 72 hours prior to injection. The GFP lentivirus was generated using 3rd generation packaging system as described in section 3.14. Whole heart genomic DNA was extracted (DNeasy kit, Qiagen) and quantitative PCR was performed to detect GFP gene (PrimeTime Predesigned qPCR probes, Integrated DNA Technologies). Using the whole heart weight and the GFP standard curve prepared by serial dilution of DNA extracted from GFP transduced EDC into non- transduced EDC, the number of engrafted cells was calculated.

3.17.3.2 Measurement of short-term retention by Luciferase

EDCs were transduced with the gene of interest (Mybl2/ Backbone) or not transduced followed by double transduction with the Luciferase reporter gene. Seven days after LCA ligation, mice were randomized to receive 100,000 EDCs split into 2 doses delivered at the cardiac apex and lateral border zone using echocardiographic guidance. Luminescence by retained cells was evaluated after subcutaneous injection of 150 mg/kg of D-Luciferin (LUCNA, Gold Biotechnology) using serial whole-body imaging (IVIS spectrum *in vivo* imaging system, PerkinElmer) for 1 hour after injection to identify peak luminescence 1, 3, 5 and 7 days after cell injection. To account for net

injection variability, and luciferase expression variability in different groups (single transduced vs. double transduced), the percentage of retained cells was calculated as the signal ratio to day 1.

3.18 Statistical analyses

All data are expressed as mean ± SEM. All analysis was performed using GraphPad Prism 6 software. Normalcy was verified prior to statistical analysis. In experiments with comparison between different groups, one-way ANOVA multiple comparison with Sidak's correction was used while Dunnett's corrected t-test was applied in experiments in which different groups are compared to single control group. To measure statistical significance for correlation (R-square), p value was calculated using t-distribution function in Microsoft Excel software. $p \leq 0.05$ was considered statistically significant.

4. RESULTS

4.1 Validation of ischemic model- Donor age did not alter cardiac function after experimental myocardial infarction

After LCA ligation, cardiac contractility was tracked using serial echocardiographic measurements of LVEF. Although old mice demonstrated a tendency towards earlier reduction in cardiac function, similar degrees of cardiac remodelling resulted as both old mice and young mice reached an equivalent final LVEF 28 days after LCA ligation (27.6±1.0 vs. 29.3±1.1 %, respectively; p=0.4; Figure 4.1, Table 4.1). Thus, post infarct EDCs were sourced from young and old mice with comparable degrees of cardiac remodeling after myocardial infarction.

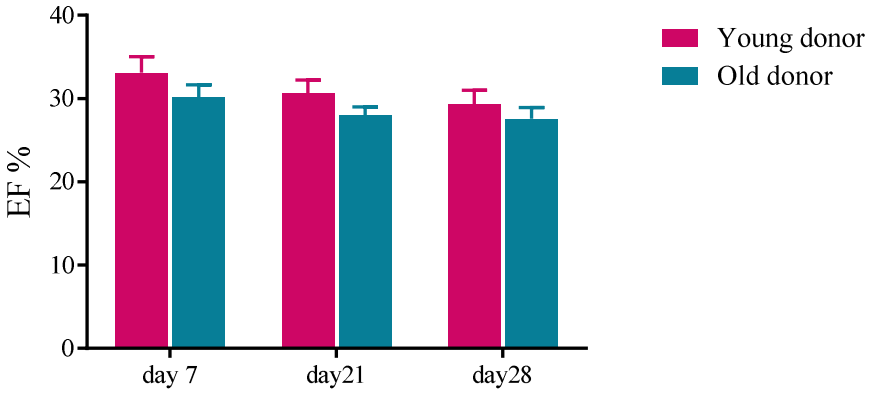

Figure 4.1. Cardiac remodeling after experimental myocardial infarction. Old and young mice underwent LCA ligation and had serial echocardiograms performed 7, 21 and 28 days later (n=17 per group). Values are mean ± SEM.

	7 DAY		21 DAY		28 DAY	
	Young	Old	Young	Old	Young	Old
End diastolic volume (µl)	55.9±4	85.4±4.7***	63.1±4	85±6.6**	68.3±4.1	91±4.2***
End systolic volume (µl)	38.3±3.6	60.8±3.9***	44.1±3.9	63±5.6**	49.1±4	66.7±3.7**
Stroke volume (µl)	17.6±0.9	24.5±1.3***	19±0.9	22±1.5	19.2±0.8	24.3±1.3**
LVEF (%)	33.1±1.9	29.3±1.4	31.4±2	26.9±1.6	29.7±1.7	27±1.4
FAC (%)	20.3±1.1	17.4±1	18.5±1.4	15.2±1.1	18.3±1.2	16.2±1

Table 4.1. Cardiac remodeling after experimental myocardial infarction. Values are mean ± SEM. **p≤0.01 ***p≤0.001 between the two age groups.

4.2. Cellular characteristics of EDCs

4.2.1 Advanced donor age reduces EDC cell culture yields

To evaluate the effects of age and ischemia on EDC yield, the number of cells collected from each harvest was manually counted by hemocytometer and cumulative yield was compared. We noted that advanced donor age reduces the overall number of EDCs collected from plated myocardial biopsies (37±8% fewer cells were collected compared to young group, $p<0.05$; Figure 4.2 A). The number of collected young EDCs from ischemic group was similar to EDCs collected from young normal hearts. In old mice, ischemia restored EDC yield back to levels comparable to its young counterpart group (10.4±0.8 vs. 9.1±0.9 million cells, respectively $p=0.28$). This observation was followed by measuring the proliferative capacity of EDCs. The population doubling time of EDCs

sourced from old and young donors with and without ischemic injury was measured in standard culture conditions (21% oxygen + 20% FBS). EDCs sourced from all donor groups demonstrated equivalent proliferative capacity (p=ns, Figure 4.2 B). The population doubling time was also measured in hypoxic culture conditions designed to mimic ischemic myocardium (1% oxygen + 1% FBS), to evaluate the effect of metabolic stress on EDC proliferation. In ischemic culture conditions, proliferation was halved in all groups compared to normoxic culture condition ($p \leq 0.05$, Figure 4.2 B). However, similar to normoxic culture condition, donor age had no effect on proliferation (p=ns).

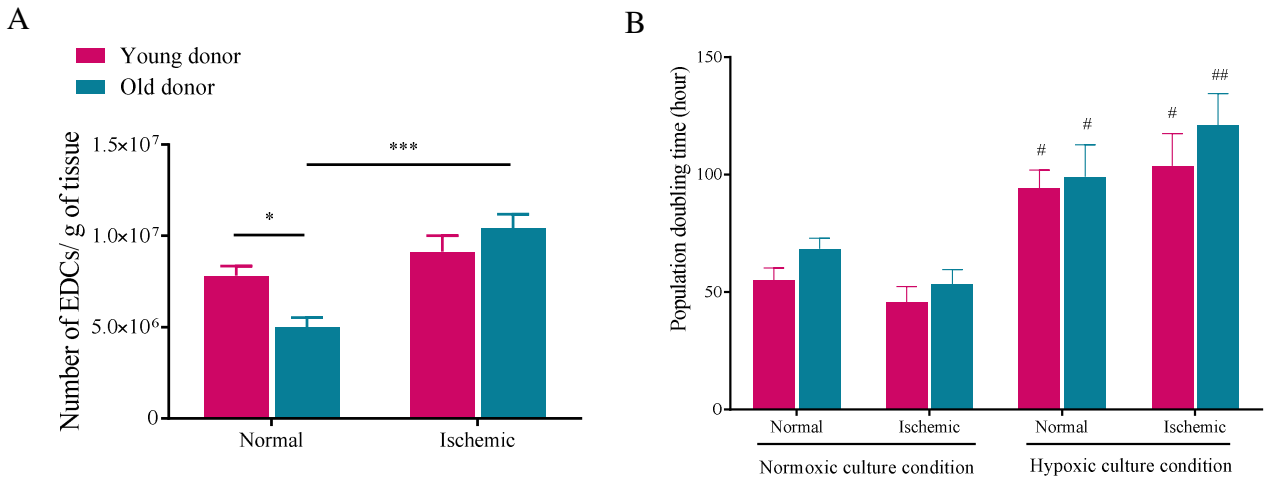

Figure 4.2. EDC culture yield measured by manual cell counting. (A) The total number of cells collected from one gram of cultured heart tissue (n=15 per group). Culture of old mice tissue provided less EDCs. (B) The doubling time measured following 48h of EDCs incubation in standard (21% oxygen, 20% serum) and ischemic (1% oxygen, 1% serum) culture conditions (n=6 per group). EDC proliferation was not affected by age or ischemia. Values are mean ± SEM. *$p \leq 0.05$; ***$p \leq 0.001$ between study groups. #$p \leq 0.05$; ##$p \leq 0.01$ between same study groups in different culture condition.

4.2.2 Advanced donor age does not influence the sub-populations found within EDCs

The EDC sub-population phenotype was analyzed using flow cytometry. We observed that advanced donor age did not alter the content of cells expressing markers indicative of cardiac (c-Kit+), mesenchymal (CD90+) or endothelial (CD34+) progenitors (Figure 4.3). Interestingly, a history of ischemia had a minor effect on the endothelial progenitor (CD34+) content within EDCs sourced from both old (7.5±1.2 to 3.7±0.6%; $p<0.05$) and young (6.8±0.9 to 3.9±0.9%, $p<0.05$) donors. While, it had no influence upon the content of cardiac (c-Kit+) and mesenchymal (CD90+) progenitors. Within ischemic groups, age had no effect on the phenotypic make-up of EDCs.

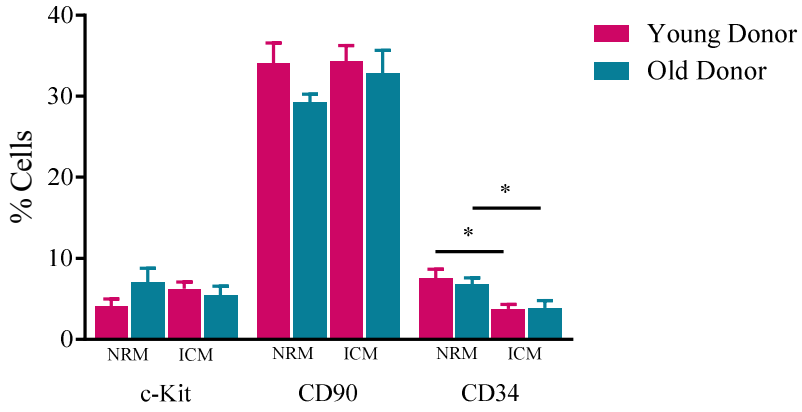

Figure 4.3. EDC phenotype. The percentage of cells positive for markers of c-Kit, CD90 and CD34 was measured by flow cytometry (n=8 per group). Age or ischemia did not influence the CD90+ and c-Kit+ portions of EDC sub-populations but ischemia background reduced the CD34+ portion of EDCs. NRM, normal; ICM, ischemic. Values are mean ± SEM *$p\leq0.05$.

4.2.3 Advanced donor age and a history of ischemia have minor effects on EDC differentiation

The effect of aging and ischemia upon the intrinsic capacity of EDCs to differentiate into myocardial lineages was investigated by exposing EDCs to *in vitro* conditions known to favour cardiac identity (Figure 4.4). We first measured the expression of transcripts indicative of cardiac, endothelial and smooth muscle lineages using the primers designed to target cardiac troponin T (cTnT), von Willebrand factor (vWF) and α-smooth muscle actin (α-SMA) mRNAs, respectively. As shown in Figure 4.4 A, EDCs cultured from old donors expressed cTnT at lower levels ($p=0.05$) when compared to EDCs culture from young mice, while vWF and α-SMA mRNA expression was not significantly different (p=ns).

EDCs cultured from old mice with a history of ischemic injury expressed more vWF and α-SMA mRNA following culture in cardiogenic media when compared to EDCs from normal old mice. In comparison, EDCs culture from young mice after ischemic injury had a reduced ability to express cTnT mRNA ($p<0.05$) when compared to EDCs cultured from young normal mice. Within ischemic groups, EDCs cultured from old mice had a higher α-SMA mRNA level ($p<0.05$ vs. ischemic young mice sourced EDCs), but vWF and cTnT expression did not significantly change (p=ns, Figure 4.4 A). These transcriptional changes were not reflected by protein expression as flow cytometry suggested that donor age and a history of ischemic injury had negligible effects on the capacity of EDCs to differentiate into cardiomyocytes or smooth muscle cells (Figure 4.4B). Interestingly, EDCs cultured from ischemic old mice displayed an increased ability to adopt endothelial lineage ($p<0.05$).

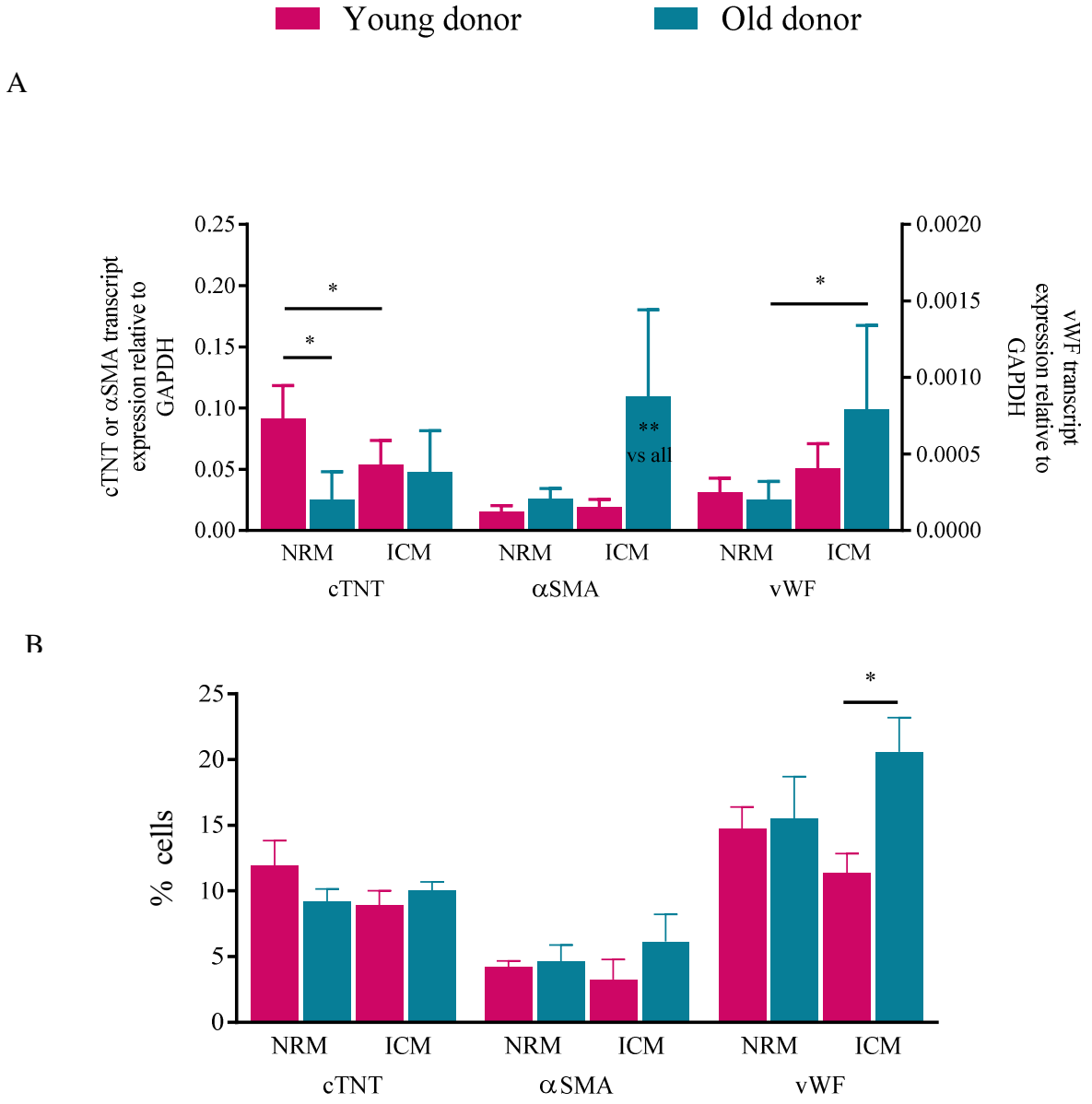

Figure 4.4. EDC ability to differentiate towards cardiac lineages. The ability of EDCs to differentiate into a cardiomyocyte, endothelial cell and smooth muscle cell was quantified using (A) qPCR for cTnT, vWF and α-SMA after 7 days of culture within conditions known to favor cardiac differentiation. The cycle thresholds (ct values) were normalized to data from normal dermal fibroblasts cultured in identical conditions (n=3 per group). (B) Flow cytometry of EDCs for cTnT, vWF and α-SMA markers after 7 days of culture in cardiogenic media. Age enhanced the ability of EDCs to differentiate into endothelial cells only when they have a history of ischemia (n=4 per group). Values are mean ± SEM *p≤0.05; **p≤0.01.

4.2.4 Advanced donor age and ischemia combine to decrease apoptosis resistance

The capacity of EDCs to withstand the harsh ischemic post-infarct environment was evaluated by exposing cells to hypoxic (1% oxygen) low serum (1% FBS) condition. After 48h, cells were stained for Annexin V and 7-AAD followed by flow cytometry quantification for positive cells. The number of double positive EDCs at late apoptotic phase was negligible and unaffected by age or history of ischemia. The number of cells that were positive for Annexin V was considered as early apoptotic cell (Figure 4.5). EDCs sourced from old and young donors demonstrated no significant difference in the number of apoptotic cells (5.2± 0.5 vs. 6.1± 1%, respectively; $p=0.43$). While a history of ischemia did not change the number of apoptotic cells in EDCs from young donors (4.8±0.4%, $p=0.23$ vs. no ischemic history), EDCs sourced from old donors with a history of ischemia showed a strong trend to reduce resistance to apoptotic stimuli (7.1±0.7%; $p=0.06$ vs. old non-ischemic donors). When considering using autologous cells (i.e., chronic ischemic old vs. young donors), advanced donor age was found to decrease the ability of cells to withstand apoptosis by 1.5±0.1 fold ($p<0.05$ vs. EDCs from young donors with a history of myocardial infarction). Taken together, this data demonstrates that advanced donor age and a history of ischemia combine to decrease the ability of EDCs to tolerate ischemic stress environment.

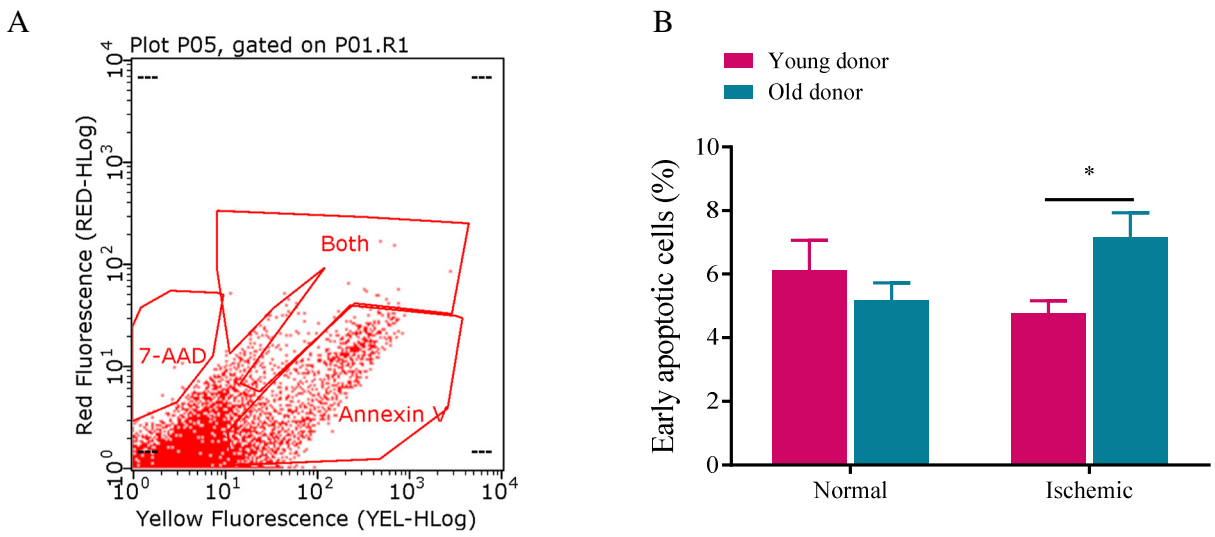

Figure 4.5. EDC resistance to apoptosis. The ability of EDCs to withstand the ischemic condition (1% oxygen, 1% serum) *in vitro* was evaluated by flow cytometry after staining the cells with Annexin V and 7-AAD (n=7 per group). (A) Representative image of flow cytometry plot. (B) The percentage of the cells that were positive for Annexin V was measured using Guava easyCyte software which showed the vulnerability of EDCs sourced from old donors with ischemic injury to ischemic condition. Values are mean ± SEM *p≤0.05

4.2.5 Advanced donor age and chronic ischemia increase senescence

The portion of senescent EDCs cultured from myocardial biopsies was evaluated after culture within normoxic condition prior to fixation with 4% paraformaldehyde and staining x-gal (the substrate for β-galactosidase). β-galactosidase is a high precision marker of cellular senescence (Lawless et al., 2010). As predicted, EDCs sourced from old mice exhibited a greater number of senescent cells as compared to EDCs cultured from young mice (14.8±2.3 vs. 3.2±0.7 %, respectively; $p<0.01$; Figure 4.6). A history of ischemia increased the number of senescent cells in EDCs from old and young donors (23.8±3% senescent EDCs cultured from old donors and 8.9±1.9 % senescent EDCs cultured from young donors, $p\leq 0.05$ vs. EDCs culture from similar age donors without a history of myocardial infarction). In old mice, a history of ischemia had a marked effect

on the number of senescent EDCs as old individual exhibited 2.7±0.3-fold more senescent cells when compared to young donors with a history of myocardial injury ($p<0.01$). This data hints that ischemia is an important parameter that induces senescence in addition to advanced donor age.

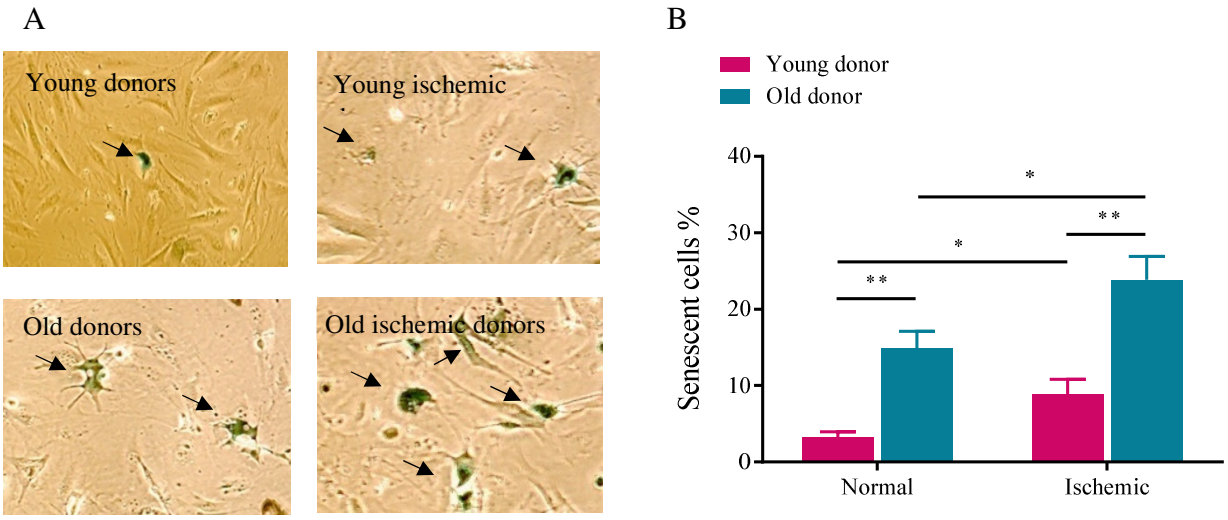

Figure 4.6. EDC senescence. Senescent cell quantification by Senescence-associated β-galactosidase staining, followed by DAPI staining to count the total number of seeded cells. The number of cells were counted in 6 random fields of view and is reported as percentage of senescent cells. (A) Representative images of senescence-associated β-galactosidase staining in EDCs sourced from old and young donors. Blue stains show the cells that have undergone senescent. (B) Quantification of senescent cells (n=8 per group). Random field analysis demonstrated that senescent cells are more abundant in aged EDCs. Values are mean ± SEM *p≤0.05; **p≤0.01

4.2.6. Antioxidant enzymes activity increases after infarction in young EDCs

The ability of cells to reduce toxic ROS generated during metabolism can greatly impact on senescence. As shown in Figure 4.7A, EDCs cultured from old donors produced equivalent amounts of ROS as compared to EDCs cultured from young donors (26.8±3.3 vs. 24.3±3.6 a.u, respectively; $p=0.59$). Interestingly, a history of myocardial infarction markedly reduced the ROS content within EDCs cultured from young donors ($p<0.05$ vs. young donors without a history of

myocardial ischemia) in contrast to EDCs cultured from old donors in which the ROS production remained unchanged. Within ischemic groups, EDCs sourced from old donors showed greater ROS burden relative to young donors (28.6±2.8 vs. 13.5±1 a.u, respectively, $p<0.05$). Given that ROS content reflects the activity of antioxidant enzymes, we probed the activity of SOD and GPx. It was interesting to see that the activity of SOD was strongly correlated to ROS levels ($R^2=0.87$, $p=0.03$ Figure 4.7 C). SOD activity remained unchanged by aging (1.24±0.07 in EDCs from young donors vs. 1.40±0.15 a.u in EDCs from old donors, $p=0.42$) but was markedly increased in EDCs cultured from young donors with a history of ischemia (1.91±0.11 a.u, $p\leq0.01$ vs. young donors without a history of myocardial ischemia). Contradictorily, a tendency for reduced SOD activity was seen in EDCs cultured from old donors with a history of ischemia (1.01±0.07 a.u, $p=0.08$). When we measured GPx activity, we observed that the difference in GPx activity of EDCs sourced from old and young donors was not significant (0.15±0.02 vs. 0.21±0.05 a.u, respectively). Nevertheless, because a history of ischemia tended to increase GPx in EDCs from young donors (0.25±0.01 a.u) and tended to decrease GPx activity in EDCs from old donors (0.11±0.02 a.u), EDCs sourced from young donors with a history of ischemia had significantly greater GPx activity compared to their old counterpart ($p<0.01$; Figure 4.7 D). This data indicates that cellular ROS production remains unaltered in EDCs, however, the activity of antioxidants markedly enhances in EDCs from young donors with ischemic injury. Therefore, enhanced clearance of toxins likely accounts for the reduced ROS content observed within these EDCs.

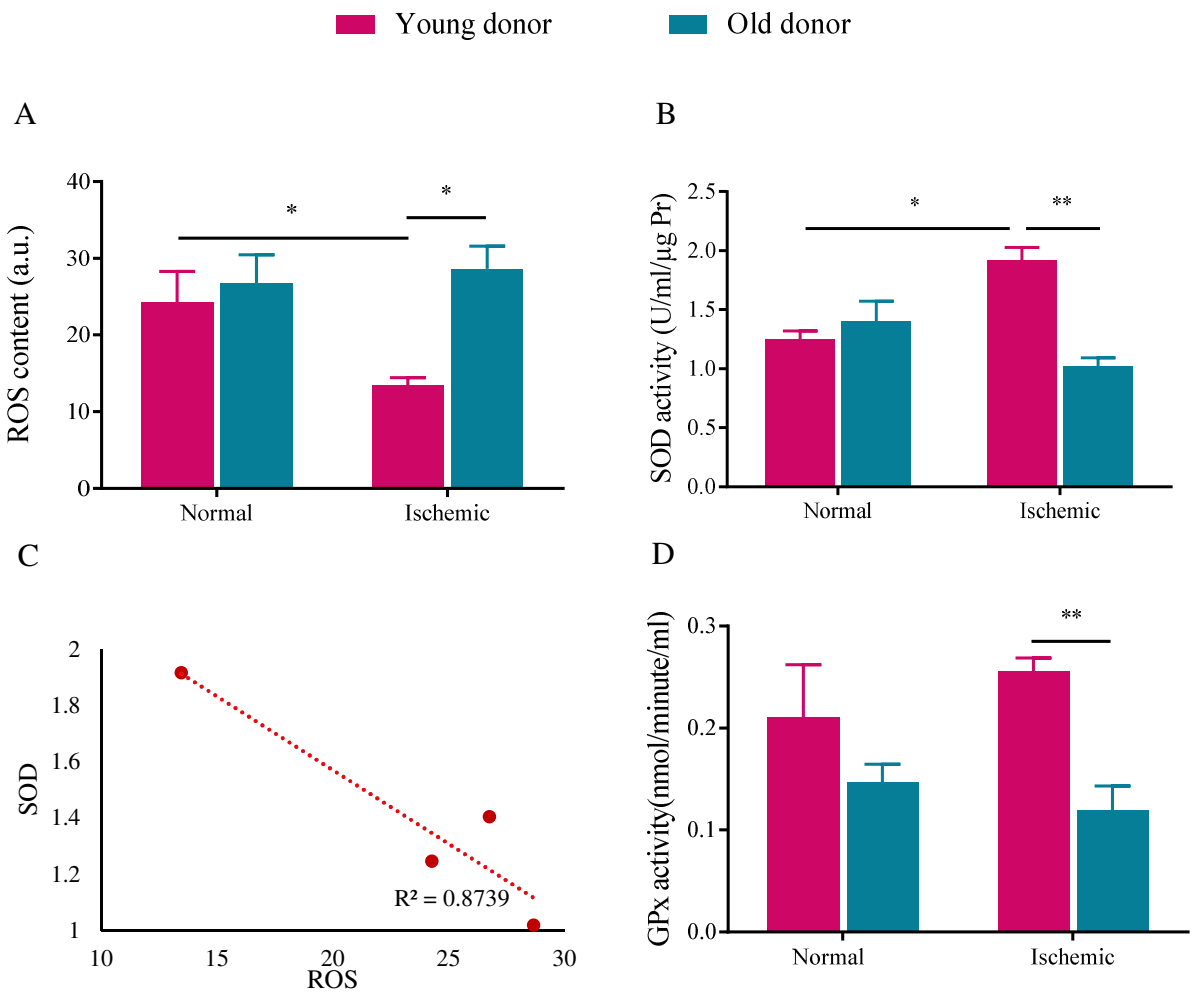

Figure 4.7. ROS formation and handling in EDCs. (A) The ROS content within EDCs was measured after incubating the cells with DCFDA for one hour followed by fluorescent reading emission at 535nm (n=5 per group). (B) Super oxide dismutase activity (n=5 per group) (C) Correlation of ROS with SOD activity (D) Glutathione peroxidase activity (n=5 per group) was measured in the supernatant of lysed EDCs. Young ischemic EDCs have increased antioxidant enzymes while aged ischemic EDCs reduced the activity of antioxidant enzymes considerably. Values are mean ± SEM *p≤0.05; **p≤0.01

4.2.7 Ischemia shortens telomere length in c-Kit+ cells but not in c-Kit- cells

Short telomere is a potent inducer of senescence. Given previous work demonstrating the myogenic and angiogenic properties of c-Kit+ cells, telomere length was quantified in magnetically sorted c-Kit+ and c-Kit- cells (Jesty et al., 2012; Cesselli et al., 2011). As shown in

Figure 4.8A, cell type influenced telomere length as c-Kit+ cells generally had longer telomeres than c-Kit- cells ($p \leq 0.05$) excepting c-Kit$^+$ cells cultured from ischemic old donors where telomere length was reduced to lengths comparable with c-Kit- cells. Telomere length in c-Kit- cells from all cohorts were equivalent. Also, advanced donor age had negligible effect on telomere length in c-Kit+ cells, while a history of ischemia reduced telomere length by 22±1.7 and 31±2.2% in young and old donor sourced EDCs, respectively ($p \leq 0.05$ vs. no ischemic history).

To account for these observed differences, the activity of the enzyme responsible for telomere lengthening (telomerase) was evaluated (Figure 4.8B). Comparing between the two population of cells within a group, the telomerase activity of c-Kit+ cells from normal young donors was greater than in c-Kit- cells (5E-04 ± 5E-05 vs. 3E-04± 1.5E-05, $p<0.5$). Akin to the telomere length results, c-Kit- cells from all cohorts showed similar telomerase activity (p=ns). Also, telomerase activity was markedly reduced in c-Kit+ cells cultured from old donors with a history of myocardial infarction ($p<0.05$ vs. non-ischemic old donor) suggesting that infarction is more apt to reduce telomerase activity in old donors. Overall, the telomere system is more vulnerable in c-Kit+ cells derived from old mice with a history of ischemia.

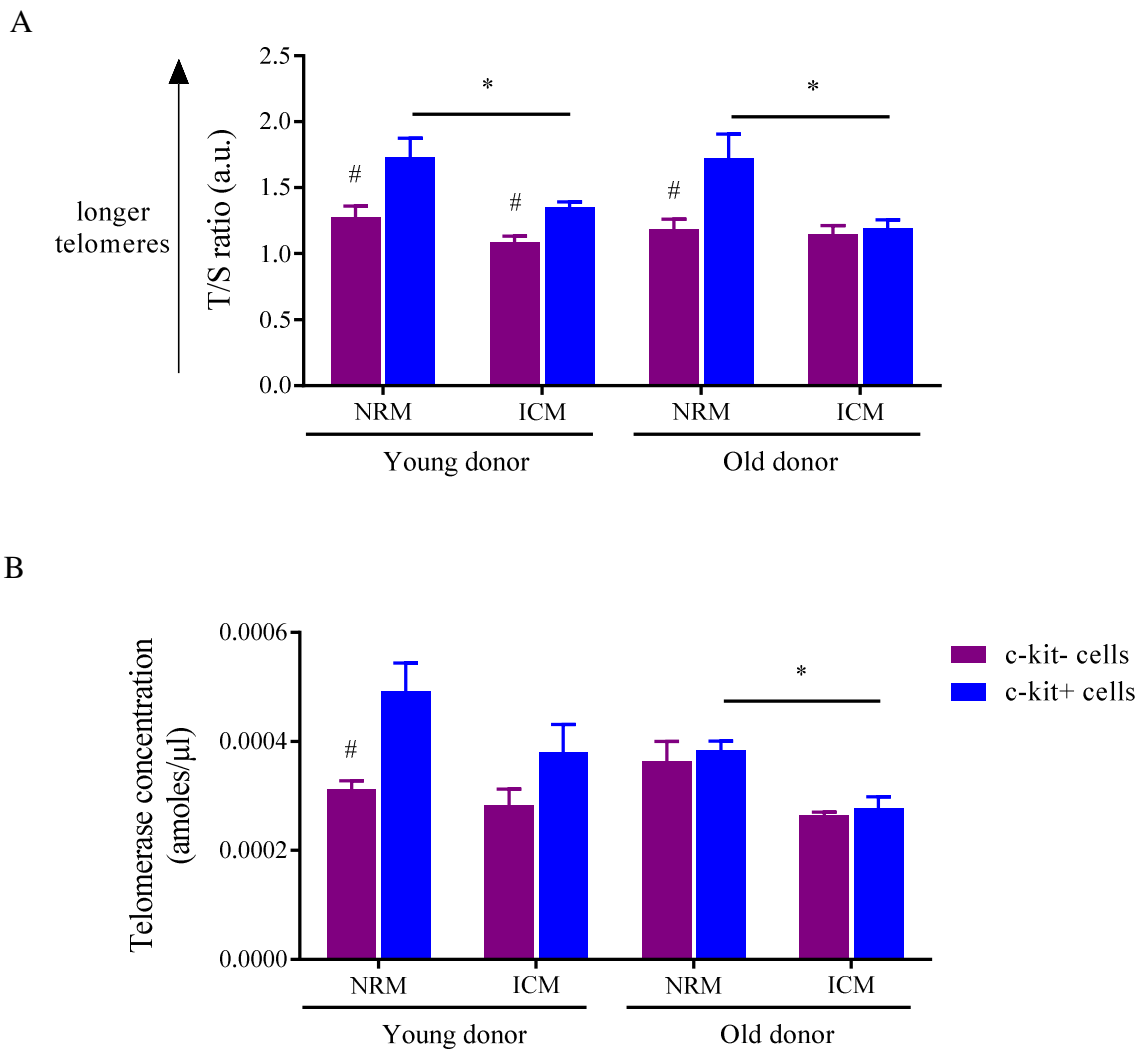

Figure 4.8. Telomere/ Telomerase system. Both telomere length and telomerase enzyme activity were assessed by qPCR after c-kit+ cell separation using magnetic sorting. (A) Telomere and reference gene levels were first calculated using standard curves for each of the genes. Telomere length was then normalized to the single copy reference gene (Albumin) in c-kit+ and c-kit- cell populations (n=6 per group). (B) Telomerase concentration in c-kit+ and c-kit- cell populations of EDCs measured by qPCR of telomerase substrate (n=5 per group). Values are mean ± SEM. *p≤0.05 between EDC cohorts; #p≤0.05 in c-kit+ vs c-kit-

4.3 Paracrine profile and potency of EDCs

4.3.1 Advanced donor age and infarction alter EDC production of cytokines

Given mounting evidence that a significant portion of cardiac repair conferred by EDC transplantation is mediated by indirect paracrine stimulation of endogenous repair, the paracrine signature of EDCs from old and young donors was quantified. Conditioned media was generated by exposing EDCs to stress conditions designed to simulate the ischemic border zone (i.e., 1% oxygen + 1% serum). The profiled cytokines of interest were selected from the work of Latham et al. (Latham et al., 2013). As shown in Figure 4.9, aging did not alter the content of angiogenin, angiopoetin-1, hepatocyte growth factor or VEGF. However, EDCs cultured from old donors secreted greater amounts of IL-6 (2481±820 vs. 1516±220 ng/ml, respectively; $p=0.05$ vs. young donors). EDCs sourced from old donors with a history of myocardial infarction demonstrated reduced secretion of the pro-angiogenic cytokines, angiogenin, angiopoietin-1 and VEGF ($p<0.05$ vs. young donors). Apart from a notable increase in IL-6 (1.7±0.24 fold greater vs. no history of myocardial infarction, $p<0.05$), ischemia had no effect on the cytokines produced by EDCs from young donors. This data demonstrates that EDCs sourced from older individuals with a history of myocardial infarction are less able maintain paracrine production hinting that the main mechanism of benefit seen after transplantation may be impaired.

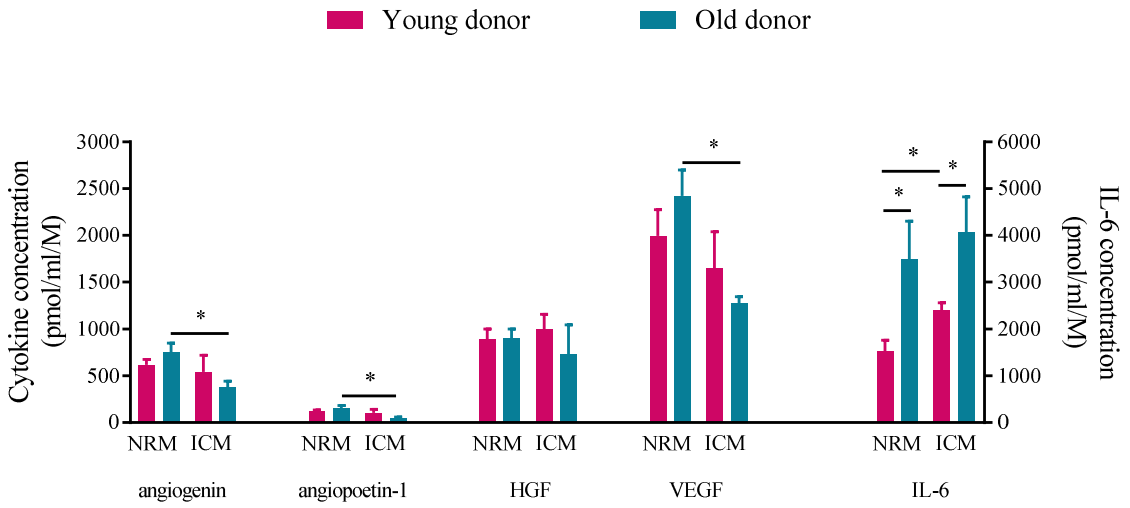

Figure 4.9. EDC secretion paracrine profile of angiogenin, angiopoietin-1, HGF, VEGF and IL-6. These cytokines are known to play a critical role in angiogenesis and cardiogenesis. The secretion levels of these cytokines within media conditioned by EDCs were determined by ELISA. Values were compared after correction for dilution factor and normalization with total protein (n=4 per group). Values are mean ± SEM. *p≤0.05

4.3.2 Ischemia increases the pro-angiogenic capacity of EDCs through proliferin angiogenic cytokine

Forming new vessels is essential for myocardial re-perfusion. We modelled vessel formation *in vitro* by analyzing HUVEC tubule formation on cytokine-depleted Matrigel while the cells were exposed to EDC conditioned media (CM). As shown in Figure 4.10A and B advanced donor age alone had little effect on tubule length (11.2±0.6 and 12.2±0.3 mm in EDCs from young and old donors, respectively; p=0.9). Surprisingly, unlike the marked reduction in pro-angiogenic cytokine production observed in EDCs cultured from old donors with a history of myocardial infarction, EDCs cultured from donors after myocardial infarction demonstrated longer tubule length (16.4±0.5mm; p<0.01 in young and 14.3±0.4mm; p=0.05 in old donors vs. no infarction history)

with the greatest increase observed in young donors with a history of myocardial infarction ($p<0.04$ vs. old donors with a history of myocardial infarction).

Misalignment between HUVEC tubule formation results and candidate pro-angiogenic cytokines' ELISA data rationalized unbiased follow-up experiments profiling the secretory angiogenic proteome profile of EDCs. Secretion of 53 different cytokines within conditioned media was assessed using an angiogenesis proteome profiler array (53 cytokines; Figure 4.10E and F). As a negative cellular control, DF conditioned media with minimal potency to form tubules (Latham et al., 2013) was used. Among cytokines whose secretion level was significantly different compared to DF cells, proliferin secretion was increased by ~5 fold in media conditioned by EDCs from both old and young donors with a history of myocardial infarction ($p\leq0.01$ vs. no infarct donors, Figure 4.10C). These differences in cytokine production corresponded to significant increase in the EDC ability to stimulate angiogenesis (1.47±0.04 and 1.15±0.03 fold more tubules in young and old donors with a history of infarction vs. no infarction, respectively; $p\leq0.05$). Proliferin depletion confirmed the suspicion that proliferin was responsible for increased tubule formation of ischemic mice sourced EDCs as in the absence of proliferin tubule formation was reduced by 27±7 and 38±6 % in young and aged ischemic EDCs, respectively ($p\leq0.05$ vs. non proliferin depleted; Figure 4.10B and D). Successful depletion of proliferin was confirmed using an IgG isotype control. Proliferin elimination resulted in reduction of HUVEC tubule formation on matrigel compared to IgG isotype control as shown in Figure 4.10G.

A

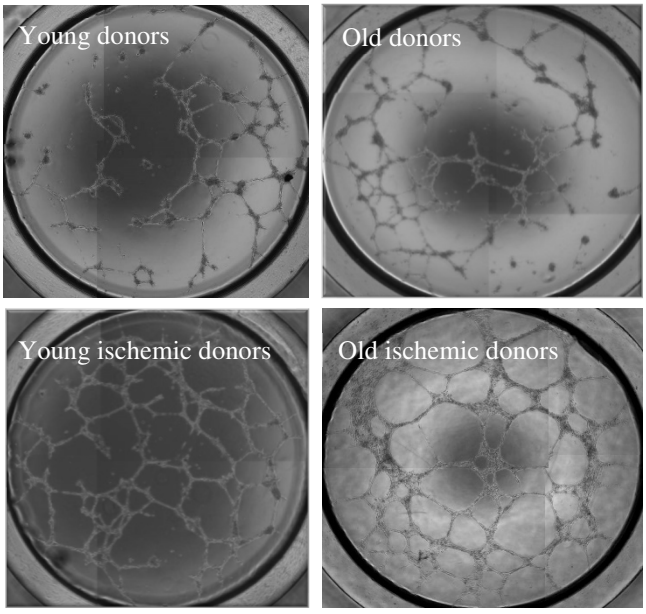
Young donors
Old donors
Young ischemic donors
Old ischemic donors

B

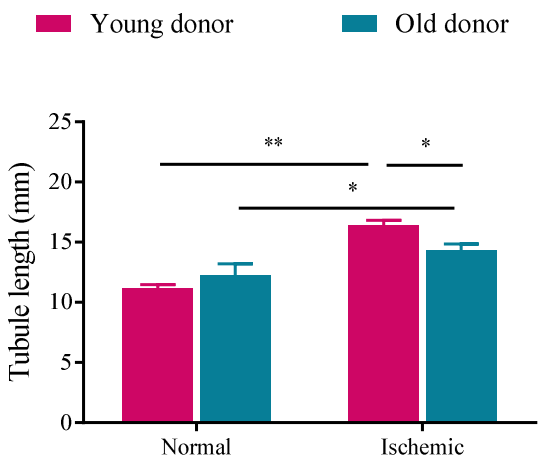
Young donor
Old donor
Tubule length (mm)
25
20
15
10
5
0
**
*
*
Normal
Ischemic

C

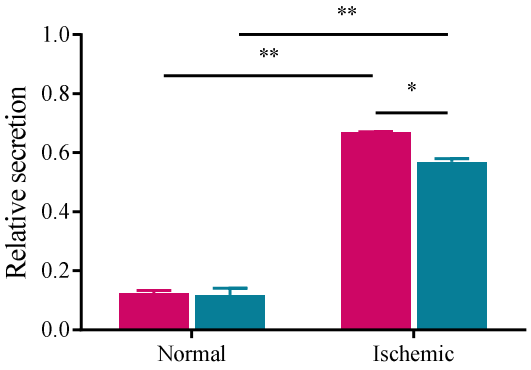
Relative secretion
1.0
0.8
0.6
0.4
0.2
0.0
**
**
*
Normal
Ischemic

D

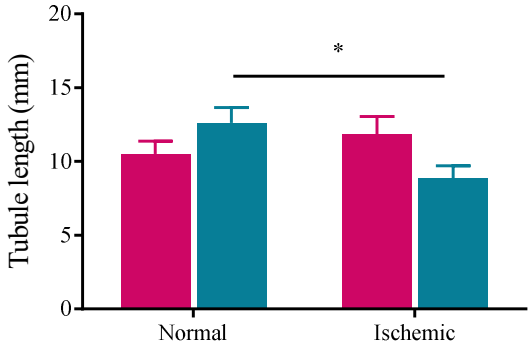
Tubule length (mm)
20
15
10
5
0
*
Normal
Ischemic

E

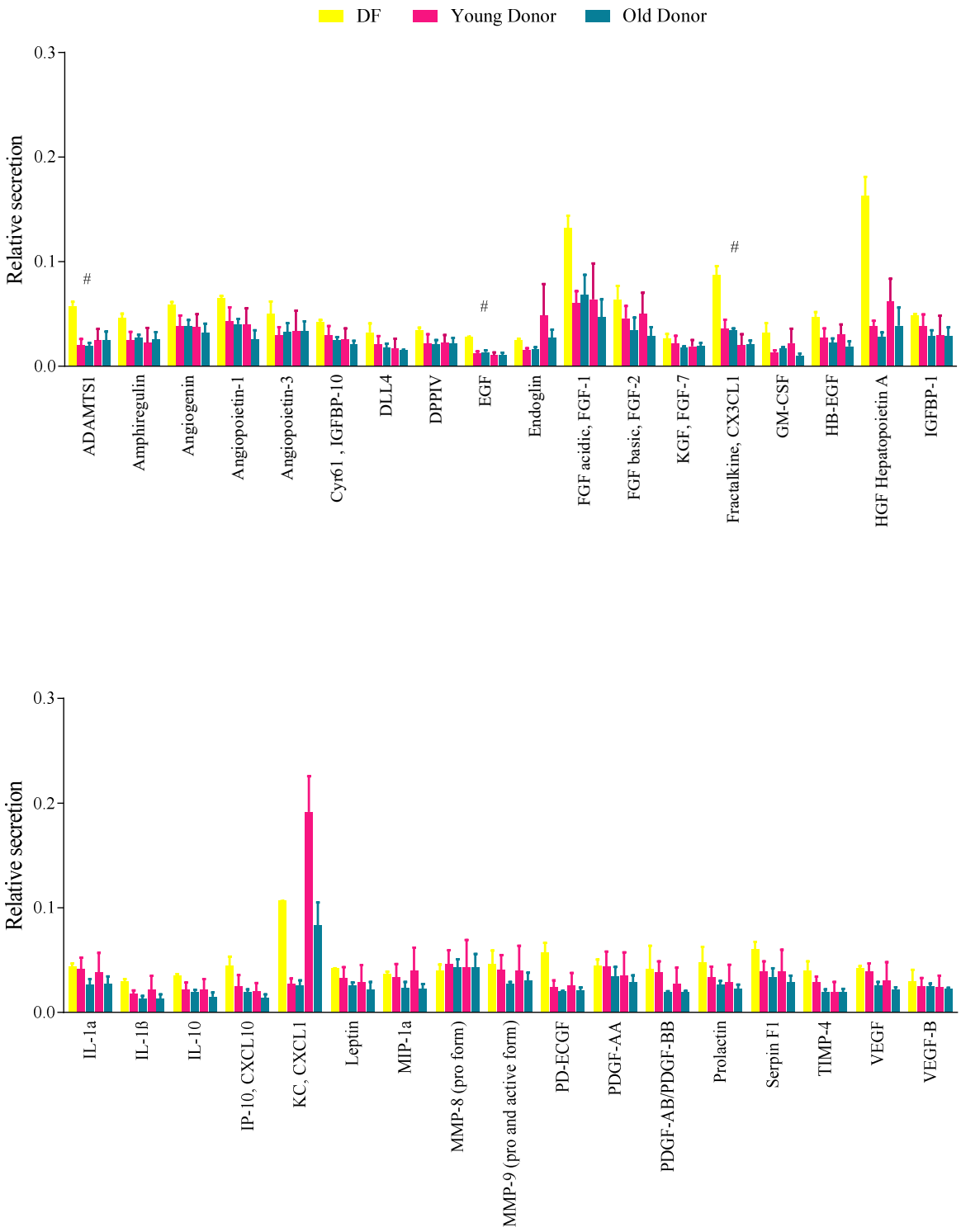
DF
Young Donor
Old Donor
Relative secretion
0.0
0.1
0.2
0.3
#
#
#
ADAMTS1
Amphiregulin
Angiogenin
Angiopoietin-1
Angiopoietin-3
Cyr61 , IGFBP-10
DLL4
DPPIV
EGF
Endoglin
FGF acidic, FGF-1
FGF basic, FGF-2
KGF, FGF-7
Fractalkine, CX3CL1
GM-CSF
HB-EGF
HGF Hepatopoietin A
IGFBP-1
Relative secretion
0.0
0.1
0.2
0.3
IL-1a
IL-1ß
IL-10
IP-10, CXCL10
KC, CXCL1
Leptin
MIP-1a
MMP-8 (pro form)
MMP-9 (pro and active form)
PD-ECGF
PDGF-AA
PDGF-AB/PDGF-BB
Prolactin
Serpin F1
TIMP-4
VEGF
VEGF-B

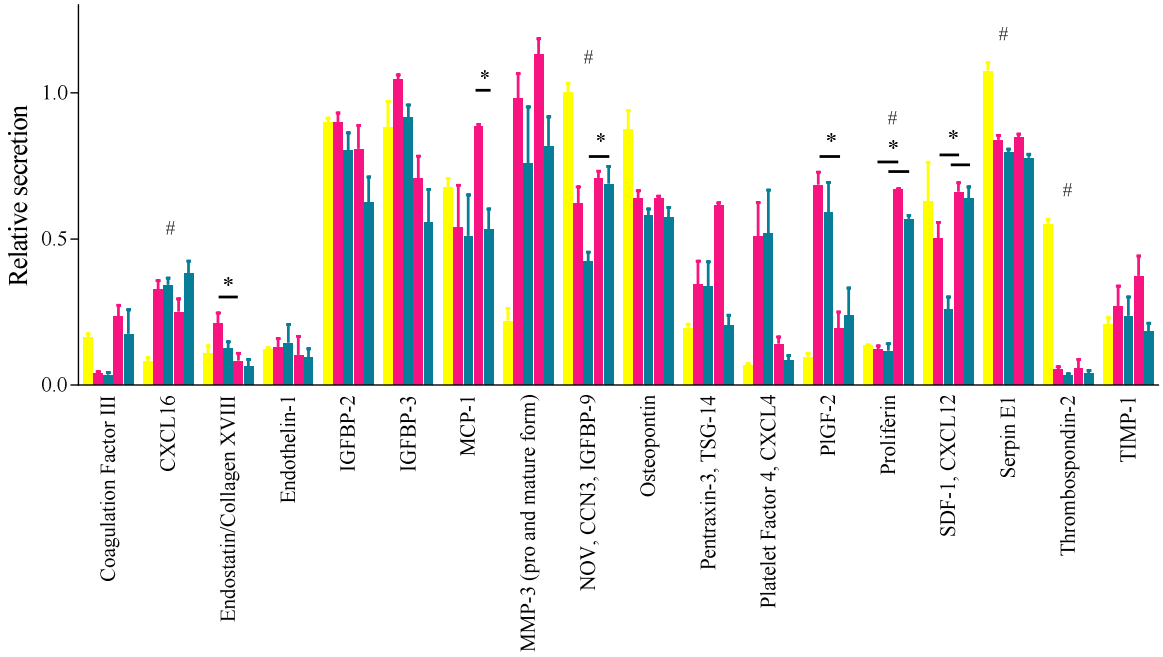
Relative secretion
1.0
0.5
0.0
Coagulation Factor III
CXCL16
Endostatin/Collagen XVIII
Endothelin-1
IGFBP-2
IGFBP-3
MCP-1
MMP-3 (pro and mature form)
NOV, CCN3, IGFBP-9
Osteopontin
Pentraxin-3, TSG-14
Platelet Factor 4, CXCL4
PIGF-2
Proliferin
SDF-1, CXCL12
Serpin E1
Thrombospondin-2
TIMP-1

F

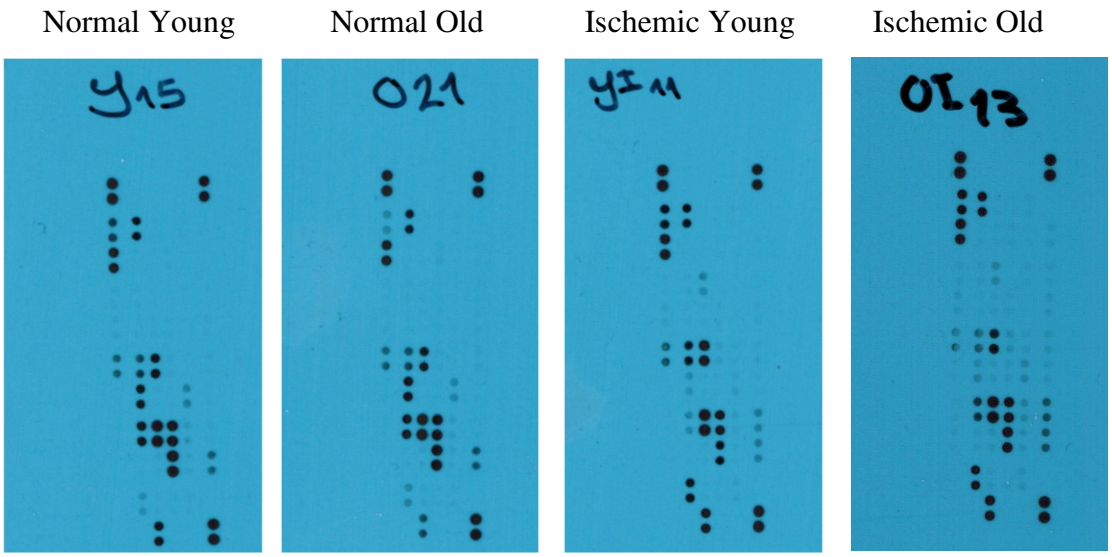
Normal Young
Normal Old
Ischemic Young
Ischemic Old

G

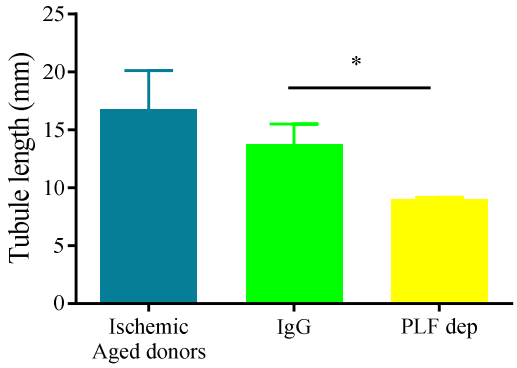

Figure 4.10. Angiogenesis capacity and profiling of secreted angiogenic cytokines. The ability of conditioned media from EDCs to induce tubule formation was assessed after seeding HUVECs on Matrigel followed by incubation with CM. (A) Representative images of tubule formation assay. (B) Quantification of tubule length using NeuronJ plugin of ImageJ software. Tubule length for each sample was averaged from 3 well replicates (n=4 per group). (C) Proliferin secretion level within EDC CM, measured by angiogenesis proteome profiler array (n=3 per group). (D) Quantification of tubule length after proliferin depletion. Depletion of proliferin from conditioned media was performed by addition of proliferin antibody to CM, followed by protein A/G magnetic beads elimination (n=4 per group). (E) Quantification of secreted cytokines. Loaded conditioned media was normalized to protein content of the cells. Following the experiment, the expression levels were normalized to reference controls on the membrane. # shows significant secretion level in all EDC groups comparing to DF cells ($p \leq 0.05$). (F) Representative images of EDC secretion of 53 angiogenesis-related proteins. Data shown from 5-minute exposure. (G) Angiogenesis assay in the presence of isotype control. The specificity of proliferin antibody was confirmed using IgG isotype control antibody (n=3 per group). Values are mean ± SEM. *$p \leq 0.05$; **$p \leq 0.01$

4.3.3 Advanced donor age increases bone-marrow derived cells recruitment by EDCs

A portion of the indirect cardiac repair seen after EDC transplantation is mediated through recruitment of circulating stem cells and/or inflammatory cells (Tilokee et al., 2016). Therefore, we evaluated the effects of advanced donor age and ischemia on the ability of EDC conditioned

media to recruit bone marrow derived cells through a standard transwell assay (Molgat et al. 2014). This assay revealed that advanced donor age markedly increases the ability of EDC conditioned media to recruit BMDCs (50±6 vs. 23±4, $p<0.05$ vs. normal young donors and 54±8 vs. 28±5, $p<0.05$ vs. young donors with a history of ischemia; Figure 4.11A, B). Interestingly, a history of ischemia had a negligible effect on the ability of conditioned media to recruit BMDCs. Consistent with previous reports, (Mayfield et al., 2016; Mayfield et al., 2017) transwell migration strongly correlated with IL-6 content within conditioned media ($R^2=0.95$; $p=0.02$). Hence, we tested the hypothesis that IL-6 is involved in increased migration of BMDCs when exposed to media conditioned by EDCs from old donors. When we performed the migration assay after IL-6 depletion, recruitment was decreased in all cohorts ($p\leq0.05$; Figure 4.11B and C) with a prominent ~75% reduction effect noted in aged EDC conditioned media. Thus, confirming the notion that IL-6 accounts for increased BMDCs recruitment seen in media conditioned by old donors.

The specificity of the IL-6 neutralizing antibody was confirmed by running the migration experiment in the presence of the IgG isotype control. Figure 4.11D shows a significant reduction in the migration of BMDCs through a Boyden chamber after depletion of IL-6 by its neutralizing antibody compared to the IgG isotype control ($p=0.05$).

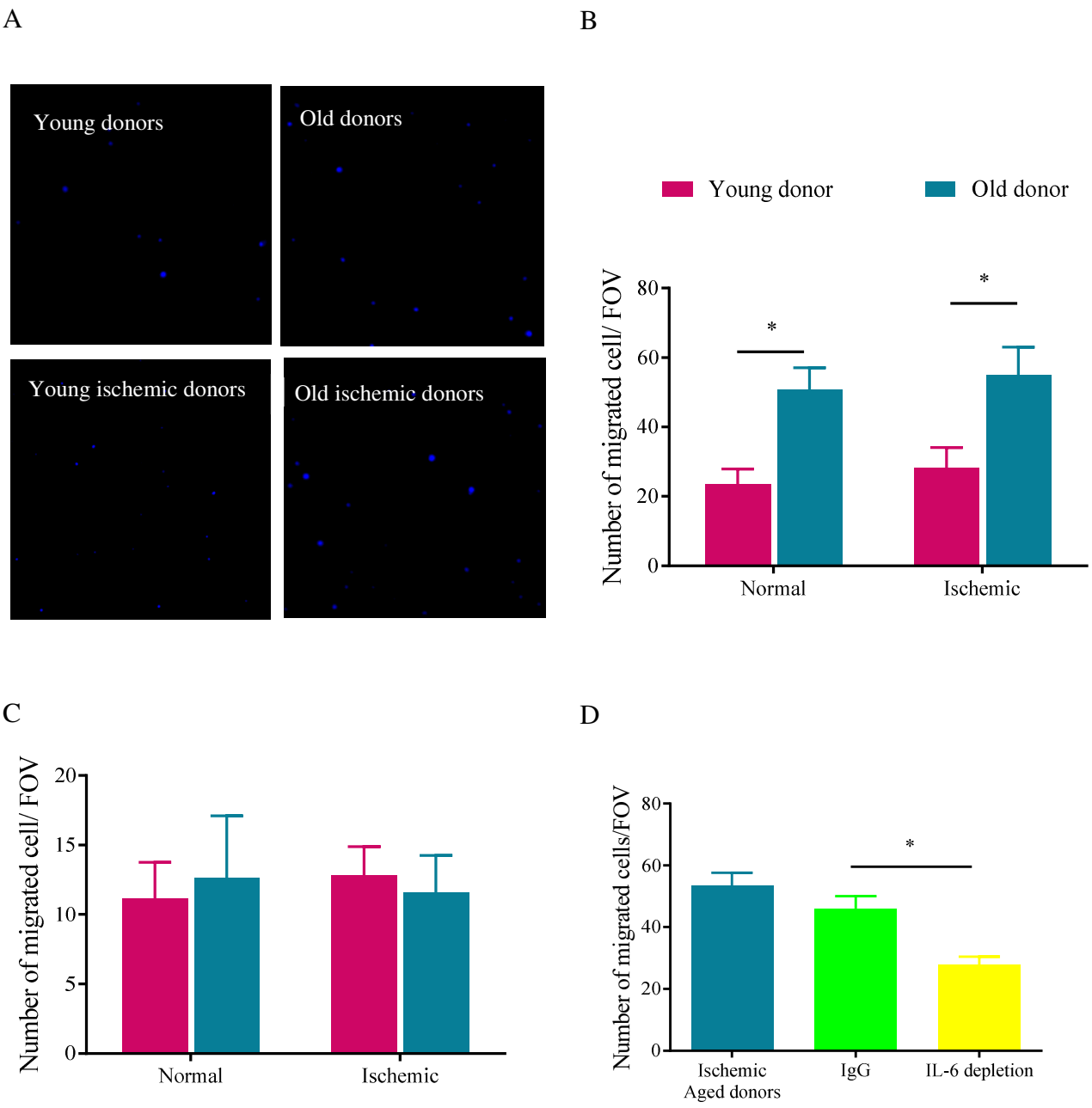

Figure 4.11. Cell migration inducing capacity. The ability of EDC conditioned media to induce migration of bone marrow derived cells was evaluated by seeding these cells on transwell inserts and calculating the number of migrated cells to the bottom compartment of transwell plate. These cells were then fixed and stained with DAPI. (A) Representative images of migration assay. (B) Quantification of migrated cells using ImageJ software. The cells were counted in 6 random fields of view (n=5 per group). (C) Quantification of migrated cells after IL-6 depletion using neutralizing IL-6 antibody. The cells were counted in 6 random fields of view (n=4 per group). IL-6 in conditioned media promoted cell migration.

(D) Migration assay in the presence of isotype control. The specificity of IL-6 antibody was confirmed using IgG isotype control antibody (n=3 per group). Values are mean ± SEM. *p≤0.05

4.3.4 Donor age and myocardial ischemia do not alter EDC extracellular vesicle production

To probe the contribution of the age and myocardial injury on extracellular vesicle production, EDCs were cultured for 48 hours in exosome -free 1% FBS media under hypoxic (1% O_2) culture condition. Microparticle quantification (NanoSight) showed that advanced donor age or a history of myocardial infarction had no effect on size and number of secreted extracellular vesicles (*p*=ns; Figure 4.12).

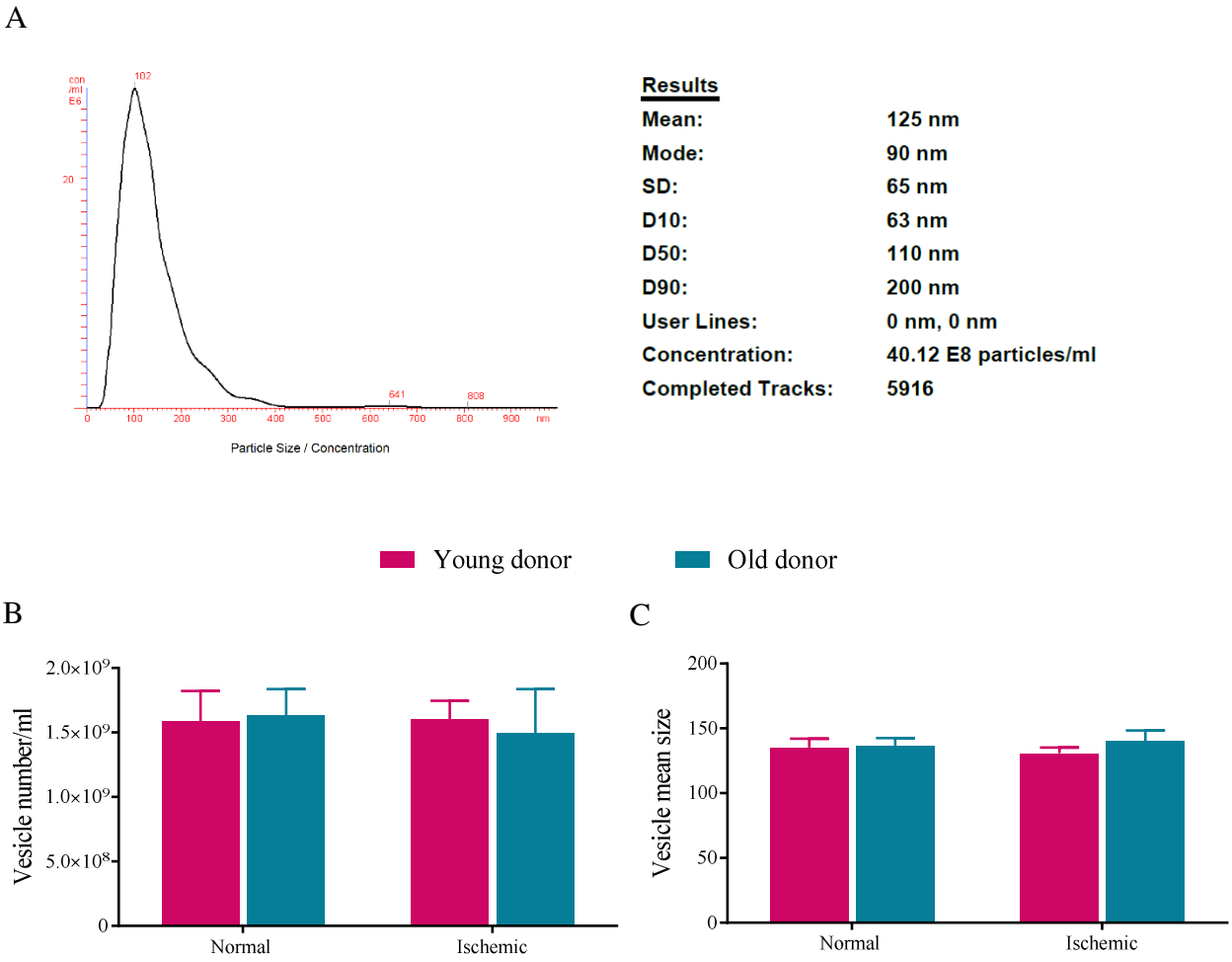

Figure 4.12. Extracellular vesicle secretion. Particle movements were captured during 60 second videos from 3 different random fields of view (n=4 per group). (A) Representative image of NanoSight result. (B) Total vesicle number collected within 48 hours time period concentrated in 1 ml of saline. (C) Average vesicle size. EDCs from all cohorts were secreting equal number of vesicles and their mean peak size remained unchanged. Values are mean ± SEM

4.4 Effects of advanced donor age and ischemia on the regenerative potency of EDCs *in vivo*

4.4.1 Advanced donor and recipient age reduce functional improvements after EDC transplantation

To evaluate the capacity of EDCs from different cohorts to improve the heart function after myocardial infarction, 100,000 EDCs were injected into the infarct border zone 7 days after LCA ligation using echocardiographic guidance (Latham et al. 2013; Molgat et al. 2014; Jackson et al., 2015). Heart function was evaluated using echocardiography at the time of injection and 3 weeks after injection (Figure 4.13 and Table 4.2). EDCs from all four cohorts were injected into young (2-month old) or old (12-month old) recipients. PBS was used as a negative control and resulted in progressive adverse cardiac remodeling over the 3 weeks after injection (-3.7±1 vs. -2.8±0.8 % EF in young and old recipients, respectively; p= 0.51 for effect of recipient age; Figure 4.13). EDCs from all cohorts significantly improved cardiac function in both young and old recipients compared to PBS injection ($p \leq 0.01$). As shown in Figure 4.13, advanced recipient age markedly attenuated the salutary benefits conferred by EDC transplantation as aged matched EDCs cultured from normal or ischemic mice provided greater improvements in cardiac contractility when injected into young recipients relative to old recipients; suggesting that old heart milieu is less responsive to regenerative (paracrine) stimuli. Donor age also had a marked effect on the regenerative performance of EDC transplant as cells from normal young donors consistently outperformed those from normal old donors (7.8±0.6 vs. 5.3±1% change in LVEF from baseline, p=0.05) in young or (5±1 vs. 1.8±0.6% change in LVEF from baseline, p<0.01) old recipients.

Comparing the effect of age within ischemic groups showed a similar trend as observed in normal groups. EDCs from young donors with a history of ischemia tended to provide greater improvement compared to those from old donors (7±0.9 vs. 4±1.2% change in LVEF from baseline, p=0.06) in young or (3.4±0.6 vs. 1.1±0.9% change in LVEF from baseline, p<0.05) old recipients. When we evaluated the effect of ischemia on EDCs, ANOVA showed that the factor of ischemia significantly reduced gains in myocardial function, however, the multiple comparison did not show any significant difference between donors with or without ischemic injury. Further details of echocardiographic measurement are available in Table 4.2. As shown in this table, cardiac dimensions indicate progressive remodeling in all groups. However, young hearts injected with young EDCs are showing greater improvement in cardiac function compared to PBS group (p<0.05).

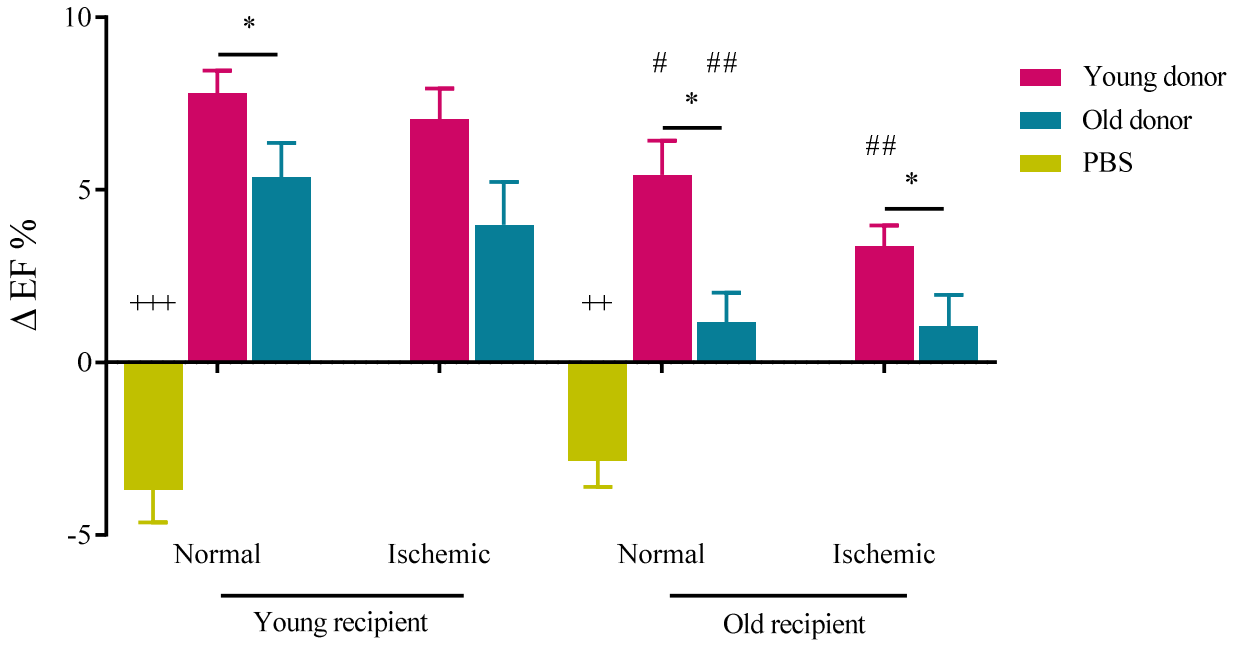

Figure 4.13. Functional evaluation measured by echocardiography. Cardiac function (ΔEF %) was assessed following injection of 100,000 cells into an LCA ligated mouse heart. The chart shows the difference in LVEF 3-weeks after EDC injection compared to baseline (n=12 per group). EDCs from young donors were more potent to ameliorate the heart function in both young and old recipients. Values are mean ± SEM. *p≤0.05 between different donor in same-age recipient; # p≤0.05; ##p≤0.01 between same donors in different-age recipients; ++p≤0.01; +++p≤0.001 between PBS group and all other donors in same-age recipients.

YOUNG RECIPIENT

Donor:	PBS control		Young mouse no ischemia		Old mouse no ischemia		Young mouse with ischemia		Old mouse with ischemia	
DAYS POST MI	7	28	7	28	7	28	7	28	7	28
EDV	64±1	76±4#	57±4	72±4#	60±4	69±2	65±3	76±3#	68±4	79±8
ESV	44±2	55±4#	41±4	46±3	42±3	45±2	48±3	51±3	48±4	55±7
SV	20±1	21±2	16±1	25±1#*	18±1	24±1#	17±1	26±1#*	19±1	24±1#
LVEF (%)	32±2	28±3	28±2	36±2#*	30±1	35±1#*	27±2	34±2#	28±2	33±2
FAC (%)	19±1	17±2	16±1	23±1#*	17±1	22±1#*	16±1	21±2#	16±1	19±2

OLD RECIPIENT

Donor:	PBS control		Young mouse no ischemia		Old mouse no ischemia		Young mouse with ischemia		Old mouse with ischemia	
DAYS POST MI	7	28	7	28	7	28	7	28	7	28
EDV	113±11	103±9	93±5	93±4	94±6	88±4	108±9+	107±5	86±3	87±4
ESV	79±9	74±8	64±4	69±4	70±5	66±4	79±8+	81±4	60±3	61±4
SV	35±3	29±2	30±2	24±2+	24±1	22±1	29±2	26±2	27±2	26±1
LVEF (%)	31±2	29±2	32±2	26±2#+	27±1	25±2	28±1	24±2	30±2	29±1
FAC (%)	18±2	18±1	19±2	16±1	16±1	14±1	16±1	14±1	18±1	17±1

Table 4.2. Echocardiographic parameters after EDC therapy at day 7 post infarction when the EDCs were injected and 28 days after infarction (21 day after EDC therapy).Values are mean ± SEM. *p≤0.05 vs.

PBS group; # p≤0.05 day 7 vs. day 28; +p≤0.05 young vs. old; EDV: End diastolic volume; ESV: End systolic volume; SV: Stroke volume; LVEF: Left ventricular ejection fraction; FAC: Fractional area shortening.

4.4.2 Advanced donor age and ischemia combine to reduce the antifibrotic effect of EDC transplant

Myocardial scar size in the left ventricle was evaluated using Masson's Trichrome staining 28 days after LCA ligation (4 sections per mouse, 100 μm separation). In contrast to the adverse effect of recipient age on EDC improvement in cardiac function, advanced recipient age did not consistently reduce the salutary effects of EDC transplant on myocardial scar burden (p=ns; Figure 4.14). As shown in Figure 4.14, intramyocardial injection of EDCs from mice with advanced donor age was consistently associated with larger scar sizes compared to young donors (29±1.4 vs 24.6±1.2%, respectively in non-ischemic and 33.7±1.3 vs. 28.6±1.7% in ischemic donors; p≤0.05) although this effect attained significance only in sections from young recipients. Injection of cells from donors with a history of myocardial infarction was also associated with larger scar sizes with significant effects noted only within young recipients injected with EDCs from old donors. Overall, these results suggest that advanced donor age and a history of myocardial infarction combine to reduce the anti-fibrotic effects of EDC transplantation, but this effect was only observed in young mice underscoring the importance of the recipient heart to pro-healing stimulation.

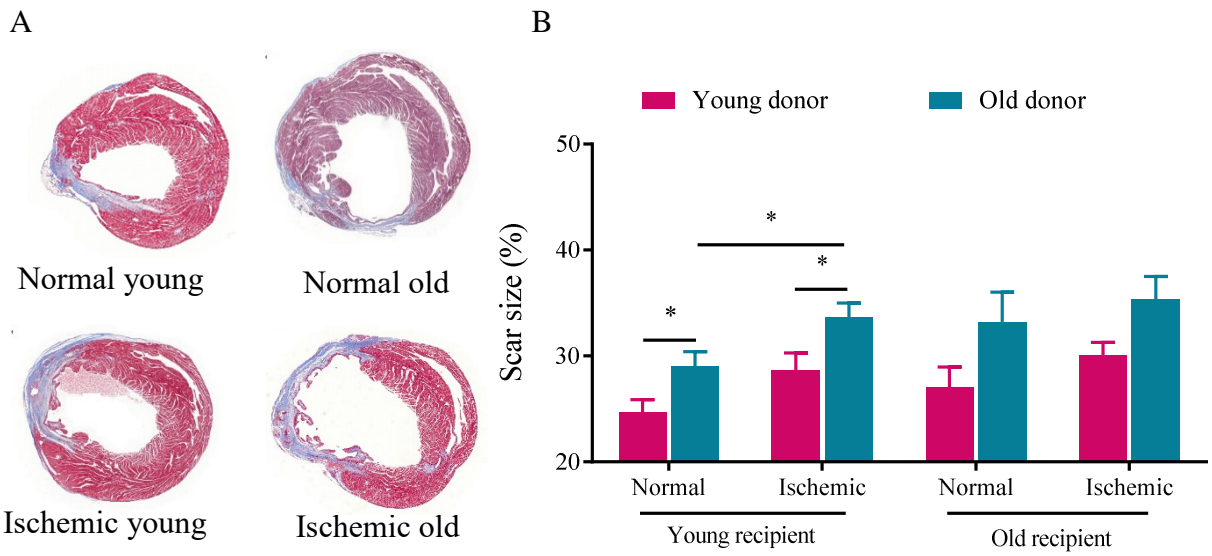

Figure 4.14. Scar size determined by Masson's trichrome staining performed on heart sections at 3 weeks post-treatment. (A) Representative images of Masson's trichrome staining. (B) Calculation of scar size by measuring color threshold of fibrotic tissue relative to the whole ventricular area using image J program. (n=6 per group). Values are mean ± SEM. *p≤0.05

4.4.3 Advanced donor age and ischemia do not alter the pro-angiogenic effect of EDC transplant

Isolectin B4 staining was performed to identify vessels within the infarct border zone of EDC-treated mice 28 days after LCA ligation. As shown in Figure 4.15A and B, EDC source had limited effects on vascularization. EDC recipient had an unanticipated effect on vessel density as old recipients treated with EDCs from young non-infarcted donors demonstrated 1.4±1 fold more vessels within the peri-infarct (4.6±0.4 vs. ~ 3.3 /FOV in all other treated groups; p≤0.05). Thus, in contrast to *in vitro* data showing ischemia increases the pro-angiogenic potential of EDCs, this capacity is not realized *in vivo* as injection of young EDCs within an aged host was the only group that experienced a marked increase in peri-infarct vascularization.

4.4.4 Age and ischemia have negligible effects on the long-term retention of transplanted EDCs

It is intuitive that increased long-term retention of transplanted cells may influence the functional benefits of cell therapy. To investigate this possibility, a separate series of mice were injected with lentiviral-labelled EDCs prior to qPCR detection of GFP transcripts within the left ventricular lysate. Although retention of transplanted EDC s from young donors was slightly greater (Figure 15C), these modest changes were not significant due to high variability and limited number of cells retained 21 days after cell injection. The sex mismatch method (injection of male donor cells to female recipients) to measure engraftment by detecting SRY or RBMY sequences was not successful, as well. This high variation might be due to modest reproducibility and low sensitivity of the technique to detect the few engrafted cells, as the copy number of GFP, SRY and RBMY are much lower than ALU sequences (which has successfully used for human cell retention measurements) and falls below the PCR detection level threshold.

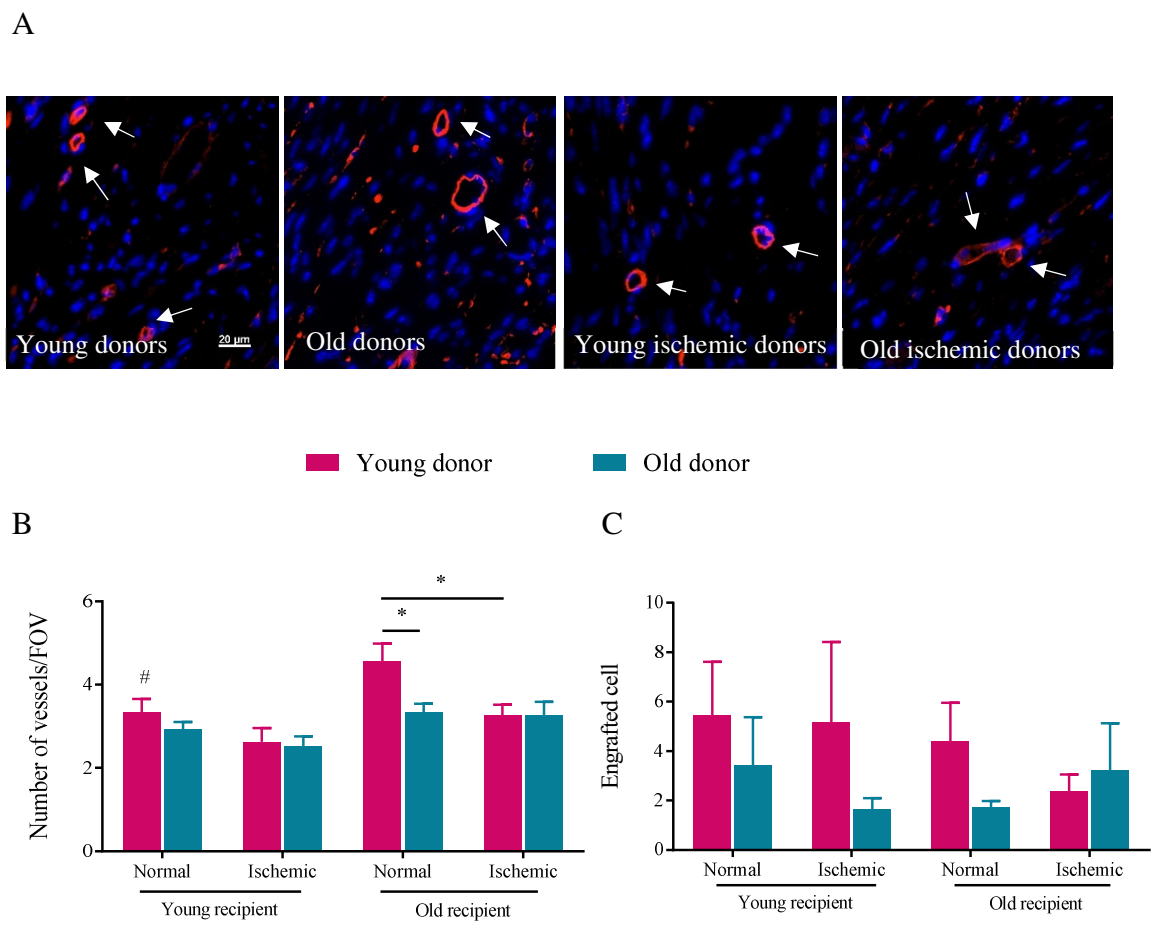

Figure 4.15. EDC mechanism of benefit. The hearts were isolated 3-weeks after EDC injection. (A) Representative images of isolectin B4 staining. (B) Total vessels in the infarct border zone was calculated after isolectin B4 staining. The number of vessels was quantified per field of view in the whole border zone area (n=6 per group). (C) Quantification of GFP+ EDC retention in the heart tissue by qPCR (n=3 per group). The number of cells were quantified using a standard curve made by serial dilution of GFP EDCs. Values are mean ± SEM. *p≤0.05; # p≤0.05 between same donors in different-age recipients

4.5 Microarray transcriptome profiling

4.5.1 Microarray data

Microarray analysis was used to explore the fundamental changes underpinning the observed differences in EDC characteristics and function. To this end, the global gene-expression profiles of EDCs from ischemic old, normal old, ischemic young and normal young mice were directly compared. While hierarchical clustering of genes with a greater than 2-fold change in expression showed substantial alterations in gene expression after ischemia (Figure 4.16A), microarray profiling revealed that aging alone prompted the differential expression of 245 genes (≥2-fold change; FDR≤0.05) that resulted in up-regulation of pro-inflammatory pathways including TREM1, NF-KB, Toll-like receptor and Death Receptor signaling by modulating the upstream regulators, TGFβ1 and IL-6. Figure 4.16B shows the 5 most significant differentially regulated pathways. A history of ischemia resulted in the differential expression of 924 and 773 genes in EDCs from old and young donors, respectively (≥2-fold change; FDR≤0.05). Although inflammatory pathways were activated in EDCs from both old and young donors with a history of myocardial ischemia (i.e., IL-6, NF-KB, TNFR2, TGFβ1 and TNF), ischemia resulted in EDCs sourced from young donors up-regulating NRF2-mediated oxidative stress response and PI3K signalling pathways (compared to normal young donors). In contrast, a history of ischemia in old donors increased the expression of P38 MAPK pathway and inflammation/oxidative stress in these EDCs. Within EDCs cultured from ischemic groups, advanced donor age promoted the differential expression of 145 genes (≥2-fold change; FDR≤0.05) which modify many of the pathways responsible for effective cell cycle regulation namely cell cycle control of chromosomal replication ($p<7.5E-06$), DNA damage induced 14-3-3σ Signaling ($p<5.2E-03$), Mitotic Roles of Polo-Like

Kinase (p<1.3E-2) and Cell Cycle: G2/M DNA Damage Checkpoint Regulation (p< 1.7E-2) (Figure 4.16B).

A

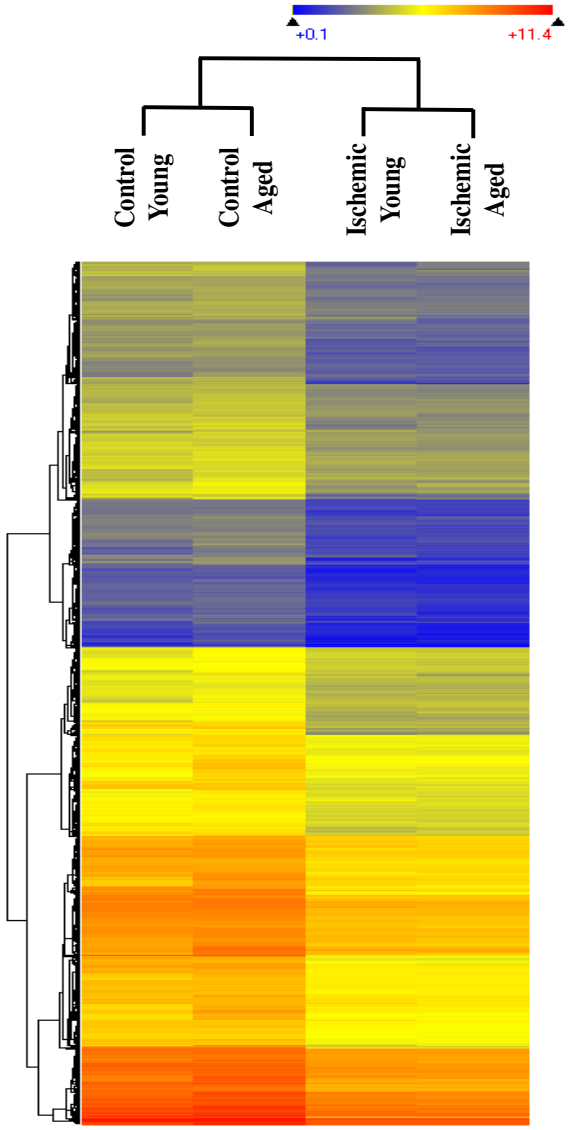

B

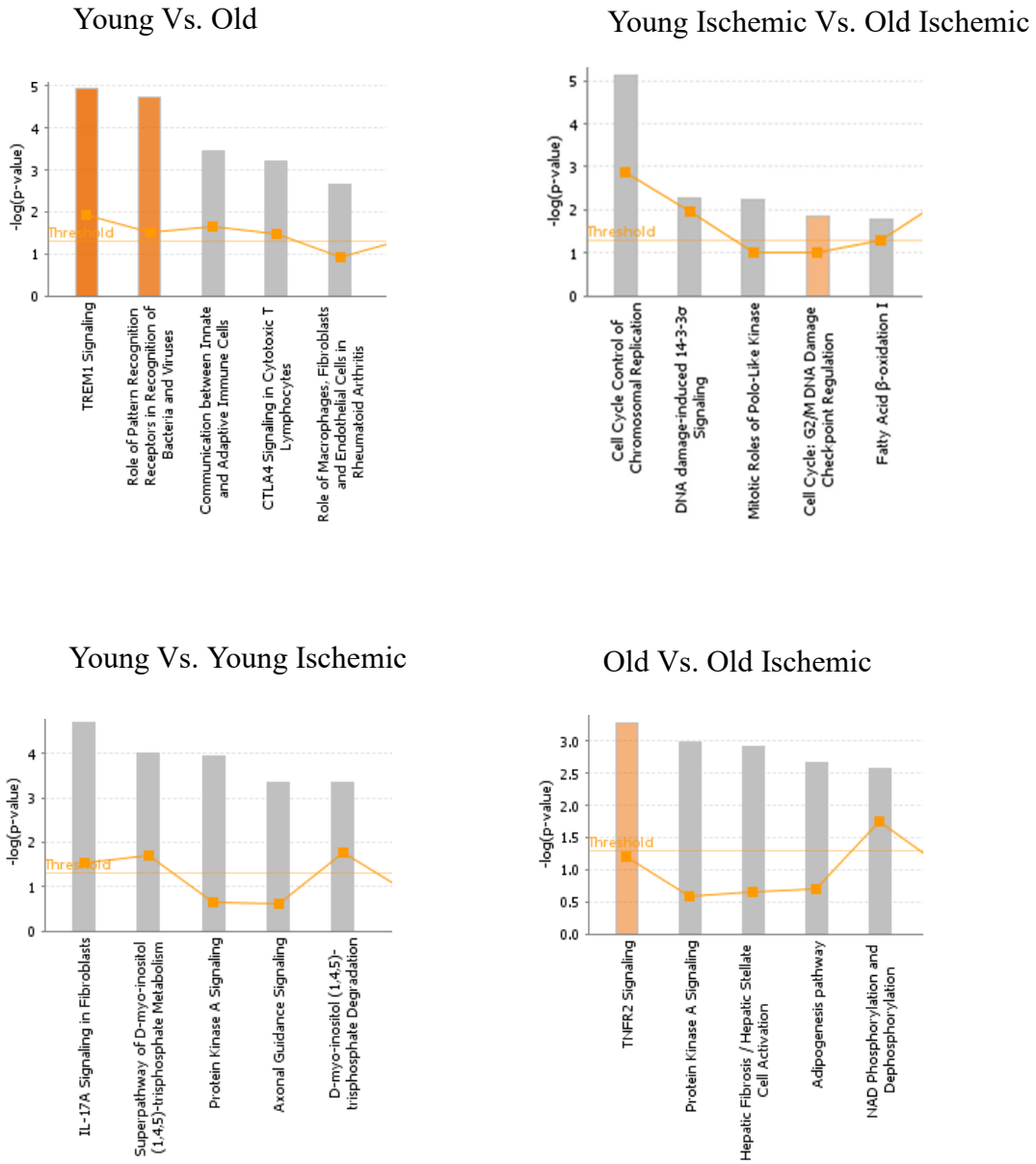

Figure 4.16. Microarray analysis. (A) Hierarchical clustering of genes with more than 2-fold differential expression (FDR≤0.05) using arraystar software. (B) Top canonical pathways determined based on genes whose expression was significantly different between groups (p≤0.01), analyzed by Ingenuity software. Orange bar: predicted to be activated; Gray bar: no activity pattern available; Orange square: the ratio of altered gene to the total genes within a pathway; Y axis shows significance of the changes in a pathway. Above the threshold line is significant (n=3 per group).

4.5.2 qPCR validated the microarray data

A series of differential expressed genes were randomly selected for microarray validation using qPCR, which were Ppp1r16b, Tnf, Cxcr4 and Rgs1 whose expressions varied from 1- to 8- fold between the experimental groups. The expression ratios of these genes between different cohorts were calculated again by qPCR data. The results showed strong correlation between qPCR and microarray data with R^2= 0.97 (p=0.001; Figure 4.17).

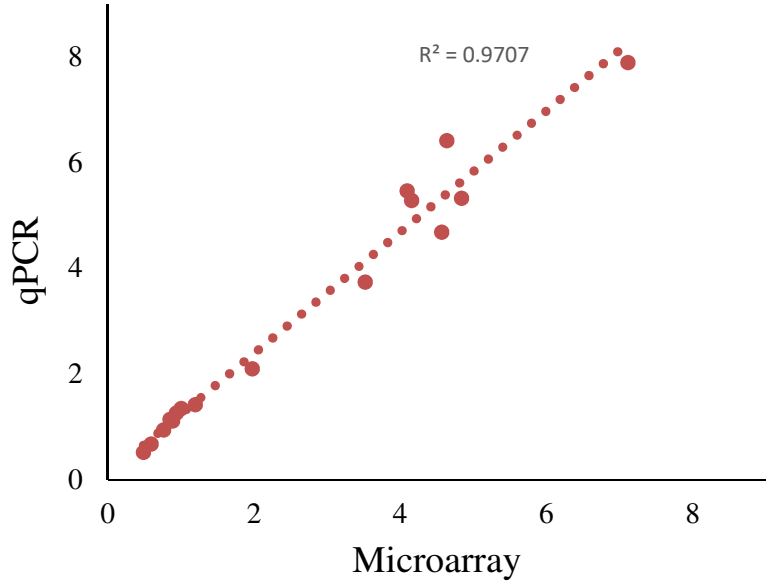

Figure 4.17. Microarray data validation. Five genes were selected for qPCR. Then the expression ratios between the experimental groups was calculated for both qPCR data and microarray data. The ratio correlation validated the accuracy of microarray data (n=3 per group).

4.5.3 Mybl2 is an attractive candidate to rejuvenate aged EDCs

To identify a potential target to rejuvenate aged EDCs prior to autologous therapy, differences between the transcriptome of EDCs from old and young donors with a history of ischemia was explored in depth. The Ingenuity analysis program specifically showed deregulation in cell cycle progression/checkpoint control, interphase/G1/S/mitosis, DNA damage/breakage, replication/

recombination, oxidative stress, p53 signaling and death receptor signaling. Based on the program pathway analysis algorithm and the changes in gene expression, the software predicted activation or inhibition of several upstream regulators including TBX2, E2F1, E2F4, FoxM1, EP400, RB1, HDAC1 and Let-7. When analyzed for any gene with a role in cell cycle control/senescence with more than 1.5 fold differential expression, we identified several molecules including Shcbp1, Mir145, Mir186, Mirlet7c-2, Mir494, Mir323, Sorl1, Mir380, Dlgap5, Fbxo5, Mybl2, Ccnb2, Ska3, COX1, Nqo1 and Chaf1b for further scrutiny. Using the Genome-scale Integrated Analysis of gene Networks in Tissues (GIANT) database to determine the networking of each of the mentioned molecules, we identified Mybl2 as a potential candidate to rejuvenate aged ischemic EDCs as it has a strong association with genes relating to DNA replication and cell cycle checkpoint regulation including some regulators that Ingenuity analysis predicted to have altered activity (such as E2Fs and FoxM1) (Figure 4.18A). Reassuringly, confirmatory qPCR analysis demonstrated a 2.5 fold expression reduction in aged ischemic EDCs compared to young ischemic EDCs (p=0.001; Figure 4.18B).

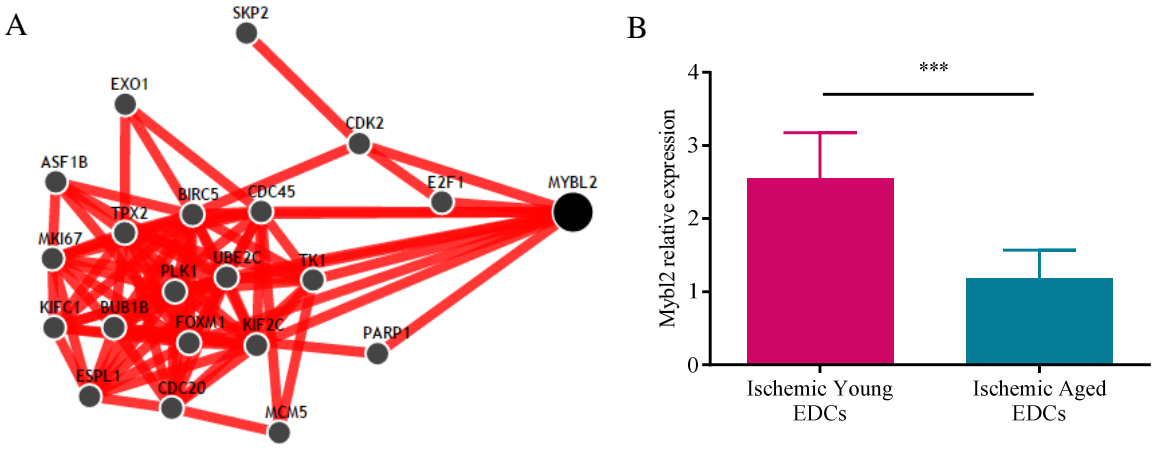

Figure 4.18. Mybl2. (A) Relationship of Mybl2 and 20 genes with high confidence relationship score as determined by GIANT database (B) Mybl2 expression measured by qPCR was normalized to GAPDH and

is shown relative to EDCs from mice with a history of ischemia (n=3 per group). Values are mean ± SEM. ***p=0.001

4.6 Genetic enhancement with Mybl2 rejuvenates aged EDCs

4.6.1 Mybl2 over-expression increases Mybl2 protein and transcription of target genes

Following Mybl2 transduction, we assessed if Mybl2 overexpression was successful. We measured the amount of Mybl2 mRNA by qPCR in EDCs from old donors with a history of myocardial infarction after transduction with Mybl2 or backbone. Figure 4.19A shows that RNA expression of Mybl2 was substantially increased in EDCs after Mybl2 transduction ($p<0.001$ vs. backbone and non-transduced aged ischemic EDCs). This increase in Mybl2 transcript resulted in 1.5±0.04 fold increase in Mybl2 protein ($p<0.05$ vs. backbone and non-transduced EDCs; Figure 4.19B). Backbone transduced, and non-transduced EDCs showed equivalent Mybl2 transcriptome expression and protein levels. As shown in Figure 4.19C, the expression of the Mybl2 target transcripts CDK1, Cyclin B and FoxM1 was increased by 1.6±0.1, 1.2±0.1 and 1.2±0.1 fold relative to backbone transduced EDCs and by 1.4±0.1, 1.15±0.03 and 1.3±0.1 fold relative to non-transduced EDCs, respectively ($p\leq0.05$).

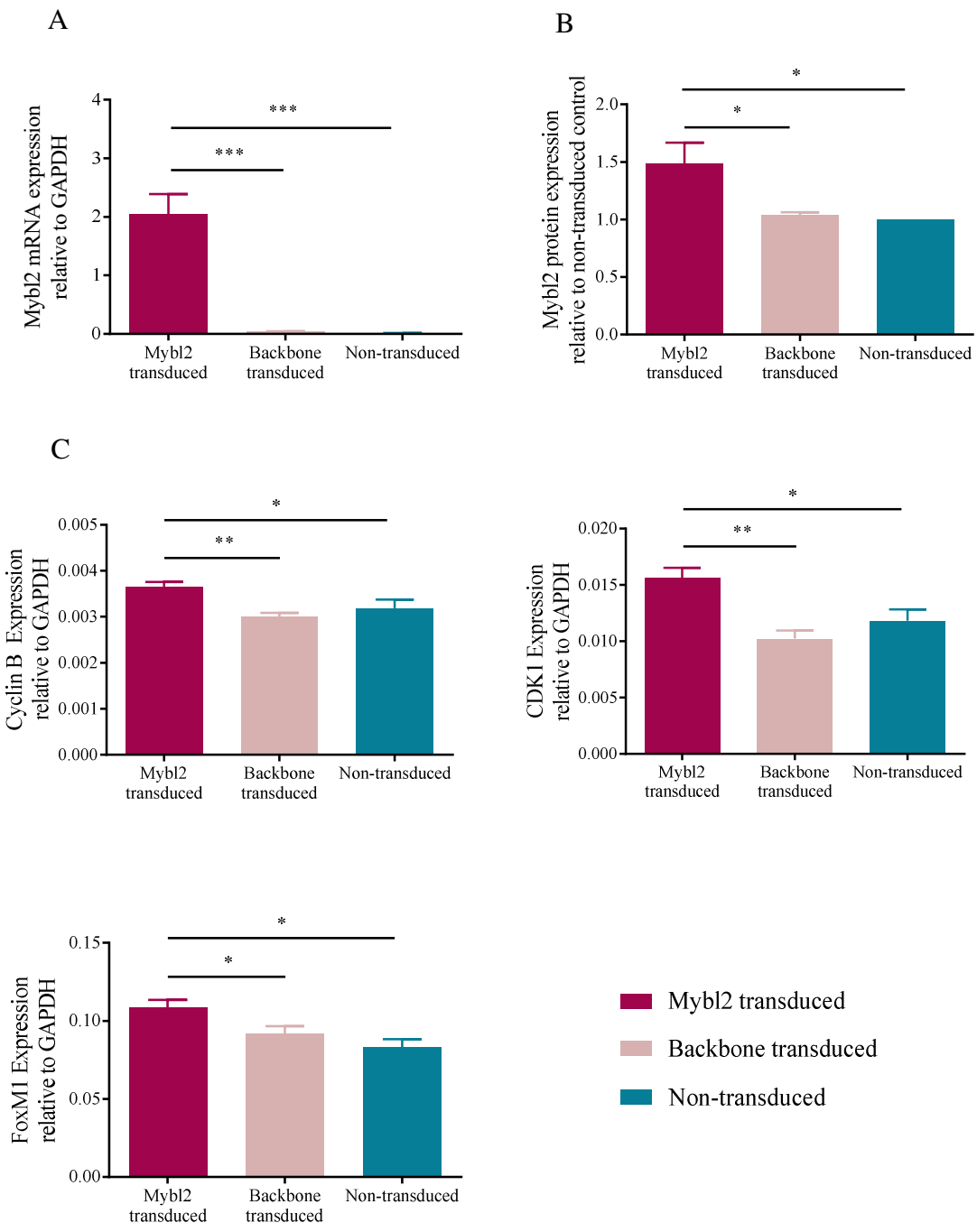

Figure 4.19. Expression of Mybl2 and its target genes. 48h after EDC transduction the expression of (A) Mybl2 mRNA relative to GAPDH by qPCR (n=4 per group) (B) Mybl2 protein by ELISA (n=4 per group) and (C) Mybl2 target gene mRNA by qPCR (n=4 per group) was measured. Values are mean ± SEM. *p≤0.05; **p≤0.01; ***p≤0.001

4.6.2 Mybl2 over-expression reduces EDC senescence

The capacity of Mybl2 to overcome senescence was evaluated by comparing the percentage of β–galactosidase positive cells in Mybl2 transduced EDCs from old ischemic donors. As shown in Figure 4.20, somatic gene transfer of Mybl2 to aged ischemic EDCs reduced the number of senescent EDCs by 61.4±6.4 % ($p<0.001$) and 63.8±5.7% ($p<0.001$) compared to backbone or non-transduced EDCs, respectively. There was no meaningful difference in EDC senescence detected between the backbone and non-transduced EDCs.

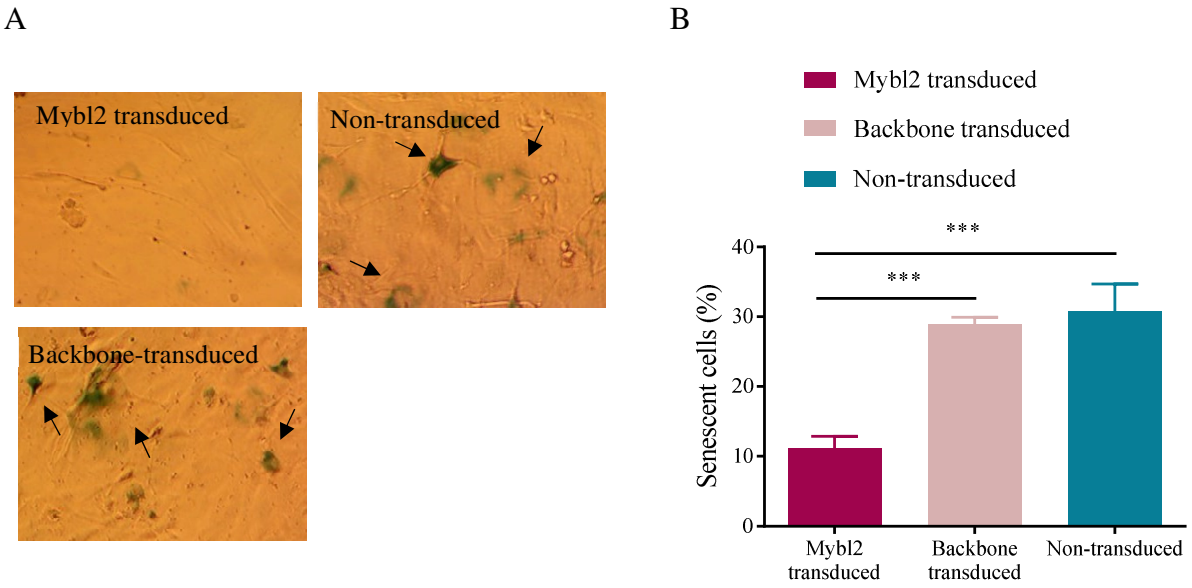

Figure 4.20. Senescence after Mybl2 over-expression. (A) Representative images of senescence-associated β-galactosidase staining (B) The senescent cell number count reported as percentage of senescent cells (n=9 per group). There was a decrease in senescent cell number for Mybl2 overexpressing EDCs compared to the two control groups. Values are mean ± SEM ***p≤0.001

4.6.3 Increased Mybl2 expression and reduced senescent cell number after treatment with senolytic compounds

To explore the hypothesis that Mybl2 is involved in anti-senescence effect of senolytic compounds, we treated EDCs from old ischemic donors with small molecules known to reverse senescence and evaluated effects on Mybl2 expression. As shown in Figure 4.21, treatment of cells with BIO or rapamycin decreased EDC senescence by 63±3 or 53±14% as compared to meBIO treated control EDCs ($p<0.05$). Consistent with a role in EDC senescence, Mybl2 transcripts were increased by 58±1 or 33±2% within BIO or Rapamycin treated EDCs ($p<0.05$ vs. meBIO-treated EDCs).

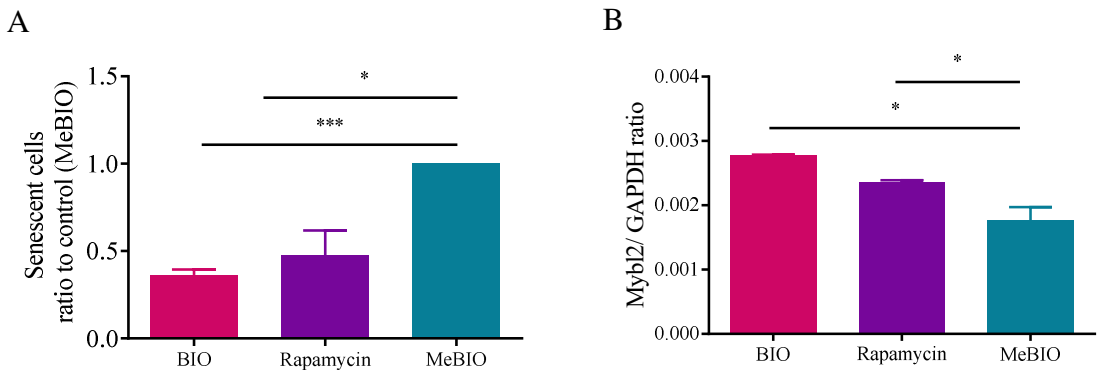

Figure 4.21. BIO and Rapamycin effect on EDCs. (A) Senescent cell quantification by Senescence-associated β-galactosidase staining, followed by DAPI staining. The total number of senescent cells were counted after treatment with Rapamycin 50nM, BIO 2μM and MeBIO 2μM. The number of cells was counted in 6 random fields of view and is reported as a ratio to negative control, MeBIO (n=4 per group). (B) Mybl2 mRNA levels after treatment with Rapamycin 50nM, BIO 2μM and MeBIO 2μM normalized by GAPDH gene. Values are mean ± SEM *$p\leq0.05$ ***$p\leq0.001$

4.6.4 Mybl2 overexpression reduces reactive oxygen species stress within EDCs

As shown in Figure 4.22A, lentiviral transduction alone significantly increased ROS generation (27098±719 a.u in backbone transduced EDCs vs. 19230±1283 units in non-transduced EDCs; $p<0.05$). However, lentiviral-mediated overexpression of Mybl2 reduced ROS content to baseline (21041±798 a.u., p=ns compared to non-transduced EDCs). Given that ROS content reflects the activity of antioxidant enzymes, SOD activity was evaluated in Mybl2 transduced EDCs. As shown in Figure 4.22B, the SOD antioxidant became more active after Mybl2 over-expression in aged ischemic EDCs as compared to non-transduced cells (18.4±1 a.u. vs. 15.3±0.6 a.u., p=0.05).

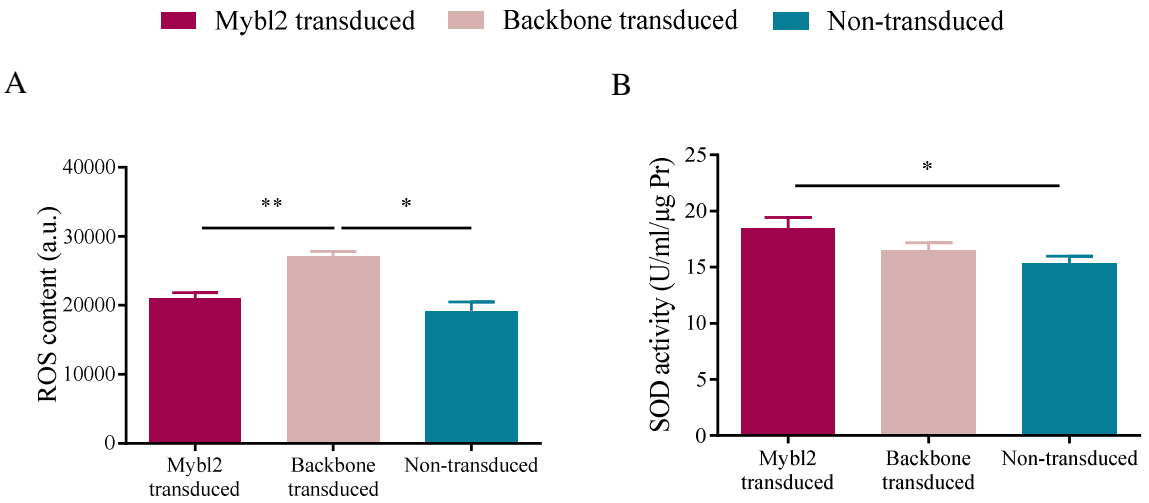

Figure 4.22. ROS formation and handling after Mybl2 over-expression. (A) ROS content within EDCs (n=3 per group). Mybl2 scavenges ROS content of EDCs generated due to transduction, possibly by increasing the SOD activity. (B) SOD activity was measured in the supernatant from sonicated EDCs (n=4 per group). Values are mean ± SEM *p≤0.05; **p≤0.01

4.6.5 Mybl2 overexpression improves the expression of inflammatory and angiogenic cytokines

Given that somatic gene transfer may disrupt the cytokine profile of heart-derived cells (Bonios et al., 2011b), the effect of Mybl2 over-expression on the paracrine signature of EDCs was evaluated using unbiased proteomic profiling of media conditioned by cells under ischemic (1% oxygen) low serum (1% serum) culture condition. As shown in Figure 4.23, lentiviral transduction altered the cytokine secretion of EDCs (Chi square value 5.115, p=0.02 vs. backbone or non-transduced EDC conditioned media). Interestingly, secretion of the angiogenesis-inhibitory cytokine, endostatin, was halved in Mybl2 overexpressing EDCs ($p \leq 0.05$ vs. backbone or non-transduced EDC conditioned media) while amphiregulin, a member of endothelial growth factor family, was increased ($p \leq 0.01$ backbone or non-transduced EDC conditioned media). Other cytokines reduced after Mybl2 overexpression of EDCs comprised the inflammatory cytokines IL-1β, IL-4 and IL-17a ($p \leq 0.01$ vs. backbone or non-transduced EDC conditioned media). Amongst the cytokines found to account for ischemia or age related differences in EDC-stimulated angiogeneiss (proliferin, section 4.3.2) or cell migration (IL-6, section 4.3.3), Mybl2 overexpression had no consistent detectable effects on cytokine content within conditioned media.

A

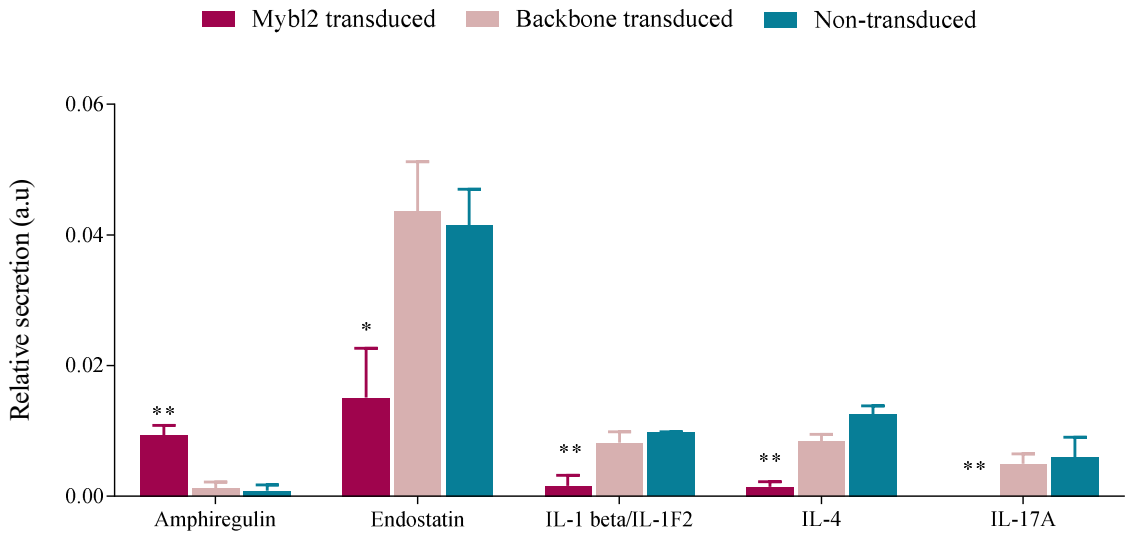
Mybl2 transduced
Backbone transduced
Non-transduced
Relative secretion (a.u)
0.06
0.04
0.02
0.00
**
*
**
**
**
Amphiregulin
Endostatin
IL-1 beta/IL-1F2
IL-4
IL-17A

B

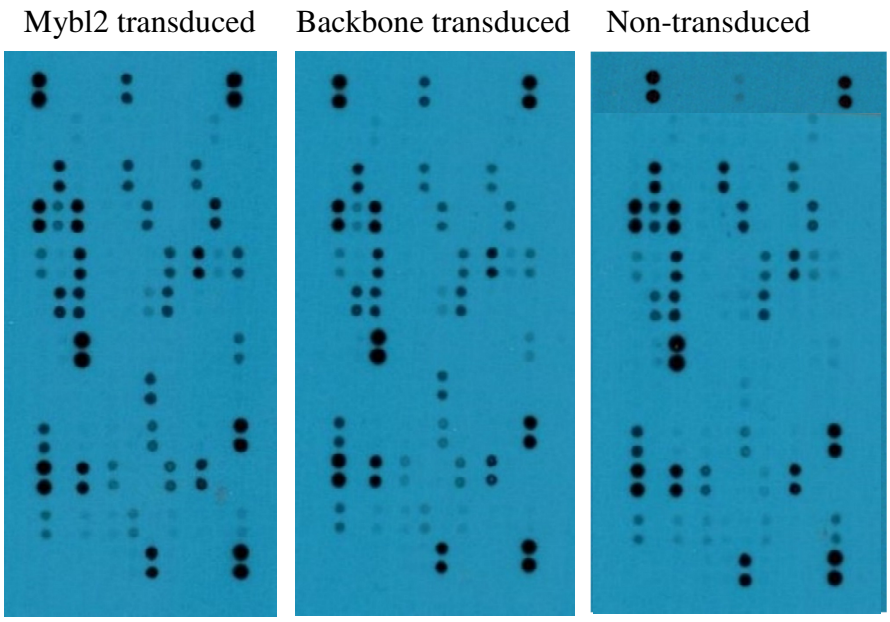
Mybl2 transduced
Backbone transduced
Non-transduced

C

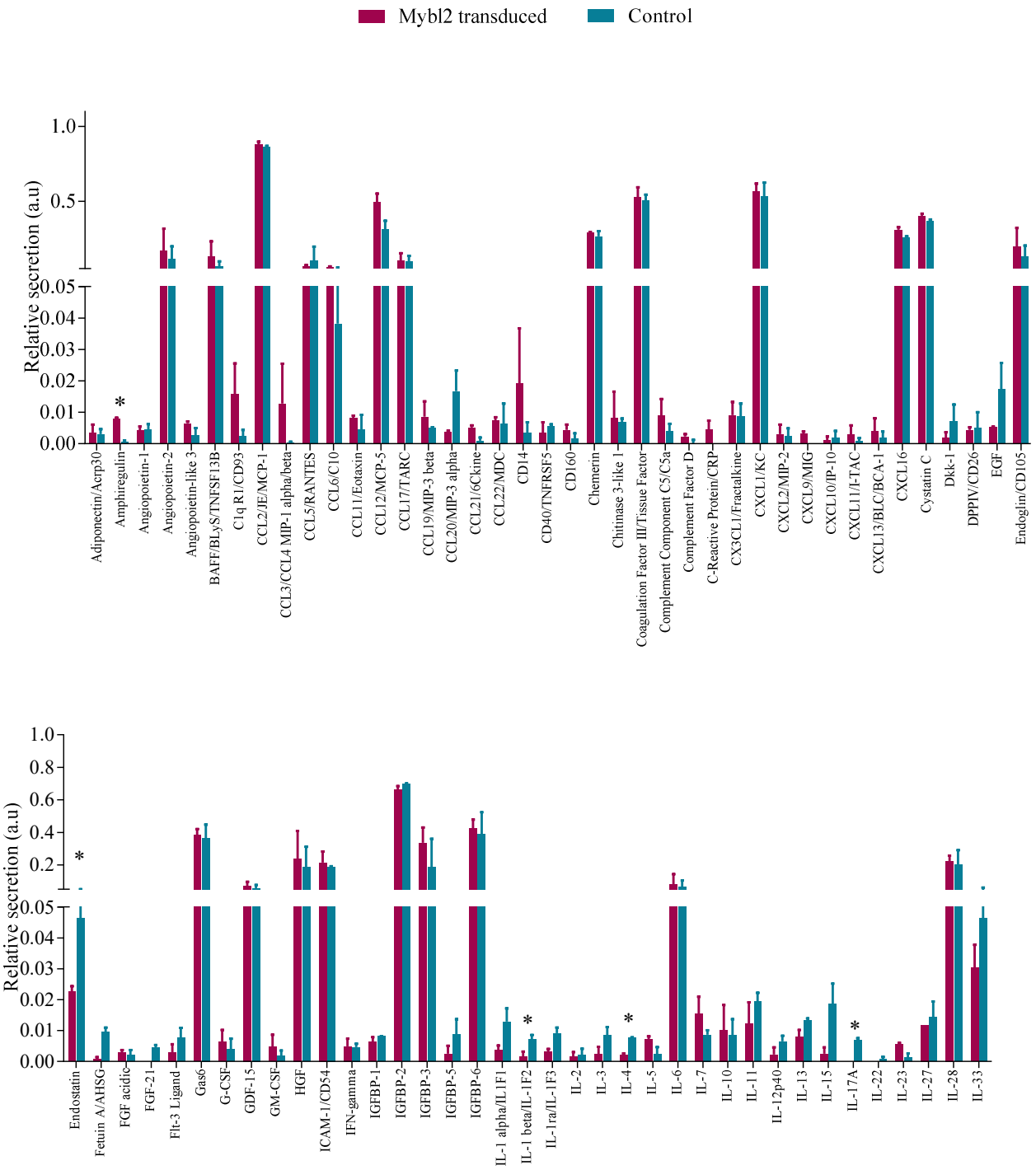
Mybl2 transduced
Control
Relative secretion (a.u)
1.0
0.5
0.05
0.04
0.03
0.02
0.01
0.00
*
Adiponectin/Acrp30
Amphiregulin
Angiopoietin-1
Angiopoietin-2
Angiopoietin-like 3
BAFF/BLyS/TNFSF13B
C1q R1/CD93
CCL2/JE/MCP-1
CCL3/CCL4 MIP-1 alpha/beta
CCL5/RANTES
CCL6/C10
CCL11/Eotaxin
CCL12/MCP-5
CCL17/TARC
CCL19/MIP-3 beta
CCL20/MIP-3 alpha
CCL21/6Ckine
CCL22/MDC
CD14
CD40/TNFRSF5
CD160
Chemerin
Chitinase 3-like 1
Coagulation Factor III/Tissue Factor
Complement Component C5/C5a
Complement Factor D
C-Reactive Protein/CRP
CX3CL1/Fractalkine
CXCL1/KC
CXCL2/MIP-2
CXCL9/MIG
CXCL10/IP-10
CXCL11/I-TAC
CXCL13/BLC/BCA-1
CXCL16
Cystatin C
Dkk-1
DPPIV/CD26
EGF
Endoglin/CD105
Relative secretion (a.u)
1.0
0.8
0.6
0.4
0.2
0.05
0.04
0.03
0.02
0.01
0.00
*
*
*
*
Endostatin
Fetuin A/AHSG
FGF acidic
FGF-21
Flt-3 Ligand
Gas6
G-CSF
GDF-15
GM-CSF
HGF
ICAM-1/CD54
IFN-gamma
IGFBP-1
IGFBP-2
IGFBP-3
IGFBP-5
IGFBP-6
IL-1 alpha/IL1F1
IL-1 beta/IL-1F2
IL-1ra/IL-1F3
IL-2
IL-3
IL-4
IL-5
IL-6
IL-7
IL-10
IL-11
IL-12p40
IL-13
IL-15
IL-17A
IL-22
IL-23
IL-27
IL-28
IL-33

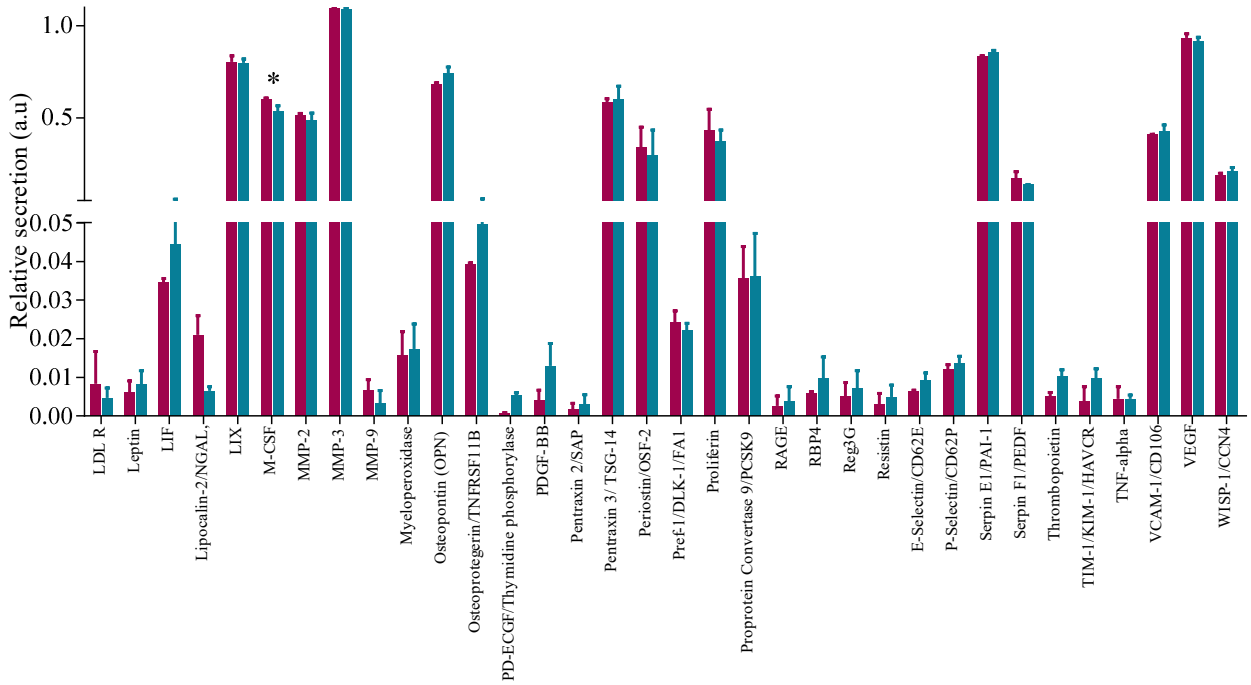

Figure 4.23. Profiling of mouse secreted cytokines after Mybl2 over-expression. After conditioned media collection, the amount of 111 cytokines was quantified. (A) Amongst all cytokines, five cytokines were expressed differently (n=3 per group). (B) Representative images of EDC expression of 111 cytokines. Data shown from 5-minute exposure. (C) Quantification of secreted cytokines (n=3 per group). The data for the two control groups are combined for this picture. There was no difference between backbone transduced and non-transduced. Values are mean ± SEM *p≤0.05; **p≤0.01 Mybl2 over-expressing compared to backbone transduced or non-transduced control groups

4.7. Mybl2 over-expression enhances therapeutic potency of transplanted aged ischemic EDCs

4.7.1 Greater functional improvement with reduced scar size was achieved after injection of Mybl2 over-expressing EDCs

The effect of Mybl2 overexpression within EDC on cardiac function after ischemic injury was evaluated in young mice randomized 1 week after LCA ligation to echocardiographic guided intra-myocardial injection of Mybl2, backbone or non-transduced EDCs. Three weeks after EDC

injection, transplant of Mybl2 overexpressing EDCs provided a 6.3±0.8% absolute increase in LVEF from baseline while transplant of backbone or non-transduced EDCs increased ejection fraction by 3.7±0.8 or 2.7±0.6% from baseline, respectively ($p \leq 0.05$; Figure 4.24A). This capacity to enhance cardiac function after ischemic injury was comparable to the effects observed following injection of EDCs from normal young donors (7.8±0.7% absolute increase in LVEF from baseline; $p=0.11$; Figure 4.13). Backbone-transduced cells provided equal benefit compared to non-transduced EDCs. After myocardial infarction remodelling occurred within the hearts regardless of the transplanted cell type. At day 28 post ischemia, the hearts from all experimental groups showed similar end diastole volumes, however, the relative change from baseline was less in Mybl2 treated group (Table 4.3).

Four weeks after LCA ligation, similar degrees of myocardial scarring were observed after injection of backbone or non-transduced EDCs (34.2±2 vs. 35.9±2.5 %, respectively; $p=0.63$; Figure 4.24 B and C). Consistent with the myocardial function effects, transplant of Mybl2 transduced EDCs reduced infarct size compared to non-transduced EDCs ($p<0.05$) and showed a promising trend compared to backbone transduced control ($p=0.06$). Mybl2 overexpressing EDCs provided scar reductions similar to the ones observed following injection of EDCs from normal young donors (27.6±2.2 vs. 25.6±1.1 %, respectively; $p=0.44$; Figure 4.14). Taken together, these results indicate an improvement in the capacity of EDCs from old ischemic donors when enhanced by somatic gene transfer of Mybl2.

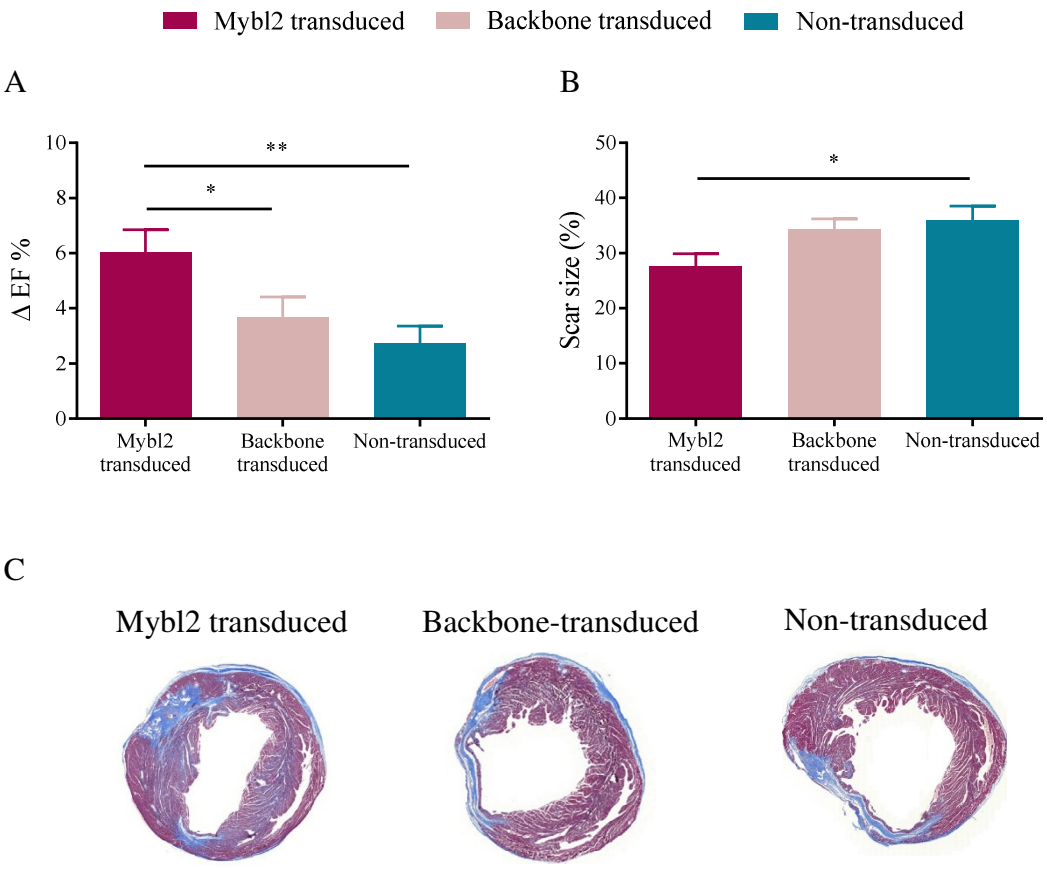

Figure 4.24. Functional evaluation and scar size calculation following Mybl2 over-expressing EDC transplantation. (A) Improvement in heart function was assessed following injection of 100,000 cells into LCA ligated mouse heart by measuring the difference in ejection fraction at baseline and after 3 weeks (n=9 per group). Mybl2 over-expressing cells provided greater benefit compared to the control groups. (B) Masson's trichrome staining was used to calculate fibrotic tissue and reported as scar size (n=5 per group). (C) Representative pictures of Masson's Trichrome staining. Values are mean ± SEM. *p≤0.05; **p≤0.01

Donor:	Mybl2 transduced		Backbone transduced		Non transduced	
Days post MI	7	28	7	28	7	28
EDV	50.6±2.4	60.7±1.8#	48.6±3.2	62.4±3.6#	48.5±2.5	60.5±2.7#
ESV	33.7±1.9	36.8±1.7	33.2±2.8	40.2±3	32.2±2.2	38.6±2.8
SV	16.9±1	23.9±1.1#	15.4±0.7	22.3±0.9#	16.3±0.8	21.9±0.7#
LVEF (%)	33.5±1.4	39.5±1.7#	32.5±1.6	36.2±1.4	33.9±1.7	36.7±1.8#
FAC (%)	20.3±1	25.3±1.2#	18.6±1.1	22.5±0.9#	20.6±1.1	21.8±1.3#

Table 4.3. Echocardiographic parameters after transgenic EDC injection at day 7 post infarction when the EDCs were injected and 28 days after infarction (21 day after EDC therapy). Values are mean ± SEM.; # $p \leq 0.05$ day 7 vs day 28; EDV: End diastolic volume; ESV: End systolic volume; SV: Stroke volume; LVEF: Left ventricular ejection fraction; FAC: Fractional area shortening.

4.7.2 Mybl2 over-expression increases vascular density

Following the observation that endostatin secretion was reduced by Mybl2 over-expression, we measured *in vivo* vessel formation using isolectin B4 staining on heart sections collected and prepared 3 weeks after EDC injection. The number of vessels were counted in the infarct/border zone area. As shown in Figure 4.25, viral transduction alone had no effect on vessel density while transplant of EDCs that overexpressed Mybl2 increased the vessel density (4.4±0.2/FOV) compared to mice injected with non-transduced EDCs (2.3±0.4/FOV, $p<0.01$) and showed a tendency to increase the vessel density compared to mice injected with backbone transduced EDCs (2.7±0.6/FOV, $p=0.06$). Interestingly, transplant of aged ischemic EDCs after Mybl2 overexpression increased peri-infarct vessel density to a greater extent than seen after transplant of EDCs cultured from normal young donors (3.3±0.3/FOV, $p<0.05$; Figure 4.15).

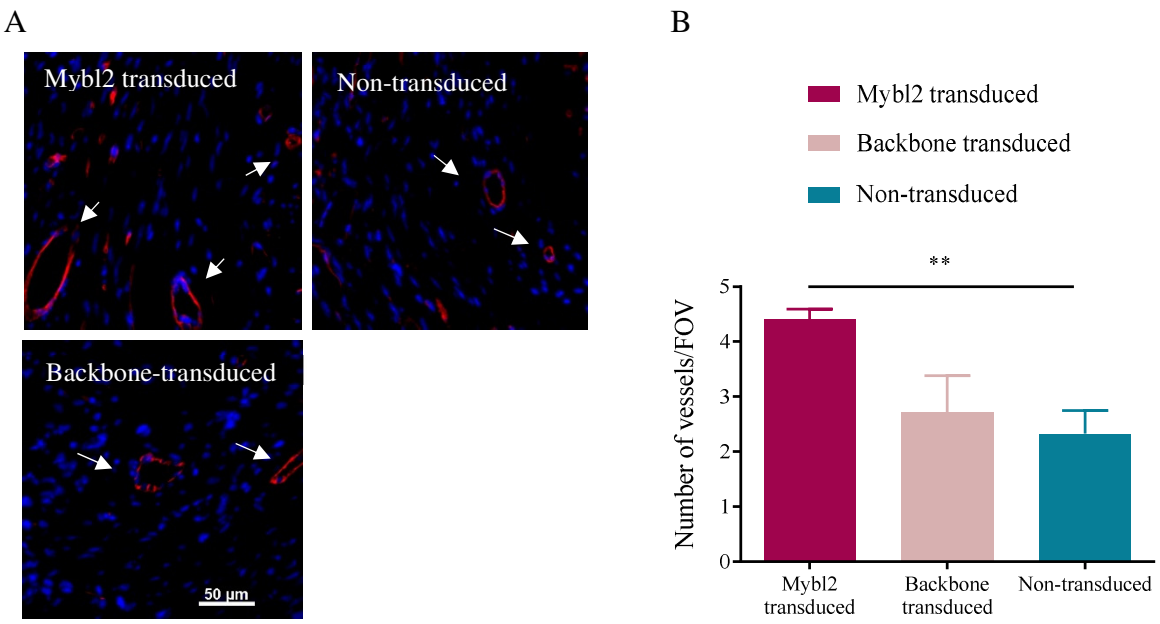

Figure 4.25. Isolectin B4 staining for assessment of vascular density in the border zone/ infarct area after Mybl2 over-expressing EDC injection. (A) Representative images of isolectin B4 staining. (B) Quantification of vessel number. The data are the average of 6 random fields (n=5 per group). We observed that Mybl2 over-expressing EDCs were more capable of inducing vessel formation. Values are mean ± SEM. **p≤0.01

4.7.3 Similar infiltration rate was observed 4 weeks after Mybl2+/- EDC injection

Proteomic-profiling suggested that Mybl2 overexpression alters the production of inflammatory cytokines. Therefore, the number of CD68 macrophages was quantified 3 weeks after EDC injection. As shown in Figure 4.26, there was no appreciable difference in CD68+ cell density between the experimental cohorts within the pre-infarct zone. This finding may be attributed to the modest production of IL-1β, IL-4 and IL-17 as seen in the non-transduced EDC conditioned media or the observation that the inflammatory phase post infarct healing (and macrophage recruitment) had essentially resolved by the time of heart collection.

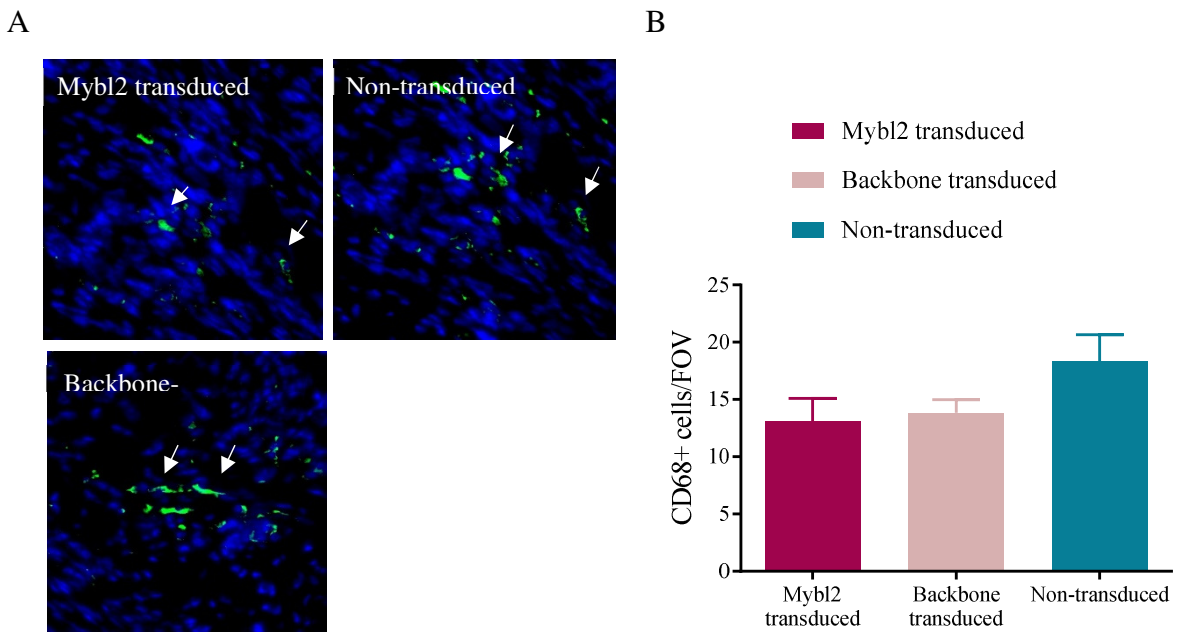

Figure 4.26. CD68 staining. Three weeks after EDC injection, the hearts were collected and sectioned. After CD68 staining, the total number of CD68+ macrophages per field of view was counted in the border zone/ infarct area. (A) Representative images of CD68+ staining. (B) Quantification of CD68+ macrophages. The data is the average of 6 random fields (n=5 per group). We did not observe any changes in the number of CD68+ cells. Values are mean ± SEM. **p≤0.01

4.7.4 Mybl2 overexpression enhances EDC retention

The effect of Mybl2 over-expression on retention was evaluated in a separate cohort of mice injected using EDCs from old ischemic donors double transduced with luciferase using lentivirus. As shown in Figure 4.27, bioluminescent imaging was performed 1, 3, 5 and 7 days after intramyocardial injection of EDCs and robust bioluminescent signals detected in all 3 groups 1 day after cell injection. These signals diminished over time with Mybl2 treated EDCs demonstrating an appreciable difference 5 days after injection (70.8±13.7 % of the peak bioluminescent signal detected 1 day after cell injection relative to 31.6±8.5 in backbone or 18.5±4 in non-transduced EDC treated mice; p≤0.05; Figure 4.27B). By 7 days after cell injection, there

was no detectable bioluminescent signal in any of the treated animals. This data hints that the benefits observed after injection of EDCs genetically engineered to overexpress Mybl2 may be partially attributable to increased (albeit transient) persistence of transplanted cells.

A

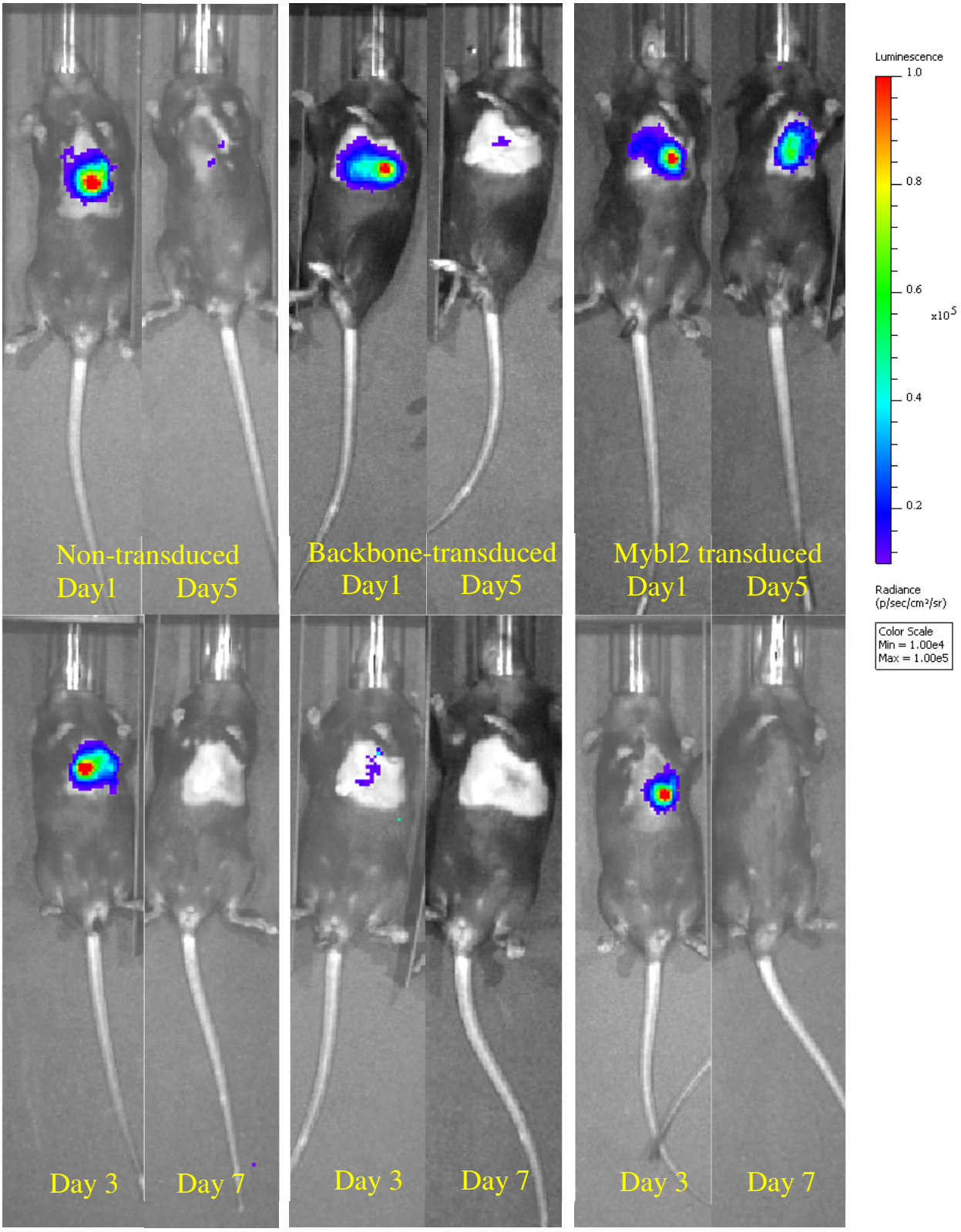
Non-transduced
Day1
Day5
Backbone-transduced
Day1
Day5
Mybl2 transduced
Day1
Day5
Day 3
Day 7
Day 3
Day 7
Day 3
Day 7
Luminescence
1.0
0.8
0.6
x10^5
0.4
0.2
Radiance
(p/sec/cm²/sr)
Color Scale
Min = 1.00e4
Max = 1.00e5

B

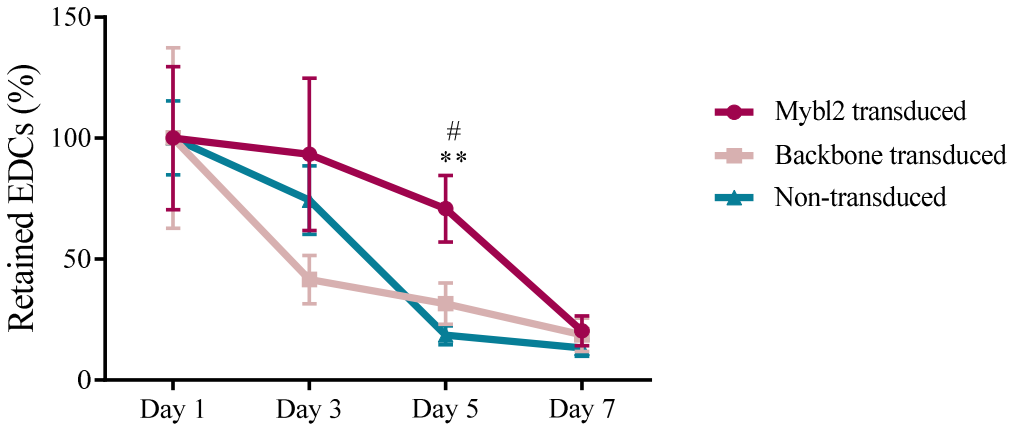

Figure 4.27. Effect of Mybl2 on EDC retention. Bioluminescence signal was evaluated 1, 3, 5 and 7 days after EDC injection using IVIS imaging system (n=6 per group). (A) Representative images of IVIS imaging. (B) Quantification of retention. The percentage of retained cells was determined by calculating the signal ratio to day 1. Evaluation of the luminescence signal by live imaging software showed a profound increase in retention after Mybl2-overexpression. Values are mean ± SEM. #p≤0.05 relative to Backbone transduced; **p≤0.01 relative to non-transduced.

5. DISCUSSION

A sophisticated carbon-dating method revealed that the annual myocyte turn-over in humans is around 1% per year at a young age (Bergmann et al., 2009). Although this data suggests that innate cardiac regeneration is very limited, it brings hope that regeneration of the heart is possible. One way to take advantage of this regeneration mechanism is through *ex vivo* expansion of cardiac stem cells and their reintroduction to the heart to boost endogenous salvage of damaged tissue. During the last fifteen years, several studies on animal models have shown significant functional improvements after cardiac stem cell transplantation; however, these results were not consistently reproducible in clinical trials (Makkar et al., 2012; Malliaras et al., 2014b). This likely arises from the common pre-clinical testing practice of using healthy young donors for stem cell preparation followed by transplantation into young recipients. Given the 1% myocyte turnover decreases to 0.1 % in people over the age of 65, it is probable that aged recipient patients do not benefit from stem cell therapy as much as young recipients (Bergmann et al., 2009). In this project, we answered some of the limitations regarding models used in cardiac stem cell therapy research. We explored the effect of age and ischemia to help in designing the next generation stem cell therapy products specific for different complication contexts. We showed aging deteriorates stem cell function mainly through activation of senescent pathways which is in turn negatively synergized by ischemia. Cell cycle dysregulation was corrected by Mybl2 over-expression as it reduced senescence to restore lost potency and improved heart function after transplant into a mouse model of myocardial ischemia.

5.1 Senescence- associated secretory phenotype

All cells are in constant communication with their microenvironment. Within the culture dish, cells respond to oxygen, pH levels and molecules that are secreted from surrounding cells but at same time they contribute to their microenvironment by secreting messenger molecules themselves. We observed that the population of senescent cells was higher in EDCs sourced from old mice. In addition to the typical characteristic of senescent cells (i.e., growth arrest), these live dynamic aged cells undergo changes in cell pathways and develop a secretory phenotype which is specific to the cell type (Coppé et al., 2010). Amongst the cytokines that characterize the SASP of EDCs, we noted greater secretion of the pleiotropic cytokine IL-6. Our lab previously has shown that IL-6 provides benefits in EDC transplantation therapy. Using hairpin RNA technology, we demonstrated that IL-6 induces migration of circulating angiogenic cells *in vitro* and reduces the apoptosis of cardiac cells *in vivo* (Mayfield et al.,2017). In this project, we observed greater migration of BMDCs through transwell pores. When we measured population doubling time, we did not observe any changes in the proliferation rate of different groups despite the existence of a population of senescent cells in aged EDCs that are not able to divide. This observation may be partially explained by the ability of IL-6 to enhance cell proliferation (Kuhn et al., 2014; Ishikawa et al., 2003); suggesting that steadiness in the overall proliferation rate in our different EDC cohorts is possibly a resultant of SASP pro-proliferation effect on dividing cells in the presence of non-dividing cells.

5.2 Notch signaling and EDC emigration from the tissue explant

The total number of EDCs collected from non-ischemic old donor tissue explants was the least among all our experimental groups whereas a history of ischemic injury improved the total EDC

yield from aged cardiac tissues. Although, the trend in the EDC yields matched the population doubling times, the change in EDC yields was significant but the change in the population doubling times was modest. We assume that this large difference in EDC yields is not attributable to different proliferation rates over time, but rather it is attributable to the generation and/or migration of EDCs out of the tissue; particularly, as we observed fewer EDCs coming out of the non-infarcted aged tissues after a significant delay. The origin of the EDCs is not known, although we know that the majority of these cells (98%) do not originate from cardiomyocytes (Davis et al., 2010a). Previous work has shown that EDC formation and growth depends on the epithelial to mesenchymal transition (EMT) within cardiac biopsies. Similarly, the EMT mechanism has been proposed to be involved in formation of progenitor cells from epicardium *in vivo* (Smits et al., 2018). This EMT transition involves Notch signaling (Zakharova et al., 2012). During aging, Notch signaling is deactivated in satellite cells leading to a decline in their regenerative function (Conboy and Rando, 2005). Our microarray data showed alteration in some of the molecules involving in Notch signalling within EDCs sourced from non-infarcted old hearts. Among the Notch-related molecules, we observed a reduction in Notch ligand, Jagged1, with further reduction in some of the downstream targets of Notch receptor namely, Hes1, Hes7 and Numb1. Ischemia, however, activated this pathway which also has been reported by other investigators (Li et al., 2010b). Hence, variations in EDC yield likely result from our observed changes in Notch signaling.

5.3 Aged stem cells derived from ischemic mice are more angiogenic

The main cause for ischemic cardiomyopathy incident is angiopathy. With age, endothelial cells show dysfunction and vessel formation decreases, while, angiogenesis is required for oxygenation of cardiac tissue and switching the stem cell niche from the hypoxic state that favors quiescence to the normoxic state that favors proliferation and differentiation. In addition, angiogenesis is

important for reperfusion of ischemic tissue (Reed and Edelberg, 2004; Cheung and Rando, 2013; Sanada et al., 2014). Although, ischemia pre-conditioning promotes angiogenesis, it is not clear if chronic heart failure would affect angiogenesis of cardiac stem cells (Maulik and Das, 2002; Fukuda et al.,2004). In this report, we evaluated both the intrinsic ability of EDCs to differentiate into endothelial cells and their ability to induce angiogenesis in progenitor cells via paracrine stimulation. As shown by flow cytometry, EDCs sourced from ischemic old mice are more angiogenic. We achieved more endothelial cells *in vitro* after EDC differentiation while the percentage of the CD34+ cells is decreasing after ischemia. This may be explained by my colleague's work showing that other fractions of EDCs also differentiate into endothelial cells (unpublished data-Davis lab). Furthermore, different cell populations within EDCs have been characterized before and other type of cells with endothelial progenitor properties were detected such as CD31+ cells (Davis et al., 2010a). Thus, the increase in percentage of differentiated cells to endothelial lineage can be because of alteration in other endothelial progenitor populations of EDCs. Alike EDCs from old ischemic donors, it is probable that the innate cardiac stem cells residing within the cardiac tissue of old infarcted recipients be more prone to differentiate into endothelial cells and form new vessels in response to paracrine signaling. Nevertheless, the increased angiogenic potency within EDCs has little manifestation *in vivo* as very few cells are retained in the heart 3 weeks after transplantation (<1% of the initial injectate) (Terrovitis et al., 2009). Thus, most of the *in vivo* angiogenesis seen after cell transplantation is provided by paracrine secretion. Others estimate that 80% of new endothelial cells originate from host tissue (Chimenti et al., 2010). The effectiveness of paracrine stimulation to injured myocardium is influenced by several factors including the number of engrafted cells, secreted cytokine abundance and the spectrum of factors released by individual EDCs and the responsiveness of host cells.

Therefore, young non-infarcted EDCs with greater retention and a broader array of cytokines produced would likely increase stimulation of endogenous angiogenic cells to form vessels. *In vivo* experiments confirmed this notion as old hearts modestly generated more vessels than young hearts when provided with equivalent cells of equivalent potency and this increase was more profound in the old hearts which received young normal EDCs. Our work agrees with research reports showing that angiogenesis impairment is due to diminished paracrine signaling within the aged individuals and presentation of exogeneous angiogenic cytokines restores vessel formation whinin ischemic hindlimb (Rivard et al., 1999) and infarcted myocardium (Edelberg et al., 2002).

Within the cytokine signature of EDCs, proliferin secretion increased tremendously after ischemia while other angiogenic cytokines declined. Following depletion of proliferin, we saw decreased tubule formation in ischemic groups *in vitro*. While we anticipated to see more vessels after EDC therapy, we did not observe this expected benefit. Given that proliferin is typically released by placenta in large quantities and HUVECs are derived from umbilical cord, it follows that HUVECs may be a more responsive target for proliferin than cardiac progenitors. The minimal effect seen *in vivo* could also be due to the low frequency of proliferin receptor on cardiac progenitor cells. Proliferin conducts its effects through the mannose 6-phosphate receptor (Volpert et al., 1996) but the prevalence of proliferin receptor in the mouse heart endothelial cells has not been reported. The only report on proliferin effect in cardiac tissue suggests a hypertrophic role for this factor (Dang et al., 2015). It is worth mentioning that proliferin (Prl2c2) is mouse specific and extension to human cells is uncertain (Jackson et al., 1994)

5.4 The importance of distinguishing effect of age and ischemia

Autologous stem cell therapy is a more desirable choice in cell therapy rather than allogenic stem cell therapy as it does pose a risk of immune rejection and provides the opportunity for engrafted cells to differentiate into working heart tissue. Autologous stem cell therapy is safer and more cost effective rather than iPS cells (Khatiwala and Cai, 2016), but as shown it is influenced by the patient's age and co-morbidities. There have been studies seeking to identify the effect of cardiac risk factors on stem cells. Our lab has previously shown that accumulating medical comorbidities determine the potency of EDCs for cardiac regeneration (Mayfield et al., 2016). The effect of aging has been evaluated in several different stem cell types. The results are not always consistent between the different types of stem cells and they seem to be affected by stem cell character. Within the Sca1+CD31- cells, the cells derived from old mice demonstrated reduced proliferation and differentiation capacity to all cardiac lineages, and their microarray data showed an impairment in vitamin B6 metabolism (Qiong et al., 2017). In the cardiac literature, c-Kit+ cells from old mice have reduced potency for inducing tubule formation and impaired response to dexamethasone treatment (Castaldi et al., 2017). These results were not identical with the data obtained from aged EDCs in our study; however, there were some similarities such as an increase in the number of senescent cells. CDCs sourced from human non-ischemic patients of different age with NYHA class I or II heart failure have been evaluated for markers of senescence. While they showed aged CDCs from patients over 65 years of age have increased p53 and markers of DNA damage, our EDC microarray showed equal p53 expression but a significant change in p16 and RB mRNA. Given that CDCs originate from EDCs, increases in p53 level in CDCs may have resulted from long culture time in these cells or the greater disparity in donor age (i.e., 65 years in a human ≈ 22 months in a mouse). In contrast to our EDCs, the IL-6 secretion level was remained

unchanged in CDCs from non-ischemic aged patients (Nakamura et al., 2016) which may be attributable to their disease condition. Although the cardiac progenitor cells collected by diverse methods are all heart derived, it is not surprising to see dissimilar SASP cytokines as SASP is different between various cell types (Coppé et al., 2010).

The effect of ischemia has been evaluated in several stem cell types; however, these studies model patients with many different medical backgrounds. Bone marrow cells from patients with ischemic heart failure had lower capacity for colony formation, migration and *in vivo* revascularization when injected into ischemic hindlimb model (Heeschen et al., 2004). In terms of cardiac-derived cells, c-Kit+ cells from healthy donor hearts were more clonogenic with less expression of markers of senescence than c-Kit+ cells from explant hearts (Cesselli et al., 2011). Also, measurement of cytokines secreted from explant heart derived c-Kit+ cells showed high secretion of IL-1β and equal secretion of IL-6 compared to the ones from young donor hearts (Avolio et al., 2014) unlike our EDCs from old donors after myocardial infarction which showed low IL-1β secretion and elevated IL-6. Unfortunately, straightforward extrapolation of these effects is not possible as the incorporation of risk factors that resulted in end stage heart failure is not well described in these studies. Our study is the first to discriminate the effect of aging and ischemia separately on stem cells. As mentioned above, the impact of other medical comorbidities may confound the straightforward interpretation of our results. For example, one study examined the effect of age on soluble molecules secreted by CDCs sourced from aged and young patients. They observed an increase in secreted Frizzled Related Protein 1 in stem cells from aged patients and demonstrated a correlation between this factor and senescence (Nakamura et al., 2017). In our microarray data, secreted Frizzled Related Protein 1 increases after ischemia in both aged and young EDCs and may help explain the increase in senescent EDCs found within cells from ischemic mice in both

age groups but it is not responsible for the higher number of senescent cell in EDCs derived from old mice relative to young mice as secreted Frizzled Related Protein 1 expression was identical in the two age groups in non-ischemic and ischemic settings. This finding suggests that the study by Nakamura and colleagues is misleading as their model inappropriately used young patients that are usually hospitalized due to reasons other than ischemic heart disease while the probability of heart failure due to ischemia rises in aged individuals (not explicitly stated in the manuscript). Hence, they observed a correlation of secreted Frizzled Related Protein 1 with age instead of ischemia (as they erroneously concluded). Moreover, dissecting the influence of age from ischemia on stem cell phenotype may help with the designing cellular therapeutic for other cardiomyopathy complications that carry the risk factor of age but not ischemia (i.e. Heart failure with preserved ejection fraction (HFpEF) or Duchenne muscular dystrophy). For example, collecting a sufficient number of EDCs from aged patient who suffer from ischemic cardiomyopathy would not be an issue because ischemia promotes EDC emigration from explant tissue, however, to apply EDC therapy for aged patients with HFpEF, collecting enough cells for therapy may be challenging as aged tissue produce fewer EDCs. Similarly, researchers have found that CDC yield decrease with age, but Duchenne muscular dystrophy does not make any additional changes on the effects of aging (Hsiao et al., 2014). Consequently, collection of EDCs for these patients would also be challenging.

5.5 Ischemia amplifies the consequences of aging

Increased SOD activity was detected in young ischemic EDCs and resulted in reduced ROS within these cells compared to old ischemic mice sourced EDCs. This result hints that unlike young EDCs the antioxidant defences of aged EDCs may be inherently restricted; however, the generated ROS level in aged ischemic EDCs was comparable to the produced ROS in the non-ischemic EDCs.

Given that stressed mitochondria generate more ROS (Cortassa et al., 2014), a consistent ROS level shows negligible alteration in mitochondrial function and cell metabolism after ischemia in old mice sourced EDCs. Other than mitochondrial oxidative phosphorylation, various other free radical producing mechanisms has been discovered in the body such as peroxisome, phagocytosis and inflammation and ischemia (Lobo et al., 2010). By generating free radicals, ischemia increases the formation of lipid peroxides that consequently damages cell membrane leading to apoptosis (Meerson et al., 1982). Antioxidants can improve the repair process of cardiac tissue after ischemia by preventing further damages and apoptosis of cardiomyocyte in the border zone. GPx activity was lower in old mice sourced EDCs that was more obvious in aged EDCs with a history of ischemia. Our microarray data also showed decreased mRNA expression of NAD(P)H dehydrogenase (NQO1), another important enzyme preventing formation of radical species. These radical scavenger molecules detoxify oxidised reagents to keep lipids, proteins and cellular molecules safe. Therefore, they may partially be accountable for higher senescent cells, p16 mRNA levels and apoptotic cells in EDCs from old donors with a history of ischemia. Consequently, EDC therapy using young cells would provide more anti-apoptotic effects.

Telomere length strongly influences cell senescence. However, the prevalence of senescence in aged EDCs seems to have other triggers as the telomere length was equivalent in c-Kit- cells from all cohorts despite variable senescent cell rates. EDCs from young mice demonstrated the lowest senescent rate permitting the conclusion that telomere length in EDCs is long enough not to trigger senescence, and senescence results from triggers other than DNA damage of telomeres. Within c-Kit+ cells, cells from young donors had longer telomere with a strong correlation to greater telomerase activity in these cells. Telomerase enzyme was active in c-Kit+ cells but ischemia

reduced its activity. The shortest telomere in c-Kit cells was equal to c-Kit- cells; therefore, short telomere is not a senescence trigger in these cells, either.

5.6 Increased senescence after ischemia directed by the Sirtuin 1

The ability of EDCs from young mice to handle free radicals after ischemia contrasts with their increased senescence cell number. Further microarray data analysis demonstrated downregulation of the Sirt1 pathway by ischemia. We noticed that mRNA expression of Sirt1 and Sirt2 was reduced in EDCs sourced from both old and young mice after ischemia. Similarly, inactivation of Sir1 has been reported in cardiac tissue after ischemia/reperfusion (Tong et al., 2013). Sirt1 epigenetically controls senescence (Ogryzko et al., 1996) by localising on Frizzled-Related Protein 1 promotor - a Wnt antagonist - decreasing Frizzled-Related Protein 1 expression to promote Wnt signaling (Pruitt et al., 2006). High secreted Frizzled-Related Protein 1 expression correlates with senescence cell occurrence (Nakamura et al., 2017). In our study, Frizzled-Related Protein 1 was elevated after ischemia in both aged and young EDCs, suggesting that Sirt1 inhibition with subsequent downregulation of Wnt signaling resulted in the higher number of senescent cells after ischemia.

5.7 The impact of age of the recipients

The marked reductions noted in cardiac functional improvement suggest that recipient age is a large obstacle in conveying the benefits of EDC therapy. A recent study showed that injection of young CDCs into old rats reduces the expression of E2F1 and Rbl1 (two Mybl2-related cell cycle genes) within treated hearts, therefore, they suggested that the young EDCs are able to rejuvenate aged host tissue. Mechanistically this was attributed to reduced secretion of IL-1β and direct salutary remodeling of cardiac structure by exosomes (Grigorian-Shamagian et al., 2017).

Although young stem cells are providing superior benefits, our data from comparison of the transplantation of young EDCs into young or aged hosts suggests this rejuvenation is not sufficient to make the aged hearts as responsive as the young hearts.

Although both systemic and cardiac tissue milieu are influenced by age, changes in diet and nutrient sensing pathways can reverse the effect of age (Murphy and Thuret, 2015). Modified cells secrete autocrine or paracrine stimulating molecules, locally or systemically. Heterochronic parabiosis studies (two mice share a common bloodstream with a young mouse surgically joined to an old partner) indicate that among the plethora of different growth factors, systemic GDF-11 brings youthful phenotype for aged hearts as it reverses cardiomyocyte hypertrophy (Loffredo et al., 2013). Exosomes also contain proteins and miRNAs with rejuvenating effects (Pusic and Kraig, 2014; Munk and Panda, 2017). Some drugs are also linked to rejuvenation (i.e., statins) which have been shown to rejuvenate endothelial progenitor cells by decreasing ROS production, improving telomere/ telomerase activity and increasing the cardio-protection by decreasing inflammation and oxidative stress (Olivieri et al., 2012; Barlaka et al., 2016). Rapamycin is another compound known for its anti-senescence effects. Administration of Rapamycin at late-life stages in mice improved overall health and cardiac function by changing cardiac metabolism and inflammation (James et al., 2013). Overall, injection of these youthful factors prior to EDC therapy may favorably pre-condition the cardiac environment for cell transplantation and may accelerate the improvement of EDC therapy in infarcted hearts of aged patients but this remains to be further investigated.

5.8 Mybl2: The missing link between senolytic compounds and senescence?

There are some compounds that accepted to have the ability to reverse senescence. Rapamycin in high doses inhibits the AKT pathway through inhibition of mTORC2 (mammalian target of rapamycin complex 2) that is linked to cell survival and proliferation, thus, it has been using clinically for cancer treatment. Interestingly, rapamycin in low doses inhibits mTORC1 which sequentially activates AKT and ERK pathways. Mechanistically, this is attributable to the inhibitory feedback within the mTORC1 target - S6K - on PI3K/AKT. When mTORC1 is inhibited by rapamycin, the amount of phosphorylated S6K decreases and through the negative feed back loop, increases the AKT pathway (Figure 5.1). Activation of the AKT pathway consequently inhibits the GSK-β (Chen et al., 2010; Ballou and Lin, 2008). In low rapamycin doses, mTORC2 is still active which can directly phosphorylate and activate AKT (Memmott and Dennis, 2009). Inhibition of GSK-3β upregulates Cyclin D1 through translocation of β-catenin to the nucleus (Diehl et al., 1998; Shtutman et al., 1999). Cyclin D negatively regulates the activation of retinoblastoma and phosphorylated retinoblastoma propel expression of Mybl2 (Rufini et al.,2013). Consitent with this, loss of GSK-3β gene bypasses senescence (Liu et al., 2008). Researchers have shown that the inhibition of GSK-3β through lithium treatment can recover some of the lost regenerative potencies of aged mesenchymal stem cells (Brunt et al., 2012).

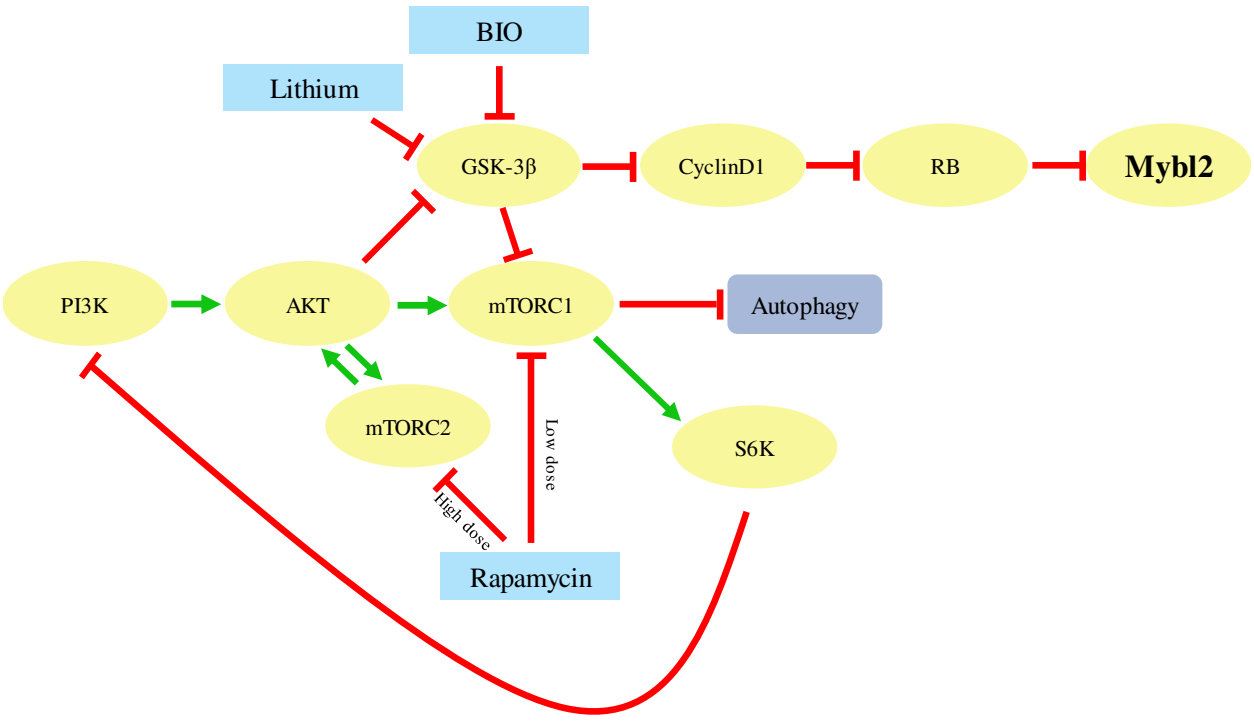

Figure 5.1. Schema of senolytic compounds link with Mybl2. Autophagy is not involved in EDC rejuvenation because in contrast to Rapamycin, BIO activates mTOR pathway and blocks autophagy, yet reduces senescence. The mutual change in both pathways is the inhibition of GSK-3β and this inhibition is linked to increased Mybl2 expression which is known for its anti-senescence effects.

The anti-senescence effect of rapamycin has been attributed to autophagy. Several pathways are recognized to be involved in autophagy. One is mTOR pathway whose inhibition is required for autophagy induction (Pyo et al., 2012), and rapamycin targets this pathway. Avolio et al. have shown that the reduced effect of c-Kit+ cells is a result of IL-1β SASP while rapamycin and Resveratrol treatments enhance the SASP of c-Kit+ cells. They proposed that the therapeutic effect ensues by activation of autophagy and AKT pathway (Avolio et al., 2014). In the field of cardiac research, some other compounds were also used to improve cardiac dysfunction by targeting autophagy (Riquelme et al., 2016); however, these administered compounds were not specific for autophagy making it difficult to exclude off target effects. Therefore, it is difficult to conclude that anti-senescence effect of rapamycin or other compounds are mediated by activation of autophagy.

Furthermore, there are contradictory opinions on the role of autophagy in senescence with some studies suggesting that autophagy is anti-senescence while others propose a pro-senescence effect for autophagy (Kwon et al., 2017). Here, we tested the effect of BIO and rapamycin on EDCs from old mice and found an antisenescence effect (Figure 4.21). The small molecule BIO activates mTOR to inhibit autophagy while while low dose Rapamycin through mTOR inhibition stimulates autophagy. In other words, both these factors reduce senescence, despite the fact that one is activating autophagy and the other one is inhibiting autophagy. Interestingly, both molecules have cross-talk on GSK-3β suggesting the observed effects on senescence are likely not mediated by autophagy but rather GSK-3β inhibition and induction of Mybl2. High dose rapamycin did not change the Mybl2 expression within EDCs whereas low dose rapamycin increased Mybl2 mRNA expression and reduced senescence; confirming the hypothesis that senescence reversal following treatment with senolytic compounds may be attributable to Mybl2 over-expression. This data also indicates that, unlike plants in which GSK-3β like protein phosphorylates and activates Mybl2 (Ye et al., 2012), in animals GSK-3β inhibition increases Mybl2. However, further investigation is essential to confirm any direct targeting of Mybl2 by GSK-3β.

5.9 Rejuvenation of EDCs by Mybl2 over-expression

Rejuvenation is the reversal of senescence to achieve youthful properties. Rejuvenation of stem cells has been shown to be possible through different strategies. Preconditioning of cells with small molecules, cytokines or hypoxia is one method of senescence reversal; however, the effects are typically transient (Haider and Ashraf, 2008; Khatiwala and Cai, 2016). Somatic gene transfer provides a more durable effect to evaluate proof of concept. Several studies have shown that gene therapy in cells or targeting the whole organ can restore a youthful phenotype. Of these, fibroblast growth factor-7 partially rejuvenates thymocyte progenitor cells (Berent-Maoz et al., 2012), while

Pim-1 kinase over-expression in cardiac c-Kit+ cells improves cell senescence by down stream targeting of Nucleostemin to activate telomerase enzyme and downregulate p16 (Mohsin et al., 2013; Cottage et al., 2012; Khatiwala et al., 2018). One group had even applied gene therapy for the heart using GDF-11 over-expression to reduce the markers of aging in cardiac tissue and protect the heart from ischemic injury (Du et al., 2017).

Mybl2 has been suggested as a determiner of cell fate, and this factor has been shown to bypass senescence better than some of the cell cycle regulatory genes such as FoxM1 and retinoblastoma (Mowla et al., 2014). Mybl2 also has anti-neoplasia properties making it a suitable factor for rejuvenation (Heinrichs et al., 2013; Clarke et al., 2013). Examination of embryonic and pluripotent stem cells showed that Mybl2 is implicated in the expression of several important pluripotency transcription factors, namely NANOG, POU5F1 and SOX. In hematopoietic stem cells, Mybl2 inactivation depleted myeloid progenitors and in intestinal epithelial cells Mybl2 promoted commitment of these cells by generating a differentiation signals (Boheler 2009; Baker et al., 2014; Papetti and Augenlicht, 2011). To date, there is no study looking for the effect of Mybl2 in stem cell senescence and rejuvenation. In our study, Mybl2 over-expression in EDCs from old ischemic donors provided functional and structural improvements to a degree that was comparable to young EDCs. These benefits were partly achieved thorough increased activity of antioxidant enzymes and greater retention of Mybl2 over-expressing EDCs as increased cell dose improves the effects of cell therapy (Shen et al.,2012). Additionally, the cytokine profile of the ischemic aged EDCs was altered following rejuvenation. These cells were secreting greater amounts of Amphiregulin growth factor and less inflammatory + anti-angiogenesis cytokines (i.e., Endostatin). The latter correlated with our *in vivo* results as we observed increased angiogenesis within Mybl2 over-expressing EDC treated hearts. The reduction of inflammatory cytokines,

however, did not alter macrophages infiltration. We believe that the observation of equal numbers of macrophages *in vivo* may be due to the resolution of inflammation in the heart at the time of heart collection (4 weeks after MI). So, it is possible that the macrophage number has been reduced to steady state phase at this point; or is due to the original low secretion of inflammatory factors in non-transduced EDC from old ischemic donors.

4.10 Future directions

Extracellular vesicles carry a cargo of several different small RNAs (i.e. miRNA and Y RNA) that represent the major bioactive constituent of these vesicles. With the recent explosion of knowledge highlighting the importance of extracellular vesicle transfer in autocrine and paracrine signalling, it seems inevitable that a portion of the benefits conferred by heart-derived cells are mediated through extracellular vesicles (Barile et al., 2014; Tseliou et al., 2015; Gallet et al., 2017). Our results showed all study cohorts are secreting vesicles with equal number and size; however, the content composition may be variable in different EDCs. In CDCs, miRNA-146-a and YF-1 are active components that are secreted through exosomes. miRNA-146-a prevents cardiomyocyte apoptosis in the ischemic heart (Ibrahim et al., 2014) and YF-1 induces IL-10 secretion and protects cardiomyocytes from oxidative stress (Cambier et al., 2017). Several miRNAs have roles in senescence such as miRNA-29 and miRNA-30 (Martinez et al., 2011). Therefore, measurement of these small RNAs within extracellular vesicles through RNA sequencing is of interest and would guide us in exploring SASP in terms of RNAs.

Cardiac tissue is constantly communicating with bone marrow cells as well as immune cells and resident macrophages. The response of these cells to stem cell paracrine secreted factors is another determinant of regeneration which could be hampered by age. Furthermore, in this study we found

that aged recipient hearts are having impaired responsiveness toward stem cell therapy. A possibility is that stem cells residing in aged cardiac tissue may not respond to the regenerative stimuli. The recipient age is important because the donor stem cells and cardiac tissue mutually interact with each other. Although the young/engineered donor stem cells are having rejuvenating effect on their surrounding recipient heart cells, the aged milieu with SASP cytokines, miRNAs and exosome content negatively affect transplanted EDCs. An extensive examination of the aged cardiac milieu and cardiac cells would help us to better understand the declined regenerative response. Albeit, regardless of the underlying mechanism, the combinatory administration of systemic rejuvenating cytokines or small molecules before and during the time of stem cell transplantation may augment the regenerative potential. This interesting topic warrants future investigation.

Genetic modification of EDCs using lentivirus is accompanied by risk of cancer because of random integration into the genome (Montini et al., 2009) making other methods of gene delivery with lower risk (such as minicircles) an option to consider. The risk of Mybl2 in oncogenicity remains to be investigated but several studies have shown a role in genome integrity for Mybl2 (Yamauchi et al., 2008; Tarasov et al., 2008; Lorvellec et al., 2010), while no studies have shown that Mybl2 over-expression induces neoplasia. Given that over-expression of Mybl2 was more efficient than small molecules BIO or Rapamycin at reducing senescence, this approach has merit. Knowing the Mybl2 activation mechanism and cellular pathways interacting with Mybl2 will help guide us to design a customized senolytic compound for cell rejuvenation in cardiac therapy and other age-related disease.

6. CONCLUSION

Aging reduced the EDC yield from explant tissue. Aged EDCs exhibited great quantities of senescent cells with a characteristic SASP signature. These changes reduced the ability of EDCs to improve cardiac function and structure after LCA ligation. Ischemia increased the number of senescent cells in both young and old mice sourced EDCs through down regulation of Sirt1 and alteration of the downstream molecule Frizzled Related Protein 1. In old mice sourced EDCs, ischemia increased the susceptibility of cells to undergo apoptosis via reduced endogenous antioxidant system activity. Ischemia increased EDC yield from old mice but reduced the regenerative performance of transplanted stem cell. Microarray data revealed alterations in cell cycle regulation and DNA damage and repair pathways in aged EDCs sourced from ischemic hearts. Mybl2 transcription factor over-expression rejuvenated aged EDCs by reducing senescent cell number and improving the paracrine profile of EDCs. This translated into greater retention of transplanted EDCs and better myocardial function to a level comparable with young EDC treatment. Overall, some of the limitations regarding the models used in cardiac stem cell therapy research were answered in this project which provides a better insight for improvement of next generation stem cell products for clinical therapy. Amongst possible enhancement procedures, stem cell rejuvenation by Mybl2 seems promising.

7. REFERENCES

Ahlbory D, Appl H, Lang D, Klempnauer KH. 2005. Disruption of B-myb in DT40 cells reveals novel function for B-Myb in the response to DNA-damage. Oncogene 24, 7127–7134.

Alcendor RR, Gao S, Zhai P, Zablocki D, Holle E, Yu X, Tian B, Wagner T, Vatner SF, Sadoshima J. 2007. Sirt1 regulates aging and resistance to oxidative stress in the heart. Circ Res. 100,1512–21.

Anders L, Ke N, Hydbring P, Choi YJ, Widlund HR, Chick JM, Zhai H, Vidal M, Gygi SP, Braun P, Sicinski P. 2011. A systematic screen for CDK4/6 substrates links FOXM1 phosphorylation to senescence suppression in cancer cells. Cancer Cell 20, 620–634.

Anversa P, Kajstura J, Leri A, Bolli R. 2006. Life and death of cardiac stem cells: a paradigm shift in cardiac biology. Circulation 113(11),1451–63.

Arslan F, de Kleijn DP, Pasterkamp G. 2011. Innate immune signaling in cardiac ischemia. Nat Rev Cardiol 8, 292-300.

Assmus B, Urbich C, Aicher A, HofmannWK, Haendeler J, Rossig L, Spyridopoulos I, Zeiher AM, Dimmeler S. 2003. HMG-CoA reductase inhibitors reduce senescence and increase proliferation of endothelial progenitor cells via regulation of cell cycle regulatory genes. Circ Res. 92(9),1049–55.

Atzmon, G. Cho M, Cawthon RM, Budagov T, Katz M, Yang X, Siegel G, Bergman A, Huffman DM, Schechter CB, Wright WE, Shay JW, Barzilai N, Govindaraju DR, Suh Y. 2010. Genetic variation in human telomerase is associated with telomere length in Ashkenazi centenarians. Proc. Natl Acad. Sci. USA 107 (suppl. 1), 1710–1717.

Avolio E, Gianfranceschi G, Cesselli D, Caragnano A, Athanasakis E, Katare R, Meloni M, Palma A, Barchiesi A, Vascotto C, Toffoletto B, Mazzega E, Finato N, Aresu G, Livi U, Emanueli C, Scoles G, Beltrami CA, Madeddu P, Beltrami AP. 2014. Ex vivo molecular rejuvenation improves the therapeutic activity of senescent human cardiac stem cells in a mouse model of myocardial infarction. Stem Cells. 32(9), 2373-85.

Baker SJ, Ma'ayan A, Lieu YK, John P, Reddy MV, Chen EY, Duan Q, Snoeck HW, Reddy EP. 2014. B-myb is an essential regulator of hematopoietic stem cell and myeloid progenitor cell development. Proc Natl Acad Sci U S A. 111(8), 3122-7.

Balaban RS, Nemoto S, Finkel T. 2005. Mitochondria, oxidants, and aging. Cell. 120, 483–495.

Ballou LM. Lin RZ. 2008. Rapamycin and mTOR kinase inhibitors. J Chem Biol. 1(1-4), 27–36.

Balsam LB, Wagers AJ, Christensen JL, Kofidis T, Weissman IL, Robbins RC. 2004. Haematopoietic stem cells adopt mature haematopoietic fates in ischaemic myocardium. Nature 428, 668-73.

Barile L, Lionetti V, Cervio E, Matteucci M, Gherghiceanu M, Popescu LM, Torre T, Siclari F, Moccetti T, Vassalli G. 2014. Extracellular vesicles from human cardiac progenitor cells inhibit cardiomyocyte apoptosis and improve cardiac function after myocardial infarction. Cardiovasc Res.103(4), 530–541.

Barlaka E, Galatou E, Mellidis K, Ravingerova T, Lazou A. 2016. Role of Pleiotropic Properties of Peroxisome Proliferator-Activated Receptors in the Heart: Focus on the Nonmetabolic Effects in Cardiac Protection. Cardiovasc Ther.34(1), 37-48.

Barzilai N, Huffman DM, Muzumdar RH, Bartke A. 2012. The critical role of metabolic pathways in aging. Diabetes 61, 1315–1322.

Beltrami AP, Urbanek K, Kajstura J, Yan SM, Finato N, Bussani R, Nadal-Ginard B, Silvestri F, Leri A, Beltrami CA, Anversa P. 2001. Evidence that human cardiac myocytes divide after myocardial infarction, N. Engl. J. Med. 344, 1750 – 1757.

Beltrami AP, Barlucchi L, Torella D, Baker M, Limana F, Chimenti S, Kasahara H, Rota M, Musso E, Urbanek K, Leri A, Kajstura J, Nadal-Ginard B, Anversa P. 2003. Adult cardiac stem cells are multipotent and support myocardial regeneration. Cell 114, 763 – 776.

Ben-Mordechai T, Palevski D, Glucksam-Galnoy Y, Elron- Gross I, Margalit R, Leor J. 2015. Targeting macrophage subsets for infarct repair. J Cardiovasc Pharmacol Ther. 20, 36–51.

Berent-Maoz B, Montecino-Rodriguez E, Signer RA, Dorshkind K. 2012. Fibroblast growth factor-7 partially reverses murine thymocyte progenitor aging by repression of Ink4a. Blood 119(24), 5715-21.

Bergmann O, Bhardwaj RD, Bernard S, Zdunek S, Barnabé-Heider F, Walsh S, Zupicich J, Alkass K, Buchholz BA, Druid H, Jovinge S, Frisén J. 2009. Evidence for cardiomyocyte renewal in humans. Science 324, 98 – 102 .

Bernardes de Jesus B, Vera E, Schneeberger K, Tejera AM, Ayuso E, Bosch F, Blasco MA. 2012. Telomerase gene therapy in adult and old mice delays aging and increases longevity without increasing cancer. EMBO Mol. Med. 4, 691–704

Bhaumik D, Scott GK, Schokrpur S, Patil CK, Orjalo AV, Rodier F, Lithgow GJ, Campisi J. 2009. MicroRNAs miR-146a/b negatively modulate the senescence-associated inflammatory mediators IL-6 and IL-8. Aging 1, 402–411.

Boheler KR. 2009. Stem Cell Pluripotency: A Cellular Trait that Depends on Transcription Factors, Chromatin State and a Checkpoint Deficient Cell Cycle. J Cell Physiol. 221(1), 10–17.

Bolli R, Chugh AR, D'Amario D, Loughran JH, Stoddard MF, Ikram S, Beache GM,Wagner SG, Leri A, Hosoda T, Sanada F, Elmore JB, Goichberg P, Cappetta D, Solankhi NK, Fahsah I, Rokosh DG, Slaughter MS, Kajstura J & Anversa P. 2011. Cardiac stem cells in patients with ischaemic cardiomyopathy (SCIPIO): initial results of a randomised phase 1 trial. Lancet 378, 1847–1857.

Bonios M, Terrovitis J, Chang CY, Engles JM, Higuchi T, Lautamäki R, Yu J, Fox J, Pomper M, Wahl RL, Tsui BM, O'Rourke B, Bengel FM, Marbán E, Abraham MR. 2011a. Myocardial substrate and route of administration determine acute cardiac retention and lung bio- distribution of cardiosphere- derived cells. J. Nucl. Cardiol. 18, 443 – 450.

Bonios M, Chang CY, Terrovitis J, Pinheiro A, Barth A, Dong P, Santaularia M, Foster D.B, Venu Raman, Abraham TP, Abraham MR. 2011b. Constitutive HIF-1alpha expression blunts the beneficial effects of cardiosphere-derived cell therapy in the heart by altering paracrine factor balance. J Cardiovasc Transl Res. 4, 363–372.

Boon RA, Iekushi K, Lechner S, Seeger T, Fischer A, Heydt S, Kaluza D, Tréguer K, Carmona G, Bonauer A, Horrevoets AJ, Didier N, Girmatsion Z, Biliczki P, Ehrlich JR, Katus HA, Müller OJ,

Potente M, Zeiher AM, Hermeking H, Dimmeler S. 2013. MicroRNA-34a regulates cardiac ageing and function. Nature 495, 107–110.

Boyle AJ, Hwang J, Ye J, Shih H, Jun K, Zhang Y, Fang Q, Sievers R, Yeghiazarians Y, Lee RJ. 2013. The Effects of Aging on Apoptosis Following Myocardial Infarction. Cardiovasc Ther. 31(6), e102–e110.

Brunt KR, Zhang Y, Mihic A, Li M, Li SH, Xue P, Zhang W, Basmaji S, Tsang K, Weisel RD, Yau TM, Li RK. 2012. Role of WNT/β-catenin signaling in rejuvenating myogenic differentiation of aged mesenchymal stem cells from cardiac patients. Am J Pathol. 181(6), 2067-78.

Bujak M, Kweon HJ, Chatila K, Li N, Taffet G, Frangogiannis NG. 2008. Aging-related defects are associated with adverse cardiac remodeling in a mouse model of reperfused myocardial infarction. J Am Coll Cardiol. 51(14), 1384-92.

Burgess ML, McCrea JC, Hedrick HL. 2001. Age-associated changes in cardiac matrix and integrins. Mech Ageing Dev. 122, 1739–1756.

Cambier L, de Couto G, Ibrahim A, Echavez AK, Valle J, Liu W, Kreke M, Smith RR, Marbán L, Marbán E. 2017. Y RNA fragment in extracellular vesicles confers cardioprotection via modulation of IL-10 expression and secretion. EMBO Mol Med. 9(3), 337-352.

Campisi J. 2005. Senescent cells, tumor suppression, and organismal aging: good citizens, bad neighbors. Cell 120, 513–522.

Campisi J. 2013. Aging, cellular senescence, and cancer. Annu. Rev. Physiol. 75, 685–705.

Cannon ROIII, Butany JW, McManus BM, Speir E, Kravitz AB, Bolli R, Ferrans VJ. 1983. Early degradation of collagen after acute myocardial infarction in the rat. Am J Cardiol. 52, 390-395.

Castaldi A, Dodia RM, Orogo AM, Zambrano CM, Najor RH, Gustafsson ÅB, Heller Brown J, Purcell NH. 2017. Decline in cellular function of aged mouse c-kit+ cardiac progenitor cells. J Physiol.595(19), 6249-6262.

Carmeliet E. 1999. Cardiac ionic currents and acute ischemia: From channels to arrhythmias. Physiol Rev. 79, 917-1017.

Catchpole S, Tavner F, Le Cam L, Sardet C, Watson RJ. 2002. A B-myb promoter corepressor site facilitates *in vivo* occupation of the adjacent E2F site by p107·E2F and p130·E2F complexes. J Biol Chem. 277, 39015–24.

Cawthon RM. 2009. Telomere length measurement by a novel monochrome multiplex quantitative PCR method. Nucleic Acids Res. 37(3), e21.

Cencioni C, Melchionna R, Straino S, Romani M, Cappuzzello C, Annese V, Wu JC, Pompilio G, Santoni A, Gaetano C, Napolitano M, Capogrossi MC. 2013. Ex vivo acidic preconditioning enhances bone marrow ckit+ cell therapeutic potential via increased CXCR4 expression. Eur Heart J. 34(26), 2007–2016.

Cencioni C, Spallotta F, Mai A, Martelli F, Farsetti A, Zeiher AM, Gaetano C. 2015. Sirtuin function in aging heart and vessels. J Mol Cell Cardiol. 83, 55-61.

Cesselli D, Beltrami AP, D'Aurizio F, Marcon P, Bergamin N, Toffoletto B, Pandolfi M, Puppato E, Marino L, Signore S, Livi U, Verardo R, Piazza S, Marchionni L, Fiorini C, Schneider C, Hosoda T, Rota M, Kajstura J, Anversa P, Beltrami CA, Leri A. 2011. Effects of Age and Heart Failure on Human Cardiac Stem Cell Function. The American Journal of Pathology 179 (1), 349-66.

Chang TC, Yu D, Lee YS, Wentzel EA, Arking DE, West KM, Dang CV, Thomas-Tikhonenko A, Mendell JT. 2008. Widespread microRNA repression by Myc contributes to tumorigenesis. Nat Genet. 40, 43–50.

Charrasse S, Carena I, Brondani V, Klempnauer KH, Ferrari S. 2000. Degradation of B-Myb byubiquitin-mediated proteolysis: involvement of the Cdc34-SCF(p45Skp2) pathway. Oncogene 19, 2986–95.

Chen ML, Logan TD, Hochberg ML, Shelat SG, Yu X, Wilding GE, Tan W, Kujoth GC, Prolla TA, Selak MA, Kundu M, Carroll M, Thompson JE. 2009. Erythroid dysplasia, megaloblastic anemia, and impaired lymphopoiesis arising from mitochondrial dysfunction. Blood 114, 4045–4053.

Chen XG, Liu F, Song XF, Wang ZH, Dong ZQ, Hu ZQ, Lan RZ, Guan W, Zhou TG, Xu XM, Lei H, Ye ZQ, Peng EJ, Du LH, Zhuang QY. 2010. Rapamycin regulates Akt and ERK

phosphorylation through mTORC1 and mTORC2 signaling pathways. Mol Carcinog. 49(6), 603-10.

Cheng K, Malliaras K, Smith RR, Shen D, Sun B, Blusztajn A, Xie Y, Ibrahim A, Aminzadeh MA, Liu W, Li T, De Robertis MA, Marbán L, Czer LSC, Trento A, Marbán E. 2014. Human Cardiosphere-Derived Cells From Advanced Heart Failure Patients Exhibit Augmented Functional Potency in Myocardial Repair. JACC Heart Fail. 2(1), 49–61.

Cheung TH, Rando TA. 2013. Molecular regulation of stem cell quiescence. Nat Rev Mol Cell Biol. 14(6), 10.

Chiao YA, Dai Q, Zhang J, Lin J, Lopez EF, Ahuja SS, Chou YM, Lindsey ML, Jin YF. 2011. Multi-analyte profiling reveals matrix metalloproteinase-9 and monocyte chemotactic protein-1as plasma biomarkers of cardiac aging. Circ Cardiovasc Genet. 4, 455–62.

Chimenti I, Smith RR, Li TS, Gerstenblith G, Messina E, Giacomello A, Marbán E. 2010. Relative roles of direct regeneration versus paracrine effects of human cardiosphere-derived cells transplanted into infarcted mice. Circ. Res. 106, 971 – 980.

Chong JJ, Yang X, Don CW, Minami E, Liu YW, Weyers JJ, Mahoney WM, Van BB, Cook SM, Palpant NJ, Gantz JA, Fugate JA, Muskheli V, Gough GM, Vogel KW, Astley CA, Hotchkiss CE, Baldessari A, Pabon L, Reinecke H, Gill EA, Nelson V, Kiem HP, Laflamme MA, Murry CE. 2014. Human embryonic-stem-cell-derived cardiomyocytes regenerate non-human primate hearts. Nature 510, 273–277.

Choudhery MS, Khan M, Mahmood R, Mohsin S, Akhtar S, Ali F, Khan SN, Riazuddin S. 2012. Mesenchymal stem cells conditioned with glucose depletion augments their ability to repairinfarcted myocardium. J Cell Mol Med. 16, 2518–29.

Choudhury AR, Ju Z, Djojosubroto MW, Schienke A, Lechel A, Schaetzlein S, Jiang H, Stepczynska A, Wang C, Buer J, Lee HW, von Zglinicki T, Ganser A, Schirmacher P, Nakauchi H, Rudolph KL. 2007. Cdkn1a deletion improves stem cell function and lifespan of mice with dysfunctional telomeres without accelerating cancer formation. Nature Genet. 39, 99–105.

Chugh AR, Beache GM, Loughran JH, Mewton N, Elmore JB, Kajstura J, Pappas P, Tatooles A, Stoddard MF, Lima JA, SlaughterMS, Anversa P, Bolli R. 2012. Administration of cardiac stem

cells in patients with ischemic cardiomyopathy: the SCIPIO trial: surgical aspects and interim analysis of myocardial function and viability by magnetic resonance. Circulation 126, S54–S64.

Chung HY, Cesari M, Anton S, Marzetti E, Giovannini S, Seo AY, Carter C, Yu BP, Leeuwenburgh C. 2009. Molecular inflammation: underpinnings of aging and age-related diseases. Ageing Res. Rev. 8, 18– 30.

Clarke M, Dumon S, Ward C, Jäger R, Freeman S, Dawood B, Sheriff L, Lorvellec M, Kralovics R, Frampton J, García P. 2013. MYBL2 haploinsufficiency increases susceptibility to age-related haematopoietic neoplasia. Leukemia 27(3), 661-70.

Cleland JGF, Torabi A, Khan NK. 2005. Epidemiology and management of heart failure and left ventricular systolic dysfunction in the aftermath of a myocardial infarction. Heart 91, ii7–ii13.

Colman RJ, Anderson RM, Johnson SC, Kastman EK, Kosmatka KJ, Beasley TM, Allison DB, Cruzen C, Simmons HA, Kemnitz JW, Weindruch R. Caloric restriction delays disease onset and mortality in rhesus monkeys. 2009. Science 325(5937), 201–204.

Colman RJ, Beasley TM, Kemnitz JW, Johnson SC, Weindruch R, Anderson RM. 2014. Caloric restriction reduces age-related and all-cause mortality in rhesus monkeys. Nat. Commun. 5, 3557.

Colombo A, Proietti R, Culić V, Lipovetzky N, Viecca M, Danna P. 2014. Triggers of acute myocardial infarction: a neglected piece of the puzzle. J Cardiovasc Med 15(1), 1-7.

Conboy IM, Conboy MJ, Wagers AJ, Girma ER, Weissman IL, Rando TA. 2005. Rejuvenation of aged progenitor cells by exposure to a young systemic environment. Nature 433, 760–764.

Conboy IM, Rando TA. Aging, stem cells and tissue regeneration: lessons from muscle. 2005. Cell Cycle 4(3), 407-10.

Coppé JP, Desprez PY, Krtolica A, Campisi J. 2010. The senescence-associated secretory phenotype: the dark side of tumor suppression. Annu Rev Pathol. 5, 99-118.

Coraboeuf E, Deroubaix E, Coulombe A. 1980. Acidosis-induced abnormal repolarization and repetitive activity in isolated dog Purkinje fibers. J Physiol 76, 97-106.

Cortassa S, O'Rourke B, Aon MA. 2014. Redox-optimized ROS balance and the relationship between mitochondrial respiration and ROS. Biochim Biophys Acta.1837(2), 287-95.

Cottage CT, Neidig L, Sundararaman B, Din S, Joyo AY, Bailey B, Gude N, Hariharan N, Sussman MA. 2012. Increased Mitotic Rate Coincident with Transient Telomere Lengthening Resulting from Pim-1 Overexpression in Cardiac Progenitor Cells. Stem Cells. 30(11), 2512–2522.

D'Amario D, Fiorini C, Campbell PM, Goichberg P, Sanada F, Zheng H, Hosoda T, Rota M, Connell JM, Gallegos RP, Welt FG, Givertz MM, Mitchell RN, Leri A, Kajstura J, Pfeffer MA, Anversa P. 2011. Functionally competent cardiac stem cells can be isolated from endomyocardial biopsies of patients with advanced cardiomyopathies. Circ. Res. 108, 857 – 861.

Dai DF, Rabinovitch PS. 2009. Cardiac aging in mice and humans: The role of mitochondrial oxidative stress. Trends in cardiovascular medicine 19, 213–220.

Dang MQ, Zhao XC, Lai S, Wang X, Wang L, Zhang YL, Liu Y, Yu XH, Liu Y, Li HH, Xia YL. 2015. Gene expression profile in the early stage of angiotensin II-induced cardiac remodeling: a time series microarray study in a mouse model. Cell Physiol Biochem. 35(2), 467-76.

Davis DR, Zhang Y, Smith RR, Cheng K, Terrovitis J, Malliaras K, Li TS, White A, Makkar R, Marban E. 2009. Validation of the cardiosphere method to culture cardiac progenitor cells from myocardial tissue. PLoS One 4, e7195.

Davis DR, Kizana E, Terrovitis J, Barth AS, Zhang Y, Smith RR, Miake J, Marban E. 2010a. Isolation and expansion of functionally-competent cardiac progenitor cells directly from heart biopsies. J Mol Cell Cardiol 49, 312–321.

Davis DR, Smith RR, Marban E. 2010b. Human cardiospheres are a source of stem cells with cardiomyogenic potential. Stem Cells 28, 903–904.

Davis DR, Stewart DJ. 2011. Autologous cell therapy for cardiac repair. Expert Opin Biol Ther 11, 489-508.

Davis DR, Stewart DJ. 2014. Cell therapy for cardiac repair – bench to bedside and back. In Cardiac Regeneration and Repair, ed. Li RK, Weisel RD, Woodhead Publishing, Sawston, UK. 138–162.

de Couto G, Liu W, Tseliou E, Sun B, Makkar N, Kanazawa H, Arditi M, Marbán E. 2015. Macrophages mediate cardioprotective cellular postconditioning in acute myocardial infarction. J Clin Invest. 125(8), 3147-62.

DeFilippis RA, Goodwin EC, Wu L, DiMaio D. 2003. Endogenous human papillomavirus E6 and E7 proteins differentially regulate proliferation, senescence, and apoptosis in HeLa cervical carcinoma cells. J Virol. 77, 1551–63.

de Lange T. 2006. Mammalian telomeres. In Telomeres, 2nd edn, de Lange T, Lundblad V, Blackburn E (eds). Cold Spring Harbor Laboratory Press: Cold Spring Harbor, NY, 387–431.

Deliang Shen, Ke Cheng, Eduardo Marbán. 2012. Dose-dependent functional benefit of human cardiosphere transplantation in mice with acute myocardial infarction. J Cell Mol Med. 16(9), 2112–2116.

Diehl JA, Cheng M, Roussel MF, Sherr CJ. 1998. Glycogen synthase kinase-3beta regulates cyclin D1 proteolysis and subcellular localization. Genes Dev. 12(22), 3499-511.

Dimri GP, Lee X, Basile G, Acosta M, Scott G, Roskelley C, Medrano EE, Linskens M, Rubelj I, Pereira-Smith O, Peacocke M, Campisi J. 1995. A biomarker that identifies senescent human cells in culture and in aging skin in vivo. Proc Natl Acad Sci USA 92, 9363–9367.

Ding A, Hwang S, Schwab R. 1994. Effect of aging on murine macrophages. Diminished response to IFN-gamma for enhanced oxidative metabolism. J Immunol 153, 2146–52.

Dobaczewski M, Bujak M, Zymek P, Ren G, Entman ML, Frangogiannis NG. 2006. Extracellular matrix remodeling in canine and mouse myocardial infarcts. Cell Tissue Res 324, 475-488.

Domenighetti AA, Wang Q, Egger M, Richards SM, Pedrazzini T, Delbridge LM. 2005. Angiotensin iimediated phenotypic cardiomyocyte remodeling leads to age-dependent cardiac dysfunction and failure. Hypertension 46, 426–432.

Dong X, Milholland B, Vijg J. 2016. Evidence for a limit to human lifespan. Nature 538, 257–259.

Down CF, Millour J, Lam EW, Watson RJ. 2012. Binding of FoxM1 to G2/M gene promoters is dependent upon B-Myb. Biochim Biophys Acta. 1819, 855–62.

Du GQ, Shao ZB, Wu J, Yin WJ, Li SH, Wu J, Weisel RD, Tian JW, Li RK. 2017. Targeted myocardial delivery of GDF11 gene rejuvenates the aged mouse heart and enhances myocardial regeneration after ischemia-reperfusion injury. Basic Res Cardiol.112(1), 7.

Dumont P, Burton M, Chen QM, Gonos ES, Frippiat C, Mazarati JB, Eliaers F, Remacle J, Toussaint O. 2000. Induction of replicative senescence biomarkers by sublethal oxidative stresses in normal human fibroblast. Free Rad. Biol. Med. 28, 361–373.

Edelberg JM, Lee SH, Kaur M, Tang L, Feirt NM, McCabe S, Bramwell O, Wong SC, Hong MK. 2002. Platelet-derived growth factor-AB limits the extent of myocardial infarction in a rat model: feasibility of restoring impaired angiogeniccapacity in the aging heart. Circulation105(5), 608–13.

Eisenberg LM, Burns L, Eisenberg CA. 2003. Hematopoietic cells from bone marrow have the potential to differentiate into cardiomyocytes in vitro . Anat Rec A Discov Mol Cell Evol Biol 274, 870 – 82 .

Elliott AC, Smith GL, Eisner DA, Allen DG. 1992. Metabolic changes during ischaemia and their role in contractile failure in isolated ferret hearts. J Physiol 454, 467-490.

Epel ES, Blackburn EH, Lin J, Dhabhar FS, Adler NE, Morrow JD, Cawthon RM. 2004. From the cover: accelerated telomere shortening in response to life stress. PNAS 101, 17312–17315.

Etoh T, Joffs C, Deschamps AM, Davis J, Dowdy K, Hendrick J, Baicu S, Mukherjee R, Manhaini M, Spinale FG. 2001. Myocardial and interstitial matrix metalloproteinase activity after acute myocardial infarction in pigs. Am J Physiol Heart Circ Physiol 281, H987-H994.

Falk E. 1982. Coronary artery narrowing without irreversible myocardial damage or development of collaterals. Assessment of "critical" stenosis in a human model. Br Heart J 48(3), 265-71.

Fazel S. Cimini M, Chen L, Li S, Angoulvant D, Fedak P, Verma S, Weisel RD, Keating A, Li RK. 2006. Cardioprotective c- kit+ cells are from the bone marrow and regulate the myocardial balance of angiogenic cytokines. J Clin Invest 116, 1865 – 77.

Fernandes S, Amirault JC, Lande G, Nguyen JM, Forest V, Bignolais O, Lamirault G, Heudes D, Orsonneau JL, Heymann MF, Charpentier F, Lemarchand P. 2006. Autologous myoblast transplantation after myocardial infarction increases the inducibility of ventricular arrhythmias. Cardiovasc Res 69, 348 – 58.

Flynn JM, O'Leary MN, Zambataro CA, Academia EC, Presley MP, Garrett BJ, Zykovich A, Mooney SD, Strong R, Rosen CJ, Kapahi P, Nelson MD, Kennedy BK, Melov S. 2013. Late-life rapamycin treatment reverses age-related heart dysfunction. Aging Cell 12(5), 851–862.

Fransioli J, Bailey B, Gude NA, Cottage CT, Muraski JA, Emmanuel G, Wu W, Alvarez R, Rubio M, Ottolenghi S, Schaefer E, Sussman MA. 2008. Evolution of the c-kit-positive cell response to pathological challenge in the myocardium. Stem Cells 26(5), 1315-24.

Frangogiannis NG, Ren G, Dewald O, Zymek P, Haudek S, Koerting A, Winkelmann K, Michael LH, Lawler J, Entman ML. 2005. The critical role of endogenous Thrombospondin (TSP)-1 in preventing expansion of healing myocardial infarcts. Circulation 111, 2935-2942.

Frangogiannis NG. 2012. Matricellular proteins in cardiac adaptation and disease. Physiol Rev. 92, 635-688.

Frangogiannis NG. 2014. The inflammatory response in myocardial injury, repair, and remodelling. Nat Rev Cardiol 11, 255-265.

Frangogiannis NG. 2015. Pathophysiology of Myocardial Infarction. Compr Physiol. 5(4), 1841-75.

Fu Z, Malureanu L, Huang J, Wang W, Li H, van Deursen JM, Tindall DJ, Chen J. 2008. Plk1-dependent phosphorylation of FoxM1 regulates a transcriptional programme required for mitotic progression. Nat Cell Biol. 10, 1076–82.

Fukuda S, Kaga S, Sasaki H, Zhan L, Zhu L, Otani H, Kalfin R, Das DK, Maulik N. 2004. Angiogenic signal triggered by ischemic stress induces myocardial repair in rat during chronic infarction. J Mol Cell Cardiol. 36(4), 547-59.

Fung SM, Ramsay G, Katzen AL. 2002. Mutations in Drosophila myb lead to centrosome amplification and genomic instability. Development 129, 347–359.

Gallet R, Dawkins J, Valle J, Simsolo E, de Couto G, Middleton R, Tseliou E, Luthringer D, Kreke M, Smith RR, Marbán L, Ghaleh B, Marbán E. 2017. Exosomes secreted by cardiosphere-derived cells reduce scarring, attenuate adverse remodelling, and improve function in acute and chronic porcine myocardial infarction. Eur Heart J.38, 201-211.

Gan B, Sahin E, Jiang S, Sanchez-Aguilera A, Scott KL, Chin L, Williams DA, Kwiatkowski DJ, DePinho RA. 2008. mTORC1-dependent and -independent regulation of stem cell renewal, differentiation, and mobilization. Proc. Natl Acad. Sci. USA 105, 19384–19389.

Garcia P, Frampton J. 2006. The transcription factor B-Myb is essential for S-phase progression and genomic stability in diploid and polyploid megakaryocytes. J Cell Sci 119, 1483–1493.

Gertz M, Steegborn C. 2010. The lifespan-regulator p66shc in mitochondria: Redox enzyme or redox sensor? Antioxidants & redox signaling 13, 1417–1428.

Ghigo A, Franco I, Morello F, Hirsch E. 2014. Myocyte signalling in leucocyte recruitment to the heart. Cardiovasc Res 102, 270-280.

Gomes AP, Price NL, Ling AJ, Moslehi JJ, Montgomery MK, Rajman L, White JP, Teodoro JS, Wrann CD, Hubbard BP, Mercken EM, Palmeira CM, de Cabo R, Rolo AP, Turner N, Bell EL, Sinclair DA. 2013. Declining NAD(+) induces a pseudohypoxic state disrupting nuclear-mitochondrial communication during aging. Cell 155, 1624–1638.

Gilbert LA, Hemann MT. 2010. DNA damage-mediated induction of a chemoresistant niche. Cell 143, 355–366.

Gottlieb RA. 2011. Cell death pathways in acute ischemia/reperfusion injury. J Cardiovasc Pharmacol Ther 16, 233-238.

Gottlieb RA, Burleson KO, Kloner RA, Babior BM, Engler RL. 1994. Reperfusion injury induces apoptosis in rabbit cardiomyocytes. J Clin Invest 94, 1621-1628.

Grigorian-Shamagian L, Liu W, Fereydooni S, Middleton RC, Valle J, Cho JH, Marbán E. 2017. Cardiac and systemic rejuvenation after cardiosphere-derived cell therapy in senescent rats. Eur Heart J. 38(39), 2957-2967.

Grillari J, Grillari-Voglauer R. 2010. Novel modulators of senescence, aging, and longevity: small non-coding RNAs enter the stage. Exp. Gerontol. 45, 302– 311.

Haendeler J, Hoffmann J, Diehl JF, Vasa M, Spyridopoulos I, Zeiher AM, Dimmeler S. 2004. Antioxidants inhibit nuclear export of telomerase reverse transcriptase and delay replicative senescence of endothelial cells. Circ. Res. 94, 768–775.

Hagège AA, Carrion C, Menasché P, Vilquin JT, Duboc D, Marolleau JP, Desnos M, Bruneval P. 2003. Viability and differentiation of autologous skeletal myoblast grafts in ischaemic cardiomyopathy. Lancet 361, 491 – 2.

Haider HKh, Ashraf M. 2008. Strategies to promote donor cell survival: combining preconditioning approach with stem cell transplantation. J Mol Cell Cardiol. 45(4), 554-66.

Han YC, Park CY, Bhagat G, Zhang J, Wang Y, Fan JB, Liu M, Zou Y, Weissman IL, Gu H. 2010. microRNA-29a induces aberrant self-renewal capacity in hematopoietic progenitors, biased myeloid development, and acute myeloid leukemia. J Exp Med 207, 475–89.

Hao M, Wang R, Wang W. 2017. Cell Therapies in Cardiomyopathy: Current Status of Clinical Trials. Anal Cell Pathol. 2017, 9404057.

Hariharan N, Quijada P, Mohsin S, Joyo A, Samse K, Monsanto M, De La Torre A, Avitabile D, Ormachea L, McGregor MJ, Tsai EJ, Sussman MA. 2015. Nucleostemin rejuvenates cardiac progenitor cells and antagonizes myocardial aging. J Am Coll Cardiol. 65, 133–147.

Hayflick L, Moorhead PS. 1961. The serial cultivation of human diploid cell strains. Exp. Cell Res. 25, 585–621.

He JQ, Ma Y, Lee Y, Thomson JA, Kamp TJ. 2003. Human embryonic stem cells develop into multiple types of cardiac myocytes: action potential characterization. Circ Res 93, 32–39.

Hees PS, Fleg JL, Lakatta EG, Shapiro EP. 2002. Left ventricular remodeling with age in normal men versus women: novel insights using three-dimensional magnetic resonance imaging. Am J Cardiol. 90, 1231–1236.

Heeschen C, Lehmann R, Honold J, Assmus B, Aicher A, Walter DH, Martin H, Zeiher AM, Dimmeler S. 2004. Profoundly reduced neovascularization capacity of bone marrow mononuclear cells derived from patients with chronic ischemic heart disease. Circulation 109(13), 1615-22.

Heidt T, Courties G, Dutta P, Sager H, Sebas M, Iwamoto Y, Sun Y, Da Silva N, Panizzi P, van der Laan AM, Swirski FK, Weissleder R, Nahrendorf M. 2014. Differential contribution of monocytes to heart macrophages in steady-state and after myocardial infarction. Circ Res 115, 284-295.

Heinrichs S, Conover LF, Bueso-Ramos CE, Kilpivaara O, Stevenson K, Neuberg D, Loh ML, Wu WS, Rodig SJ, Garcia-Manero G, Kantarjian HM, Look AT. 2013. MYBL2 is a sub-haploinsufficient tumor suppressor gene in myeloid malignancy. Elife 16(2), e00825.

Heiss C, Keymel S, Niesler U, Ziemann J, Kelm M, Kalka C. 2005. Impaired progenitor cell activity in age-related endothelial dysfunction. J Am Coll Cardiol 45(9), 1441–8.

Hensley K, Robinson KA, Gabbita SP, Salsman S, Floyd RA. 2000. Reactive oxygen species, cell signaling, and cell injury. Free Radic Biol Med 28, 1456-1462.

Herbig, U., W.A. Jobling, B.P. Chen, D.J. Chen, and J.M. Sedivy. 2004. Telomere shortening triggers senescence of human cells through a pathway involving ATM, p53, and p21(CIP1), but not p16(INK4a). Mol. Cell. 14, 501– 513.

Herskind C, Rodemann HP. 2000. Spontaneous and radiation-induced differentiation of fibroblasts. Exp. Gerontol. 35, 747–755.

Hierlihy AM, Seale P, Lobe CG, Rudnicki MA, Megeney LA. 2002. The post- natal heart contains a myocardial stem cell population, FEBS Lett. 530, 239 – 243.

Hill JH, Ward PA. 1971. The phlogistic role of C3 leukotactic fragments in myocardial infarcts of rats. J ExpMed 133, 885-900.

Horn MA, Graham HK, Richards MA, Clarke JD, Greensmith DJ, Briston SJ, Hall MC, Dibb KM, Trafford AW. 2012. Age-related divergent remodeling of the cardiac extracellular matrix in heart failure: collagen accumulation in the young and loss in the aged. J Mol Cell Cardiol. 53(1), 82-90.

Hsiao LC, Perbellini F, Gomes RS, Tan JJ, Vieira S, Faggian G, Clarke K, Carr CA. 2014. Murine cardiosphere-derived cells are impaired by age but not by cardiac dystrophic dysfunction. Stem Cells Dev. 23(9), 1027-36.

Hsieh PC, Segers VF, Davis ME, MacGillivray C, Gannon J, Molkentin JD, Robbins J, Lee RT. 2007. Evidence from a genetic fate- mapping study that stem cells refresh adult mammalian cardiomyocytes after injury. Nat. Med. 13, 970 – 974.

http://www.genecards.org/cgi-bin/carddisp.pl?gene=MYBL2

Huang Y, Wu J, Li R, Wang P, Han L, Zhang Z, Tong T. 2011. B-MYB delays cell aging by repressing p16 (INK4a) transcription. Cell Mol Life Sci. 68, 893–901.

Ye H, Li L, Guo H, Yin Y. 2012. MYBL2 is a substrate of GSK3-like kinase BIN2 and acts as a corepressor of BES1 in brassinosteroid signaling pathway in Arabidopsis. Proc Natl Acad Sci U S A. 109(49), 20142–20147.

Hulsmans M, Clauss S, Xiao L, Aguirre AD, King KR, Hanley A, Hucker WJ, Wülfers EM, Seemann G, Courties G, Iwamoto Y, Sun Y, Savol AJ, Sager HB, Lavine KJ, Fishbein GA, Capen DE, Da Silva N, Miquerol L, Wakimoto H, Seidman CE, Seidman JG, Sadreyev RI, Naxerova K, Mitchell RN, Brown D, Libby P, Weissleder R, Swirski FK, Kohl P, Vinegoni C, Milan DJ, Ellinor PT, Nahrendorf M. 2017. Macrophages facilitate electrical conduction in the heart. Cell 169, 510–522.

Hutchins GM, Bulkley BH. 1978. Infarct expansion versus extension: two different complications of acute myocardial infarction. AmJ Cardiol. 41, 1127–32.

Ibrahim AG, Cheng K, Marban E. 2014. Exosomes as critical agents of cardiac regeneration triggered by cell therapy. Stem Cell Rep. 2(5), 606–619.

Ishikawa H, Tsuyama N, Kawano MM. 2003. Interleukin-6-induced proliferation of human myeloma cells associated with CD45 molecules. Int J Hematol. 78(2), 95-105.

Jackson D, Volpert OV, Bouck N, Linzer DI. 1994. Stimulation and inhibition of angiogenesis by placental proliferin and proliferin-related protein. Science 266(5190), 1581-4.

Jackson R, Tilokee EL, Latham N, Mount S, Rafatian G, Strydhorst J, Ye B, Boodhwani M, Chan V, Ruel M, Ruddy TD, Suuronen EJ, Stewart DJ, Davis DR. 2015. Paracrine engineering of human cardiac stem cells with insulin-like growth factor 1 enhances myocardial repair. J Am Heart Assoc. 11, 4(9): e002104.

Jackson R, Mount S, Ye B, Mayfield AE, Chan V, Boodhwani M, Davies RA, Haddad H, Davis DR. 2017. Isolation of human explant derived cardiac stem cells from cryopreserved heart tissue. PLoS One. 12(4), e0176000.

Jennings RB, Reimer KA.1981. Lethal myocardial ischemic injury. Am J Pathol 102, 241-255.

Jeong JO, Han JW, Kim JM, Cho HJ, Park C, Lee N, Kim DW, Yoon YS. 2011. Malignant tumor formation after transplantation of short-term cultured bone marrow mesenchymal stem cells in experimental myocardial infarction and diabetic neuropathy. Circ. Res. 108(11), 1340–1347.

Jesty SA, Steffey MA, Lee FK, Breitbach M, Hesse M, Reining S, Lee JC, Doran RM, Nikitin AY, Fleischmann BK, Kotlikoff MI. 2012. c-kit+ precursors support postinfarction myogenesis in the neonatal, but not adult, heart. Proc. Natl. Acad. Sci. U. S. A 109, 13380-13385.

Jeyaraman MM, Rabbani R, Copstein L, Sulaiman W, Farshidfar F, Kashani HH, Qadar SMZ, Guan Q, Skidmore B, Kardami E, Ducas J, Mansour S, Zarychanski R, Abou-Setta AM. 2017. Autologous bone marrow stem cell therapy in patients with ST-elevation myocardial infarction: a systematic review and meta-analysis. Can J Cardiol. 33, 1611–1623.

Jie KE, Goossens MH, van OO, Lilien MR, Verhaar MC. 2009. Circulating endothelial progenitor cell levels are higher during childhood than in adult life. Atherosclerosis 202(2), 345-7.

Joaquin M, Watson RJ. 2003. Cell cycle regulation by the B-Myb transcription factor. Cell Mol Life Sci. 60, 2389–401.

Johnston PV, Sasano T, Mills K, Evers R, Lee ST, Smith RR, Lardo AC, Lai S, Steenbergen C, Gerstenblith G, Lange R, Marban E. 2009. Engraftment, differentiation, and functional benefits of autologous cardiosphere-derived cells in porcine ischemic cardiomyopathy. Circulation 120, 1075–1083.

Johung K, Goodwin EC, DiMaio D. 2007. Human papillomavirus E7 repression in cervical carcinoma cells initiates a transcriptional cascade driven by the retinoblastoma family, resulting in senescence. J Virol. 81, 2102–16.

Jopling C, Sleep E, Raya M, Martí M, Raya A, Izpisúa Belmonte JC. 2010. Zebrafish heart regeneration occurs by cardiomyocyte dedifferentiation and proliferation. Nature 464, 606-609.

Kajstura J, Leri A, Finato N, Di Loreto C, Beltrami CA, Anversa P. 1998. Myocyte proliferation in end- stage cardiac failure in humans. Proc. Natl. Acad. Sci. U.S.A. 95, 8801 – 8805.

Kanamori H, Takemura G, Goto K, Maruyama R, OnoK,Nagao K, Tsujimoto A, Ogino A, Takeyama T, Kawaguchi T,Watanabe T, Kawasaki M, Fujiwara T, Fujiwara H, Seishima M, Minatoguchi S. 2011. Autophagy limits acute myocardial infarction induced by permanent coronaryartery occlusion. Am J Physiol Heart Circ Physiol 300, H2261-H2271.

Kanda P, Davis DR. 2017. Cellular mechanisms underlying cardiac engraftment of stem cells. Expert Opin Biol Ther.17, 1127–1143.

Kang HT, Lee HI, Hwang ES. 2006. Nicotinamide extends replicative lifespan of human cells. Aging Cell 5, 423–436.

Karoubi G, Ormiston ML, Stewart DJ, Courtman DW. 2009. Single-cell hydrogel encapsulation for enhanced survival of human marrow stromal cells. Biomaterials 30, 5445-55.

Kenyon CJ. 2010. The genetics of ageing. Nature 464, 504–512.

Khan SS, Singer BD, Vaughan DE. 2017. Molecular and physiological manifestations and measurement of aging in humans. Aging Cell 16(4), 624-633.

Khatiwala R, Cai C. 2016. Strategies to Enhance the Effectiveness of Adult Stem Cell Therapy for Ischemic Heart Diseases Affecting the Elderly Patients. Stem Cell Rev. 12(2), 214–223.

Khatiwala RV, Zhang S, Li X, Devejian N, Bennett E, Cai C. 2018. Inhibition of p16INK4A to Rejuvenate Aging Human Cardiac Progenitor Cells via the Upregulation of Anti-oxidant and NFκB Signal Pathways. Stem Cell Rev.14(4), 612-625.

Khongkow P, Karunarathna U, Khongkow M, Gong C, Gomes AR, Yag€ue E, Monteiro LJ, Kongsema M, Zona S, Man EP, Tsang JW, Coombes RC, Wu KJ, Khoo US, Medema RH, Freire R, Lam EW. 2013. FOXM1 targets NBS1 to regulate DNA damage-induced senescence and epirubicin resistance. Oncogene, 33(32), 4144-55.

Kocher AA, Schuster MD, Szabolcs MJ, Takuma S, Burkhoff D, Wang J, Homma S, Edwards NM, Itescu S. 2001. Neovascularization of ischemic myocardium by human bone- marrow-derived angioblasts prevents cardiomyocyte apoptosis, reduces remodeling and improves cardiac function. Nat Med 7, 430 – 6.

Kollman C, Howe CW, Anasetti C, Antin JH, Davies SM, Filipovich AH, Hegland J, Kamani N, Kernan NA, King R, Ratanatharathorn V, Weisdorf D, Confer DL. 2001. Donor characteristics as risk factors in recipients after transplantation of bone marrow from unrelated donors: the effect of donor age. Blood 98, 2043–2051.

Krtolica A, Parrinello S, Lockett S, Desprez PY, Campisi J. 2001. Senescent fibroblasts promote epithelial cell growth and tumorigenesis: a link between cancer and aging. Proc. Natl. Acad. Sci. USA. 98, 12072– 12077.

Kubler W, Spieckermann PG. 1970. Regulation of glycolysis in the ischemic and the anoxic myocardium. J Mol Cell Cardiol 1, 351-377.

Kuhn HG, Dickinson-Anson H, Gage FH. 1996. Neurogenesis in the dentate gyrus of the adult rat: age-related decrease of neuronal progenitor proliferation. J. Neurosci. 16, 2027–2033.

Kuhn KA, Manieri NA, Liu TC, Stappenbeck TS. 2014. IL-6 stimulates intestinal epithelial proliferation and repair after injury. PLoS One 9(12), e114195.

Kuilman T, Michaloglou C, Mooi WJ, Peeper DS. 2010. The essence of senescence. Genes Dev. 24, 2463–2479.

Kurz DJ, Decary S, Hong Y, Erusalimsky JD. 2000. Senescence-associated (beta)-galactosidase reflects an increase in lysosomal mass during replicative ageing of human endothelial cells. J Cell Sci. 113 (Pt 20), 3613-22.

Laberge RM, Sun Y, Orjalo AV, Patil CK, Freund A, Zhou L, Curran SC, Davalos AR, Wilson-Edell KA, Liu S, Limbad C, Demaria M, Li P, Hubbard GB, Ikeno Y, Javors M, Desprez PY, Benz CC, Kapahi P, Nelson PS, Campisi J. 2015. MTOR regulates the pro-tumorigenic senescence-associated secretory phenotype by promoting IL1A translation. Nat Cell Biol 17, 1049–61.

Lakatta EG. 1990. Changes in cardiovascular function with aging. European heart journal 11(Suppl C), 22–29.

Lane S, Farlie P, Watson R. 1997. B-Myb function can be markedly enhanced by cyclin A-dependent kinase and protein truncation. Oncogene. 14, 2445–53.

Latham N, Davis DR. 2014. Chapter 8- Recent advances in cardiac stem cell therapy to restore left ventricular function. In: Li RK, Weisel RD (eds). Cardiac Regeneration and Repair. Woodhead Publishing, Sawston, UK, 163–194.

Latham N, Ye B, Jackson R, Lam B, Kuraitis D, Ruel M, Suuronen EJ, Stewart DJ, Davis DR. 2013. Human blood and cardiac stem cells synergize to enhance cardiac repair when cotransplanted into ischemic myocardium. Circulation 128, S1–S8.

Laviano A. 2014. Young blood. N. Engl. J. Med. 371, 573–575.

Lawless C, Wang C, Jurk D, Merz A, Zglinicki Tv, Passos JF. 2010. Quantitative assessment of markers for cell senescence. Exp Gerontol. 45(10), 772-8.

Lee BY, Han JA, Im JS, Morrone A, Johung K, Goodwin EC, Kleijer WJ, DiMaio D, Hwang ES. 2006. Senescence-associated β-galactosidase is lysosomal acid β-galactosidase. Aging Cell 5, 187–195.

Lee IH, Cao L, Mostoslavsky R, Lombard DB, Liu J, Bruns NE, Tsokos M, Alt FW, Finkel T. 2008. A role for the NAD dependent deacetylase Sirt1 in the regulation of autophagy. Proc Natl Acad Sci U S A 105, 3374–9.

Lee ST, White AJ, Matsushita S, Malliaras K, Steenbergen C, Zhang Y, Li TS, Terrovitis J, Yee K, Simsir S, Makkar R, Marban E. 2011. Intramyocardial injection of autologous cardiospheres or cardiosphere-derived cells preserves function and minimizes adverse ventricular remodeling in pigs with heart failure post-myocardial infarction. J AmColl Cardiol 57, 455–465.

Lee WW, Marinelli B, van der Laan AM, Sena BF, Gorbatov R, Leuschner F, Dutta P, Iwamoto Y, Ueno T, Begieneman MP, Niessen HW, Piek JJ, Vinegoni C, Pittet MJ, Swirski FK, TawakolA, DiCarli M, Weissleder R, Nahrendorf M. 2012. PET/MRI of inflammation in myocardial infarction. J Am Coll Cardiol 59, 153-163.

Levy D, Kenchaiah S, Larson MG, Benjamin EJ, Kupka MJ, Ho KK, Murabito JM, Vasan RS. 2002. Long-term trends in the incidence of and survival with heart failure. N Engl J Med. 347(18), 1397-402.

Li TS, Cheng K, Lee ST, Matsushita S, Davis DR Malliaras K, Zhang Y, Smith RR, Marban E. 2010a. Cardiospheres recapitulate a niche-like microenvironment rich in stemness and cell-matrix interactions, rationalizing their enhanced functional potency for myocardial repair. Stem Cells 28, 2088–2098.

Li TS, Cheng K, Malliaras K, Matsushita N, Sun B, Marbán L, Zhang Y, Marbán E. 2011. Expansion of human cardiac stem cells in physiological oxygen improves cell production efficiency and potency for myocardial repair. Cardiovasc Res. 89,157-65.

Li TS, Cheng K, Malliaras K, Smith RR, Zhang Y, Sun B, Matsushita N, Blusztajn A, Terrovitis J, Kusuoka H, Marban L, Marban E. 2012. Direct comparison of different stem cell types and

subpopulations reveals superior paracrine potency and myocardial repair efficacy with cardiosphere-derived cells. J Am Coll Cardiol 59, 942–953.

Li X, McDonnell DP. 2002. The transcription factor B-Myb is maintained in an inhibited state in target cells through its interaction with the nuclear corepressors N-CoR and SMRT. Mol Cell Biol. 22, 3663–3673.

Li Y, Hiroi Y, Liao JK. 2010b. Notch signaling as an important mediator of cardiac repair and regeneration after myocardial infarction. Trends Cardiovasc Med. 20(7), 228-31.

Lin D, Fiscella M, O'Connor PM, Jackman J, Chen M, Luo LL. 1994. Constitutive expression of B-myb can bypass p53-induced Waf1/Cip1-mediated G1 arrest. Proc. Natl Acad. Sci. USA 91, 10079–10083.

Liu S, Fang X, Hall H, Yu S, Smith D, Lu Z, Fang D, Liu J, Stephens LC, Woodgett JR, Mills GB. 2008. Homozygous deletion of glycogen synthase kinase 3beta bypasses senescence allowing Ras transformation of primary murine fibroblasts. Proc Natl Acad Sci U S A.105(13), 5248-53.

Liu P, Xu B, Cavalieri TA, Hock CE. 2002. Age-related difference in myocardial function and inflammation in a rat model of myocardial ischemia-reperfusion. Cardiovasc Res.56(3), 443-53.

Litovchick L, Sadasivam S, Florens L, Zhu X, Swanson SK, Velmurugan S, Chen R, Washburn MP, Liu XS, DeCaprio JA. 2007. Evolutionarily conserved multisubunit RBL2/p130 and E2F4 protein complex represses human cell cycle-dependent genes in quiescence. Mol Cell. 26, 539–51.

Litovchick L, Florens LA, Swanson SK, Washburn MP, DeCaprio JA. 2011. DYRK1A protein kinase promotes quiescence and senescence through DREAM complex assembly. Genes Dev. 25, 801–13.

Lobo V, Patil A, Phatak A, Chandra N. 2010. Free radicals, antioxidants and functional foods: Impact on human health, Pharmacogn Rev. 4(8), 118–126.

Loffredo FS, Steinhauser ML, Jay SM, Gannon J, Pancoast JR, Yalamanchi P, Sinha M, Dall'Osso C, Khong D, Shadrach JL, Miller CM, Singer BS, Stewart A, Psychogios N, Gerszten RE, Hartigan AJ, Kim MJ, Serwold T, Wagers AJ, Lee RT. 2013. Growth differentiation factor 11 is a circulating factor that reverses agerelated cardiac hypertrophy. Cell 153, 828–839.

López-Otín C, Blasco MA, Partridge L, Serrano M, Kroemer G. 2013. The hallmarks of aging. Cell 153, 1194–1217.

Lorvellec M, Dumon S, Maya-Mendoza A, Jackson D, Frampton J, Garcia P. 2010. B-Myb is critical for proper DNA duplication during an unperturbed S phase in mouse embryonic stem cells. Stem Cells 28, 1751–1759.

Lowe SW, Sherr CJ. 2003. Tumor suppression by Ink4aArf: progress and puzzles. Curr. Opin. Genet. Dev. 13, 77–83.

Lujambio A. 2016.To clear, or not to clear (senescent cells)? That is the question. Bioessays 38 Suppl 1, S56-64.

Ma Y, Chiao YA, Clark R, Flynn ER, Yabluchanskiy A, Ghasemi O, Zouein F, Lindsey ML, Jin YF. 2015. Deriving a cardiac ageing signature to reveal MMP-9-dependent inflammatory signalling in senescence. Cardiovasc Res. 106, 421–31.

Ma Y, Mouton AJ, Lindsey ML. 2018. Cardiac macrophage biology in the steady-state heart, the aging heart, and following myocardial infarction. Transl Res. 191, 15-28.

Makkar RR, Smith RR, Cheng K, Malliaras K, Thomson LE, Berman D, Czer LS, Marban L, Mendizabal A, Johnston PV, Russell SD, Schuleri KH, Lardo AC, Gerstenblith G. Marban E. 2012. Intracoronary cardiosphere-derived cells for heart regeneration after myocardial infarction (CADUCEUS): a prospective, randomised phase 1 trial. Lancet 379, 895–904.

Malliaras K, Zhang Y, Seinfeld J, Galang G, Tseliou E, Cheng K, Sun B, Aminzadeh M, Marbán E. 2013. Cardiomyocyte proliferation and progenitor cell recruitment underlie therapeutic regeneration after myocardial infarction in the adult mouse heart. EMBO Mol Med. 5, 191-209.

Malliaras K, Ibrahim A, Tseliou E, Liu W, Sun B, Middleton RC, Seinfeld J, Wang L, Sharifi BG, Marbán E. 2014a. Stimulation of endogenous cardioblasts by exogenous cell therapy after myocardial infarction. EMBO Mol Med. 6(6), 760–777.

Malliaras K, Makkar RR, Smith RR, Cheng K, Wu E, Bonow RO, Marban L, Mendizabal A, Cingolani E, Johnston PV, Gerstenblith G, Schuleri KH, Lardo AC, Marban E. 2014b. Intracoronary cardiosphere-derived cells after myocardial infarction: evidence of therapeutic

regeneration in the final 1-year results of the CADUCEUS trial (CArdiosphere-Derived aUtologous stem CElls to reverse ventricUlar dySfunction). J Am Coll Cardiol 63, 110–122.

Mannefeld M, Klassen E, Gaubatz S. 2009. B-MYB is required for recovery from the DNA damageinduced G2 checkpoint in p53 mutant cells. Cancer Res. 69:4073–80.

Marelli D, Desrosiers C, el-Alfy M, Kao RL, Chiu RC. 1992. Cell transplantation for myocardial repair: an experimental approach. Cell Transplant 1, 383 – 90.

Martin CM, Meeson AP, Robertson SM, Hawke TJ, Richardson JA, Bates S, Goetsch SC, Gallardo TD, Garry DJ. 2004. Persistent expression of the ATP-binding cassette transporter, Abcg2, identifies cardiac SP cells in the developing and adult heart. Dev. Biol. 265, 262 – 275.

Martinez I, Cazalla D, Almstead LL, Steitz JA, DiMaio D. 2011. miR-29 and miR-30 regulate B-Myb expression during cellular senescence. Proc Natl Acad Sci U S A 108, 522–7.

Martinez I, DiMaio D. 2011. B-Myb, Cancer, Senescence, and MicroRNAs. Cancer Res. 71(16), 5370–5373.

Masselink H, Vastenhouw N, Bernards R. 2001. B-myb rescues ras-induced premature senescence, which requires its transactivation domain. Cancer Lett. 171, 87–101.

Matsui Y, Morimoto J, Uede T. 2010. Role of matricellular proteins in cardiac tissue remodeling after myocardial infarction. World J Biol Chem.1(5), 69-80.

Matsui Y, Takagi H, Qu X, Abdellatif M, Sakoda H, Asano T, Levine B, Sadoshima J. 2007. Distinct roles of autophagy in the heart during ischemia and reperfusion: Roles of AMP-activated protein kinase and Beclin 1 in mediating autophagy. Circ Res. 100, 914-922.

Matthews C, Gorenne I, Scott S, Figg N, Kirkpatrick P, Ritchie A, Goddard M, Bennett M. 2006. Vascular smooth muscle cells undergo telomere-based senescence in human atherosclerosis: effects of telomerase and oxidative stress. Circ. Res. 99, 156–164.

Maulik N, Das DK. 2002. Potentiation of angiogenic response by ischemic and hypoxic preconditioning of the heart. J Cell Mol Med. 6(1), 13-24.

Mayfield AE, Tilokee EL, Latham N, McNeill B, Lam BK, Ruel M, Suuronen EJ, Courtman DW, Stewart DJ, Davis DR. 2014. The effect of encapsulation of cardiac stem cells within matrix-

enriched hydrogel capsules on cell survival, post-ischemic cell retention and cardiac function. Biomaterials 35(1), 133-42.

Mayfield AE, Fitzpatrick ME, Latham N, Tilokee EL, Villanueva M, Mount S, Lam BK, Ruel M, Stewart DJ, Davis DR. 2016. The impact of patient co-morbidities on the regenerative capacity of cardiac explant-derived stem cells. Stem Cell Research and Therapy, 7, 60.

Mayfield AE., Kanda P, Nantsios A, Parent S, Mount S, Dixit S, Ye B, Seymour R, Stewart DJ, Davis DR. 2017. Interleukin-6 Mediates Post-Infarct Repair by Cardiac Explant-Derived Stem Cells. Theranostics 7 (19), 4850-4861.

Meerson FZ, Kagan VE, Kozlov YuP, Belkina LM, Arkhipenko YuV. 1982. The role of lipid peroxidation in pathogenesis of ischemic damage and the antioxidant protection of the heart. Basic Res Cardiol.77(5), 465-85.

Memmott RM, Dennis PA. 2009. Akt-dependent and independent mechanisms of mTOR regulation in cancer. Cell Signal 21(5), 656–664.

Menasché P, Hagège AA, Scorsin M, Pouzet B, Desnos M, Duboc D, Schwartz K, Vilquin JT, Marolleau JP. 2001. Myoblast transplantation for heart failure. Lancet 357, 279 – 80.

Menasché P, Alfieri O, Janssens S, McKenna W, Reichenspurner H, Trinquart L, Vilquin JT, Marolleau JP, Seymour B, Larghero J, Lake S, Chatellier G, Solomon S, Desnos M, Hagège AA. 2008. The Myoblast Autologous Grafting in Ischemic Cardiomyopathy (MAGIC) trial: first randomized placebo- controlled study of myoblast transplantation. Circulation 117, 1189 – 200.

Meschiari CA, Ero OK, Pan H, Finkel T, Lindsey ML. 2017. The impact of aging on cardiac extracellular matrix. Geroscience 39, 7–18.

Messina E, De Angelis L, Frati G, Morrone S, Chimenti S, Fiordaliso F, Salio M, Battaglia M, Latronico MV, Coletta M, Vivarelli E, Frati L, Cossu G, Giacomello A. 2004. Isolation and expansion of adult cardiac stem cells from human and murine heart, Circ. Res. 95, 911 – 921.

Min JN, Whaley RA, Sharpless NE, Lockyer P, Portbury AL, Patterson C. 2008. CHIP deficiency decreases longevity, with accelerated aging phenotypes accompanied by altered protein quality control. Mol. Cell. Biol. 28, 4018–4025.

Mishra R, Vijayan K, Colletti EJ, Harrington DA, Matthiesen TS, Simpson D, Goh SK, Walker BL, Almeida-Porada G, Wang D, Backer CL, Dudley SC, Jr., Wold LE, Kaushal S. 2011. Characterization and functionality of cardiac progenitor cells in congenital heart patients. Circulation 123(4), 364-73.

Mohsin S, Khan M, Toko H, Bailey B, Cottage CT, Wallach K, Nag D, Lee A, Siddiqi S, Lan F, Fischer KM, Gude N, Quijada P, Avitabile D, Truffa S, Collins B, Dembitsky W, Wu JC, Sussman MA. 2012. Human cardiac progenitor cells engineered with pim-i kinase enhance myocardial repair. J Am Coll Cardiol. 60(14), 1278-87.

Mohsin S, Khan M, Nguyen J, Alkatib M, Siddiqi S, Hariharan N, Wallach K, Monsanto M, Gude NA, Dembitsky WP, Sussman MA. 2013. Rejuvenation of human cardiac progenitor cells with pim-1 kinase. Circulation research 113(10), 1169-79.

Molawi K, Wolf Y, Kandalla PK, Favret J, Hagemeyer N, Frenzel K, Pinto AR, Klapproth K, Henri S, Malissen B, Rodewald HR, Rosenthal NA, Bajenoff M, Prinz M, Jung S, Sieweke MH. 2014. Progressive replacement of embryo-derived cardiac macrophages with age. J Exp Med 211, 2151–8.

Molgat AS, Tilokee EL, Rafatian G, Vulesevic B, Ruel M, Milne R, Suuronen EJ, Davis DR 2014. Hyperglycemia inhibits cardiac stem cell-mediated cardiac repair and angiogenic capacity. Circulation 130, S70–S76.

Montini E, Cesana D, Schmidt M, Sanvito F, Bartholomae CC, Ranzani M, Benedicenti F, Sergi Sergi L, Ambrosi A, Ponzoni M, Doglioni C, Di Serio C, von Kalle C, Naldini L. 2009. The genotoxic potential of retroviral vectors is strongly modulated by vector design and integration site selection in a mouse model of HSC gene therapy. J Clin Invest. 119, 964–975.

Mowla SN, Lam EW, Jat PS. 2014. Cellular senescence and aging: the role of B-MYB. Aging Cell 13(5), 773-9.

Mukherjee R, Brinsa TA, Dowdy KB, Scott AA, Baskin JM, Deschamps AM, Lowry AS, Escobar GP, Lucas DG, Yarbrough WM, Zile MR, Spinale FG. 2003. Myocardial infarct expansion and matrix metalloproteinase inhibition. Circulation 107, 618-625.

Muller GA, Engeland K. 2010.The central role of CDE/CHR promoter elements in the regulation of cell cycle-dependent gene transcription. FEBS J. 277, 877–93.

Müller-Ehmsen J, Krausgrill B, Burst V, Schenk K, Neisen UC, Fries JW, Fleischmann BK, Hescheler J, Schwinger RH. 2006. Effective engraftment but poor mid-term persistence of mononuclear and mesenchymal bone marrow cells in acute and chronic rat myocardial infarction. J Mol Cell Cardiol. 41(5), 876-84.

Muller-Hocker J. 1989. Cytochrome-c-oxidase deficient cardiomyocytes in the human heart–an age-related phenomenon. A histochemical ultracytochemical study. Am. J. Pathol. 134, 1167–1173.

Munk R, Panda AC, Grammatikakis I, Gorospe M, Abdelmohsen K. 2017. Senescence-Associated MicroRNAs. Chapter 4- Int Rev Cell Mol Biol. 334, 177-205.

Murphy T, Thuret S. 2015. The systemic milieu as a mediator of dietary influence on stem cell function during ageing. Ageing Res Rev.19, 53-64.

Murry CE, Wiseman RW, Schwartz SM, Hauschka SD. 1996. Skeletal myoblast transplantation for repair of myocardial necrosis. J Clin Invest 98, 2512 – 23.

Murry CE, Soonpaa MH, Reinecke H, Nakajima H, Nakajima HO, Rubart M, Pasumarthi KB, Virag JI, Bartelmez SH, Poppa V, Bradford G, Dowell JD, Williams DA, Field LJ. 2004. Haematopoietic stem cells do not transdifferentiate into cardiac myocytes in myocardial infarcts. Nature 428, 664 – 8.

Musa J, Aynaud MM, Mirabeau O, Delattre O, Grünewald TG. 2017. MYBL2 (B-Myb): a central regulator of cell proliferation, cell survival and differentiation involved in tumorigenesis. Cell Death Dis. 8(6), e2895.

Nakamura T, Hosoyama T, Kawamura D, Takeuchi Y, Tanaka Y, Samura M, Ueno K, Nishimoto A, Kurazumi H, Suzuki R, Ito H, Sakata K, Mikamo A, Li TS, Hamano K. 2016. Influence of aging on the quantity and quality of human cardiac stem cells. Sci Rep.6, 22781.

Nakamura T, Hosoyama T, Murakami J, Samura M, Ueno K, Kurazumi H, Suzuki R, Mikamo A, Hamano K. 2017. Age-related increase in Wnt inhibitor causes a senescence-like phenotype in human cardiac stem cells. Biochem Biophys Res Commun. 487(3), 653-659.

Narita M, Nũnez S, Heard E, Narita M, Lin AW, Hearn SA, Spector DL, Hannon GJ, Lowe SW. 2003. Rb-mediated heterochromatin formation and silencing of E2F target genes during cellular senescence. Cell 113, 703–716.

Nelson G, Wordsworth J, Wang C, Jurk D, Lawless C, Martin-Ruiz C, von Zglinicki T. 2012. A senescent cell bystander effect: senescence-induced senescence. Aging Cell 11, 345–349.

Nguyen N, Sussman MA. 2015. Rejuvenating the senescent heart. Curr Opin Cardiol. 30(3), 235–239.

Ogryzko VV, Hirai TH, Russanova VR, Barbie DA, Howard BH. 1996. Human fibroblast commitment to a senescence-like state in response to histone deacetylase inhibitors is cell cycle dependent. Mol. Cell. Biol. 16, 5210–5218.

Oh H, Bradfute SB, Gallardo TD, Nakamura T, Gaussin V, Mishina Y, Pocius J, Michael LH, Behringer RR, Garry DJ, Entman ML, Schneider MD. 2003. Cardiac progenitor cells from adult myocardium: homing, differentiation, and fusion after infarction. Proc Natl Acad Sci U S A 100 (21), 12313-8.

Oh IH, Reddy EP. 1999. The myb gene family in cell growth, differentiation and apoptosis. Oncogene 18, 3017–33.

Ong SB, Gustafsson AB. 2012. New roles for mitochondria in cell death in the reperfused myocardium. Cardiovasc Res 94, 190-196.

Olivetti G, Giordano G, Corradi D, Melissari M, Lagrasta C, Gambert SR, Anversa P. 1995. Gender differences and aging: effects in the human heart. J Am Coll Cardiol. 26, 1068–1079.

Olivieri F, Mazzanti I, Abbatecola AM, Recchioni R, Marcheselli F, Procopio AD, Antonicelli R. 2012. Telomere/Telomerase system: a new target of statins pleiotropic effect? Curr Vasc Pharmacol. 10(2), 216-24.

Orjalo, A.V., D. Bhaumik, B.K. Gengler, G.K. Scott, and J. Campisi. 2009. Cell surface-bound IL-1α is an upstream regulator of the senescence-associated IL-6/IL-8 cytokine network. Proc. Natl. Acad. Sci. USA. 106, 17031– 17036.

Ounpuu S, Negassa A, Yusuf S. 2001. INTER-HEART: A global study of risk factors for acute myocardial infarction. Am Heart J. 141(5), 711-21.

Paik JH, Ding Z, Narurkar R, Ramkissoon S, Muller F, Kamoun WS, Chae SS, Zheng H, Ying H, Mahoney J, Hiller D, Jiang S, Protopopov A, Wong WH, Chin L, Ligon KL, DePinho RA. 2009. FoxOs cooperatively regulate diverse pathways governing neural stem cell homeostasis. Cell Stem Cell 5, 540–553.

Papetti M, Augenlicht LH. 2011. MYBL2, a link between proliferation and differentiation in maturing colon epithelial cells. J Cell Physiol. 226(3), 785–791.

Park SY, Lee JH, Ha M, Nam JW, Kim VN. 2009. miR-29 miRNAs activate p53 by targeting p85 alpha and CDC42. Nat Struct Mol Biol 16, 23–29.

Passos JF, Saretzki G, von Zglinicki T. 2007. DNA damage in telomeres and mitochondria during cellular senescence: is there a connection? Nucleic Acids Res. 35(22), 7505–7513.

Pfeffer MA, Braunwald E. 1990. Ventricular remodeling after myocardial infarction. Experimental observations and clinical implications. Circulation 81, 1161-1172.

Pinto AR, Paolicelli R, Salimova E, Gospocic J, Slonimsky E, Bilbao-Cortes D, Godwin JW, Rosenthal NA. 2012. An abundant tissue macrophage population in the adult murine heart with a distinct alternatively-activated macrophage profile. PLoS One 7, e36814.

Poss KD, Wilson LG, Keating MT. 2002. Heart regeneration in zebrafish. Science 298, 2188-2190.

Porrello ER, Mahmoud AI, Simpson E, Hill JA, Richardson JA, Olson EN, Sadek HA. 2011. Transient regenerative potential of the neonatal mouse heart. Science 331, 1078-1080.

Porrello ER, Mahmoud AI, Simpson E, Johnson BA, Grinsfelder D, Canseco D, Mammen PP, Rothermel BA, Olson EN, Sadek HA. 2013. Regulation of neonatal and adult mammalian heart regeneration by the miR-15 family. Proc. Natl. Acad. Sci. U. S. A 110, 187-192.

Povsic TJ, O'Connor CM, Henry T, Taussig A, Kereiakes DJ, Fortuin FD, Niederman A, Schatz R, Spencer R 4th, Owens D, Banks M, Joseph D, Roberts R, Alexander JH, Sherman W. 2011. A doubleblind, randomized, controlled, multicenter study to assess the safety and cardiovascular

effects of skeletal myoblast implantation by catheter delivery in patients with chronic heart failure after myocardial infarction. Am Heart J. 162, 654 – 62.

Pruitt K, Zinn RL, Ohm JE, McGarvey KM, Kang SH, Watkins DN, Herman JG, Baylin SB. 2006. Inhibition of SIRT1 reactivates silenced cancer genes without loss of promoter DNA hypermethylation. PLoS Genet. 2(3), e40.

Pusic AD, Kraig RP. 2014. Youth and environmental enrichment generate serum exosomes containing miR-219 that promote CNS myelination. Glia 62(2), 284-99.

Pyo JO, Nah J, Jung YK. 2012. Molecules and their functions in autophagy. Exp Mol Med. 44(2), 73–80.

Quaas M, M€uller GA, Engeland K. 2012. p53 can repress transcription of cell cycle genes through a p21 (WAF1/CIP1)-dependent switch from MMB to DREAM protein complex binding at CHR promoter elements. Cell Cycle 11, 4661–4672.

Quaini F, Urbanek K, Beltrami AP, Finato N, Beltrami CA, Nadal-Ginard B, Kajstura J, Leri A, Anversa P. 2002. Chimerism of the transplanted heart. N. Engl. J. Med. 346, 5 – 15.

Rabbani N, Thornalley PJ. 2008. Dicarbonyls linked to damage in the powerhouse: glycation of mitochondrial proteins and oxidative stress. Biochem Soc Trans. 36, 1045–1050.

Reed MJ, Edelberg JM. 2004. Impaired angiogenesis in the aged. Sci Aging Knowledge Environ. 2004(7), pe7.

Ren G, Michael LH, Entman ML, Frangogiannis NG. 2002. Morphological characteristics of the microvasculature in healing myocardial infarcts. J Histochem Cytochem 50, 71-79.

Riquelme JA, Chavez MN, Mondaca-Ruff D, Bustamante M, Vicencio JM, Quest AF, Lavandero S. 2016. Therapeutic targeting of autophagy in myocardial infarction and heart failure. Expert Rev Cardiovasc Ther.14(9), 1007-19.

Rivard A, Fabre JE, Silver M, Chen D, Murohara T, Kearney M, Magner M, Asahara T, Isner JM. 1999. Age-dependent impairment of angiogenesis. Circulation 99(1), 111-20.

Rodier F, Campisi J. 2011. Four faces of cellular senescence. J Cell Biol. 192(4), 547-56.

Rodier F, Muñoz DP, Teachenor R, Chu V, Le O, Bhaumik D, Coppé JP, Campeau E, Beauséjour CM, Kim SH, Davalos AR, Campisi J. 2011. DNA-SCARS: distinct nuclear structures that sustain damage-induced senescence growth arrest and inflammatory cytokine secretion. J. Cell Sci. 124, 68–81.

Rossi DJ, Bryder D, Zahn JM, Ahlenius H, Sonu R, Wagers AJ, Weissman IL. 2005. Cell intrinsic alterations underlie hematopoietic stem cell aging. Proc. Natl Acad. Sci. USA 102, 9194–9199.

Rufini A, Tucci P, Celardo I, Melino G. 2013. Senescence and aging: the critical roles of p53. Oncogene 32, 5219–5243.

Sablina AA, Budanov AV, Ilyinskaya GV, Agapova LS, Kravchenko JE, Chumakov PM. 2005. The antioxidant function of the p53 tumor suppressor. Nature Med. 11, 1306–1313.

Sadasivam S, Duan S, DeCaprio JA. 2012. The MuvB complex sequentially recruits B-Myb and FoxM1 to promote mitotic gene expression. Genes Dev. 26, 474–89.

Sadasivam S, DeCaprio JA. 2013. The DREAM complex: Master coordinator of cell cycle dependent gene expression. Nat Rev Cancer. 13(8), 585–595.

Sagiv A, Biran A, Yon M, Simon J, Lowe SW, Krizhanovsky V. 2013. Granule exocytosis mediates immune surveillance of senescent cells. Oncogene 32, 1971–7.

Sagiv A, Krizhanovsky V. 2013. Immunosurveillance of senescent cells: the bright side of the senescence program. Biogerontology 14, 617–28.

Sala A, Kundu M, Casella I, Engelhard A, Calabretta B, Grasso L, Paggi MG, Giordano A, Watson RJ, Khalili K, Peschle C. 1997. Activation of human B-MYB by cyclins. Proc Natl Acad Sci U S A 94, 532–6.

Sala A, Calabretta B. 1992. Regulation of BALB/c 3T3 fibroblast proliferation by B-myb is accompanied by selective activation of cdc2 and cyclin D1 expression. Proc Natl Acad Sci U S A 89, 10415–9.

Sanada F, Kim J, Czarna A, Chan NY, Signore S, Ogórek B, Isobe K, Wybieralska E, Borghetti G, Pesapane A, Sorrentino A, Mangano E, Cappetta D, Mangiaracina C, Ricciardi M, Cimini M, Ifedigbo E, Perrella MA, Goichberg P, Choi AM, Kajstura J, Hosoda T, Rota M, Anversa P, Leri

A. 2014. c-Kit-positive cardiac stem cells nested in hypoxic niches are activated by stem cell factor reversing the aging myopathy. Circ Res. 114(1), 41-55.

Sastry L, Johnson T, Hobson M J, Smucker B, Cornetta K. 2002. Titering lentiviral vectors: comparison of DNA, RNA and marker expression methods. Gene Ther. 9(17), 1155-1162.

Schubert S, Horstmann S, Bartusel T, Klempnauer K-H. 2004. The cooperation of B-Myb with the coactivator p300 is orchestrated by cyclins A and D1. Oncogene 23, 1392–1404.

Sciarretta S, Hariharan N, Monden Y, Zablocki D, Sadoshima J. 2011. Is autophagy in response to ischemia and reperfusion protective or detrimental for the heart? Pediatr Cardiol. 32, 275–81.

Segers VF, Tokunou T, Higgins LJ, MacGillivray C, Gannon J, Lee RT. 2007. Local delivery of proteaseresistant stromal cell derived factor-1 for stem cell recruitment after myocardial infarction. Circulation 116(15), 1683–1692.

Senyo SE, Steinhauser ML, Pizzimenti CL, Yang VK, Cai L, Wang M, Wu TD, Guerquin-Kern JL, Lechene CP, Lee RT. 2013. Mammalian heart renewal by pre-existing cardiomyocytes. Nature 493, 433–436.

Sharpless, NE, DePinho RA. 2007. How stem cells age and why this makes us grow old. Nature Rev. Mol. Cell Biol. 8, 703–713.

Shay JW, Wright WE. 2007. Hallmarks of telomeres in ageing research. J Pathol. 211(2), 114-23.

Shih H, Lee B, Lee RJ, Boyle AJ. 2010. The Aging Heart and Post-Infarction Left Ventricular Remodeling. J Am Coll Cardiol. 57(1), 9–17.

Shiloh Y. 2003. ATM and related protein kinases: safeguarding genome integrity. Nat. Rev. Cancer 3, 155–168.

Shinde AV, Frangogiannis NG. 2014. Fibroblasts in myocardial infarction: A role in inflammation and repair. J Mol Cell Cardiol 70, 74-82.

Shtutman M, Zhurinsky J, Simcha I, Albanese C, D'Amico M, Pestell R, Ben-Ze'ev A. 1999. The cyclin D1 gene is a target of the beta-catenin/LEF-1 pathway. Proc Natl Acad Sci U S A 96(10), 5522-7.

Siddiqi S, Sussman MA. 2013. Cardiac Hegemony of Senescence. Curr Transl Geriatr Exp Gerontol Rep. 2(4).

Siminiak T, Kalawski R, Fiszer D, Jerzykowska O, Rzeźniczak J, Rozwadowska N, Kurpisz M. 2004. Autologous skeletal myoblast transplantation for the treatment of postinfarction myocardial injury: phase I clinical study with 12 months of follow- up. Am Heart J. 148, 531 – 7.

Simpson DL, Mishra R, Sharma S, Goh SK, Deshmukh S, Kaushal S. 2012. A strong regenerative ability of cardiac stem cells derived from neonatal hearts. Circulation 126, S46-S53. Smith RR, Barile L, Cho HC, Leppo MK, Hare JM, Messina E, Giacomello A, Abraham MR, Marbán E. 2007. Regenerative potential of cardiosphere-derivedcellsexpandedfrom percutaneous endomyocardial biopsy specimens. Circulation 115(7), 896-908.

Singla DK, Long X, Glass C, Singla RD, Yan B. 2011. Induced pluripotent stem (iPS) cells repair and regenerate infarcted myocardium. Mol Pharm 8, 1573–1581.

Smith RR, Barile L, Cho HC, Leppo MK, Hare JM, Messina E, Giacomello A, Abraham MR, Marbán E. 2007. Regenerative potential of cardiosphere-derived cells expanded from percutaneous endomyocardial biopsy specimens. Circulation 115, 896 – 908.

Smits AM, Dronkers E, Goumans MJ. 2018. The epicardium as a source of multipotent adult cardiac progenitor cells: Their origin, role and fate. Pharmacol Res. 127, 129-140.

Sousounis K, Baddour JA, Tsonis PA. 2014. Chapter Eight Aging and Regeneration in Vertebrates In: Mechanisms of Regeneration. Current Topics in Developmental Biology, Vol. 108, 217-246.

St John Sutton M, Lee D, Rouleau JL, Goldman S, Plappert T, Braunwald E, Pfeffer MA. 2003. Left ventricular remodeling and ventricular arrhythmias after myocardial infarction. Circulation 107, 2577-2582.

Sultana N, Zhang L, Yan J, Chen J, Cai W, Razzaque S, Jeong D, Sheng W, Bu L, Xu M, Huang GY, Hajjar RJ, Zhou B, Moon A, Cai CL. 2015. Resident c-Kit+ cells in the heart are not cardiac stem cells. Nat Commun. 6, 8701.

Sun Y, Firestein GS, Wenger L, Huang CY, Cheung HS. 2004. Telomerase-transduced osteoarthritic fibroblast-like synoviocyte cell line. Biochem Biophys Res Commun. 323(4), 1287-92.

Sundaresan NR, Gupta M, Kim G, Rajamohan SB, Isbatan A, Gupta MP. 2009. Sirt3 blocks the cardiac hypertrophic response by augmenting Foxo3a-dependent antioxidant defense mechanisms in mice. J Clin Invest. 119, 2758–71.

Tanaka Y, Patestos NP, Maekawa T, Ishii S. 1999. B-myb is required for inner cell mass formation at an early stage of development. J Biol Chem. 274, 28067–70.

Tarasov KV, Tarasova YS, Tam WL, Riordon DR, Elliott ST, Kania G, Li J, Yamanaka S, Crider DG, Gianluca Testa, Li RA, Lim B, Stewart CL, Liu Y, Van Eyk JE, Wersto RP, Wobus AM, Boheler KR. 2008. BMYB is Essential for Normal Cell Cycle Progression and Chromosomal Stability of Embryonic Stem Cells. PLoS One 3, e2478.

ter Horst EN, Hakimzadeh N, van der Laan AM, Krijnen PA, NiessenHW, Piek JJ. 2015. Modulators of macrophage polarization Influence healing of the infarcted myocardium. Int J Mol Sci 16, 29583–91.

Terrovitis J, Lautamaki R, Bonios M, Fox J, Engles JM, Yu J, Leppo MK, Pomper MG, Wahl RL, Seidel J, Tsui BM, Bengel FM, MR Abraham, Marbán E. 2009. Noninvasive quantification and optimization of acute cell retention by in vivo positron emission tomography after intramyocardial cardiac- derived stem cell delivery. J. Am. Coll. Cardiol. 54, 1619 – 1626.

The Lancet Editors. 2014. Expression of concern: the SCIPIO trial. Lancet 383, 1279.

Tilokee EL, Latham N, Jackson R, Mayfield AE, Ye B, Mount S, Lam BK, Suuronen EJ, Ruel M, Stewart DJ, Davis DR. 2016. Paracrine engineering of human explant-derived cardiac stem cells to over-express stromal cell derived factor 1alpha enhances myocardial repair. Stem Cells 34(7), 1826-35.

Tomaru U, Takahashi S, Ishizu A, Miyatake Y, Gohda A, Suzuki S, Ono A, Ohara J, Baba T, Murata S, Tanaka K, Kasahara M. 2012. Decreased proteasomal activity causes age-related phenotypes and promotes the development of metabolic abnormalities. Am. J. Pathol. 180, 963–972.

Tong C, Morrison A, Mattison S, Qian S, Bryniarski M, Rankin B, Wang J, Thomas DP, Li J. 2013. Impaired SIRT1 nucleocytoplasmic shuttling in the senescent heart during ischemic stress. FASEB J. 27(11), 4332–4342.

Tothova Z, Gilliland DG. 2007. FoxO transcription factors and stem cell homeostasis: insights from the hematopoietic system. Cell Stem Cell 1, 140–152.

Tseliou E, Reich H, de Couto G, Terrovitis J, Sun B, Liu W, Marbán E. 2014. Cardiospheres reverse adverse remodeling in chronic rat myocardial infarction: roles of soluble endoglin and Tgf-β signaling. Basic Res Cardiol.109 (6), 443.

Tseliou E, Fouad J, Reich H, Slipczuk L, de Couto G, Aminzadeh M, Middleton R, Valle J, Weixin L, Marbán E. 2015. Fibroblasts Rendered Antifibrotic, Antiapoptotic, and Angiogenic by Priming With Cardiosphere-Derived Extracellular Membrane Vesicles. J Am Coll Cardiol. 66, 599-611.

Urbanek K, Torella D, Sheikh F, De Angelis A, Nurzynska D, Silvestri F, Beltrami CA, Bussani R, Beltrami AP, Quaini F, Bolli R, Leri A, Kajstura J, Anversa P. 2005. Myocardial regeneration by activation of multipotent cardiac stem cells in ischemic heart failure. Proc Natl Acad Sci U S A. 102(24), 8692-7.

Uygur A, Lee RT. 2016. Mechanisms of Cardiac Regeneration. Dev Cell. 36 (4), 362–374.

Vaitkevicius PV, Fleg JL, Engel JH, O'Connor FC, Wright JG, Lakatta LE, Yin FC, Lakatta EG. 1993. Effects of age and aerobic capacity on arterial stiffness in healthy adults. Circulation 88, 1456–1462.

Valdes AM, Andrew T, Gardner JP, Kimura M, Oelsner E, Cherkas LF, Aviv A, Spector TD. 2005. Obesity, cigarette smoking, and telomere length in women. The Lancet 366, 662–664.

Vakhrusheva O, Smolka C, Gajawada P, Kostin S, Boettger T, Kubin T, Braun T, Bober E. 2008. Sirt7 increases stress resistance of cardiomyocytes and prevents apoptosis and inflammatory cardiomyopathy in mice. Circ Res. 102(6), 703-10.

van Berlo JH, Kanisicak O, Maillet M, Vagnozzi RJ, Karch J, Lin SC, Middleton RC, Marban E, Molkentin JD. 2014. c-kit+ cells minimally contribute cardiomyocytes to the heart. Nature 509, 337–341.

Van der Bogt KE, Sheikh AY, Schrepfer S, Hoyt G, Cao F, Ransohoff KJ, Swijnenburg RJ, Pearl J, Lee A, Fischbein M, Contag CH, Robbins RC, Wu JC. 2008. Comparison of different adult stem cell types for treatment of myocardial ischemia. Circulation 118(14 Suppl), S121-9.

Verma S, Fedak PW, Weisel RD, Butany J, Rao V, Maitland A, Li RK, Dhillon B, Yau TM. 2002. Fundamentals of reperfusion injury for the clinical cardiologist. Circulation 21, 105(20), 2332-6.

Volpert O, Jackson D, Bouck N, Linzer DI. 1996. The insulin-like growth factor II/mannose 6-phosphate receptor is required for proliferin-induced angiogenesis. Endocrinology 137(9), 3871-6.

Vousden KH, Lane DP. 2007. p53 in health and disease. Nature Rev. Mol. Cell Biol. 8, 275–283.

Walter DH, Rittig K, Bahlmann FH, Kirchmair R, Silver M, Murayama T, Nishimura H, Losordo DW, Asahara T, Isner JM. 2002. Statin therapy accelerates reendothelialization: a novel effect involving mobilization and incorporation of bone marrow-derived endothelial progenitor cells. Circulation. 105(25), 3017–24.

Wells J, Boyd KE, Fry CJ, Bartley SM, Farnham PJ. 2000. Target gene specificity of E2F and pocket protein family members in living cells. Mol Cell Biol. 20, 5797–807.

Williams AR, Hatzistergos KE, Addicott B, McCall F, Carvalho D, Suncion V, Morales AR, Da Silva J, Sussman MA, Heldman AW, Hare JM. 2013. Enhanced effect of combining human cardiac stem cells and bone marrow mesenchymal stem cells to reduce infarct size and to restore cardiac function after myocardial infarction. Circulation 127, 213–223.

Wolf D, Reinhard A, Seckinger A, Gross L, Katus HA, Hansen A. 2009. Regenerative capacity of intravenous autologous, allogeneic and human mesenchymal stem cells in the infarcted pig myocardiumcomplicated by myocardial tumor formation. Scand. Cardiovasc. J. 43(1), 39–45.

Wu Q, Zhan J, Pu S, Qin L, Li Y, Zhou Z. 2017. Influence of aging on the activity of mice Sca-1+CD31− cardiac stem cells. Oncotarget 8(1), 29–41.

Yamauchi T, Ishidao T, Nomura T, Shinagawa T, Tanaka Y, Yonemura S, Ishii S. 2008. A B-Myb complex containing clathrin and filamin is required for mitotic spindle function. EMBO J. 27, 1852–62.

Kwon Y, Kim JW, Jeoung JA, Kim MS, Kang C. 2017. Autophagy Is Pro-Senescence When Seen in Close-Up, but Anti-Senescence in Long-Shot. Mol Cells. 40(9): 607–612.

Yoon YS, Park JS, Tkebuchava T, Luedeman C, Losordo DW. 2004. Unexpected severe calcification after transplantation of bone marrow cells in acute myocardial infarction. Circulation 109, 3154-7.

Yusuf S, Hawken S, Ounpuu S, Dans T, Avezum A, Lanas F, McQueen M, Budaj A, Pais P, Varigos J, Lisheng L. 2004. Effect of potentially modifiable risk factors associated with myocardial infarction in 52 countries (the INTERHEART study): case-control study. Lancet 364(9438):937-52.

Zakharova L, Nural-Guvener H, Gaballa MA. 2012. Cardiac explant-derived cells are regulated by Notch-modulated mesenchymal transition. PLoS One 7(5):e37800.

Zeisberg EM, Tarnavski O, Zeisberg M, Dorfman AL, McMullen JR, Gustafsson E, Chandraker A, Yuan X, Pu WT, Roberts AB, Neilson EG, Sayegh MH, Izumo S, Kalluri R. 2007. Endothelial-to-mesenchymal transition contributes to cardiac fibrosis. Nat Med 13, 952-961.

Zhan M, Riordon DR, Yan B, Tarasova YS, Bruweleit S, Tarasov KV, Li RA, Wersto RP, Boheler KR. 2012. The B-MYB transcriptional network guides cell cycle progression and fate decisions to sustain self-renewal and the identity of pluripotent stem cells. PLoS One.7(8):e42350.

Zhang J, Wilson GF, Soerens AG, Koonce CH, Yu J, Palecek SP, Thomson JA, Kamp TJ. 2009. Functional cardiomyocytes derived from human induced pluripotent stem cells. Circ Res 104, e30–e41.

Zhang X, Klein AL, Alberle NS, Norby FL, Ren BH, Duan J, Ren J. 2003. Cardiac-specific overexpression of catalase rescues ventricular myocytes from ethanol-induced cardiac contractile defect. Journal of molecular and cellular cardiology 35, 645–652.

Zhu J, Woods D, McMahon M, Bishop JM. 1998. Senescence of human fibroblasts induced by oncogenic Raf. Genes Dev. 12, 2997–3007.

Zhu JH, Tao QM, Chen JZ, Wang XX, Shang YP. 2004a. Statins contribute to enhancement of the number and the function of endothelial progenitor cells from peripheral blood. Sheng Li Xue Bao 56(3), 357–64.

Zhu W, Giangrande PH, Nevins JR. 2004b. E2Fs link the control of G1/S and G2/M transcription. EMBO J. 23, 4615–26.

Zhu F, Li Y, Zhang J, Piao C, Liu T, Li HH, Du J. 2013. Senescent cardiac fibroblast is critical for cardiac fibrosis after myocardial infarction. PLoS One 8(9), e74535.